NTNU – Trondheim
Norwegian University of
Science and Technology

3D seismic interpretation in a deep-marine depositional environment from Lower Congo Basin offshore Angola

Ines Gomes Bartolomeu

Petroleum Geosciences
Submission date: June 2013
Supervisor: Egil Tjåland, IPT
Co-supervisor: Eilert Hilde, Statoil
Nils Erik Janbu, Statoil
Helge Løseth, Statoil

Norwegian University of Science and Technology
Department of Petroleum Engineering and Applied Geophysics

NTNU

Norges teknisk-naturvitenskapelige universitet

Fakultet for ingeniørvitenskap og teknologi

Faculty of Engineering and Technology

Studieprogram i Geoffag og petroleumsteknologi

Study Programme in Earth Sciences and Petroleum Engineering

Institutt for petroleumsteknologi og anvendt geofysikk

Department of Petroleum Engineering and Applied Geophysics

Kandidatens navn/ The candidate's name: **Ines Gomes Bartolomeu**

Oppgavens tittel, engelsk/Title of Thesis, English: **3D seismic interpretation in a deep-marine depositional environment from Lower Congo Basin offshore Angola**

Utfyllende tekst/Extended text:

1.

2.

Studieretning/Area of specialization: **Petroleum Geosciences**
Fagområde/Combination of subjects: **Petroleum Geophysics**
Tidsrom/Time interval: **January to June, 2013**

_____Egil Tjåland_____

Faglærer/Teacher

Original: Student
Kopi: Fakultet
Kopi:Institutt

Table of content

List of Figure

Acknowledgements

Those who are enchanted with practice without science are like the helmsmen entering the ship without rudder or compass, never being sure of their destiny (Leonardo da Vinci).

During the time of the preparation of this thesis, I had to fend many activities that were common in my daily life and at the same time I approached some people that helped much in the progress and conclusion of this work. Therefore, I would like to tank primarily:

Almighty God, the creator and source of all knowledge, because without Him I would not have the opportunity to make this scientific work and for the light of wisdom that He conceived me during this period.

My acknowledgements go also to Statoil Angola in the person of Mr. Jose Frey-Martinez, Knut Graue, Manuel Seque, Makutulo Ndongala and Ragnar Poulsen for having selected me and all indispensable availability in conceiving me all means for this work, allowing greater quality and efficiency in the conclusion of this work that will make this product an asset in the oil business. In particular, Statoil Research Centre in Trondheim – Rotvoll , especially to my advisors Eilert Hilde, Helge Løseth, Nils Erik Janbu and Richard John Wild for the patience and dedication during the project.

In another hand I appreciate the opportunity given to me by NTNU and ANHEI program all support given to me, particularly Professor Egil Tjåland, Jon Kleppe and Mrs. Tone Sanne (Trondheim), Professor Emilio Silva (Angola). To all Staff, Thank you.

Not to mention, my family especially my parents, Mariana Gomes, my dear brothers Antonio, Janiss, Suzana, and Manuel Bartolomeu. My Fiance Pedro Kinanga dos Santos to whom I dedicate this work since much has been done to the success of this work.

My colleagues from NTNU and the ANHEI program Ahanor David, Celsa Cesar, Esperanca Caetano, Edvaldo Agostino, Genilson Andre, Marina Salamanca, Pedro Bengui and Vania Costa, I thank you for the fellowship and support during this time.

To all once again, thank you very much.

Abstract

3D seismic data from the offshore Congo Basin, Angola has been performed in order to do geological interpretation of deep-marine deposits and understand the depositional system in the basin. Architectural elements, such as submarine channels, were mapped to see the geomorphologic characteristic.

The interpretation was done by dividing the seismic section into three stratigraphic units that are bounded by horizons interpreted. In order to help the interpretation, surface maps, isopach and attribute maps were extracted and the time slices was also displayed to show the channels migration. Analyses of the channelized depositional environments reveal two distinct depositional styles and results morphologies. Channels interpreted within Unit I and II are defined laterally migrating. The channels of Unit III exhibit a pronounced vertical aggradational motif.

Keyword: Submarine channel, lateral channel migration, vertical aggradational channel

Chapter 1 : Introduction and aims

1.1 Introduction

The present project is the master thesis for my MSc in Petroleum Geophysics at Norwegian University of Science and Technology (NTNU). It was written from January to June of 2013 at Statoil Research Centre in Trondheim – Rotvoll. Statoil has provided a 3D seismic data set from Congo Basin, Angola, Petrel Software, workstation and supervisors to help the execution of the project.

The thesis is organized into 8 chapters. The present chapter (Chapter 1) provides the list of principal aims of this thesis and subsequently, a concise overview. Chapter 2 comprises the geological setting of the study area. Chapter 3 comprises a short literature review of the most important characteristic of deep-marine depositional environment. Chapter 4, 5 and 6 describes how the interpretations was done and show the result. Chapter 7 and 8 shows the discussion, and conclusion.

Angolan margin comprises three main basins namely Congo Basin in the north, Kwanza Basin in the central part and Namibe Basin in south part (Stark, 1991). The thesis focuses on the Congo Basin west of block 31 (Figure 1.1). Seismic studies have been limited of the late Cenozoic, Malembo Group. I have interpreted submarine channel in 3D seismic section.

The interpretation stated by picking four horizons. This was bounded by three units. In order to help the interpretation, surface maps, isopach and attribute maps were extracted and the time slices was also displayed to see how the channels are migrate.

1.2 Aims and Objectives

The aim of this thesis is seismic interpretation of 3D seismic data from Congo Basin in order to do geological interpretation of submarine channels, to see how the salt influences evolution of the channel. It was also to understand the geology and depositional system in the basin. The main objectives are:

- ✓ Geological interpretation of submarine channel.
- ✓ Geomorphology and geometry of the channels.
- ✓ Understanding of the depositional system in the study area.
- ✓ Salt influence on channels development.

The most important seismic horizons were mapped in order to interpret the channel systems. The interpretation methodology divides the channel into several intervals, which are imaged by both variance and RMS amplitude maps. Therefore, workstation applications and Petrel techniques were applied to aid the interpretation such as:

- Seismic horizons interpretation.
- Generation of surfaces horizon maps.
- Seismic attribute map extractions.
- Time slice extraction.

1.3 Data provided/ software

Seismic Data: The seismic data are 3D pre stack time migration (PSTM). The seismic survey comprises 2026 inlines and 2811 cross lines. The inline interval is 25 m and the length is 70255.50 m. The cross line interval is 25 m and the cross line length is 50628.66 m. The seismic sections were acquired in a NW-SE direction. The seismic 3D survey covers an area of 655.36 km^2. It was recorded in TWT ms.

Petrel Workstation: The 3D seismic data was interpreted with Petrel software.

Time of Interpretation work/Deadline: It was written from January to June of 2013. The interpretation was done during 2 months (23th of January to 29th of March). The deadline was 17th of June

No available data:

- Seismic depth data,
- Wells
- Velocity Data
- LFP (Lithological fluid prediction data)

1.4 Location

The Lower Congo Basin is located in the West African continental margin, in the north part of Angolan margin between 5^0S and $8^0$30'S of latitude. The study area is located offshore, in the western part of Lower Congo Basin (Figure 1.1).

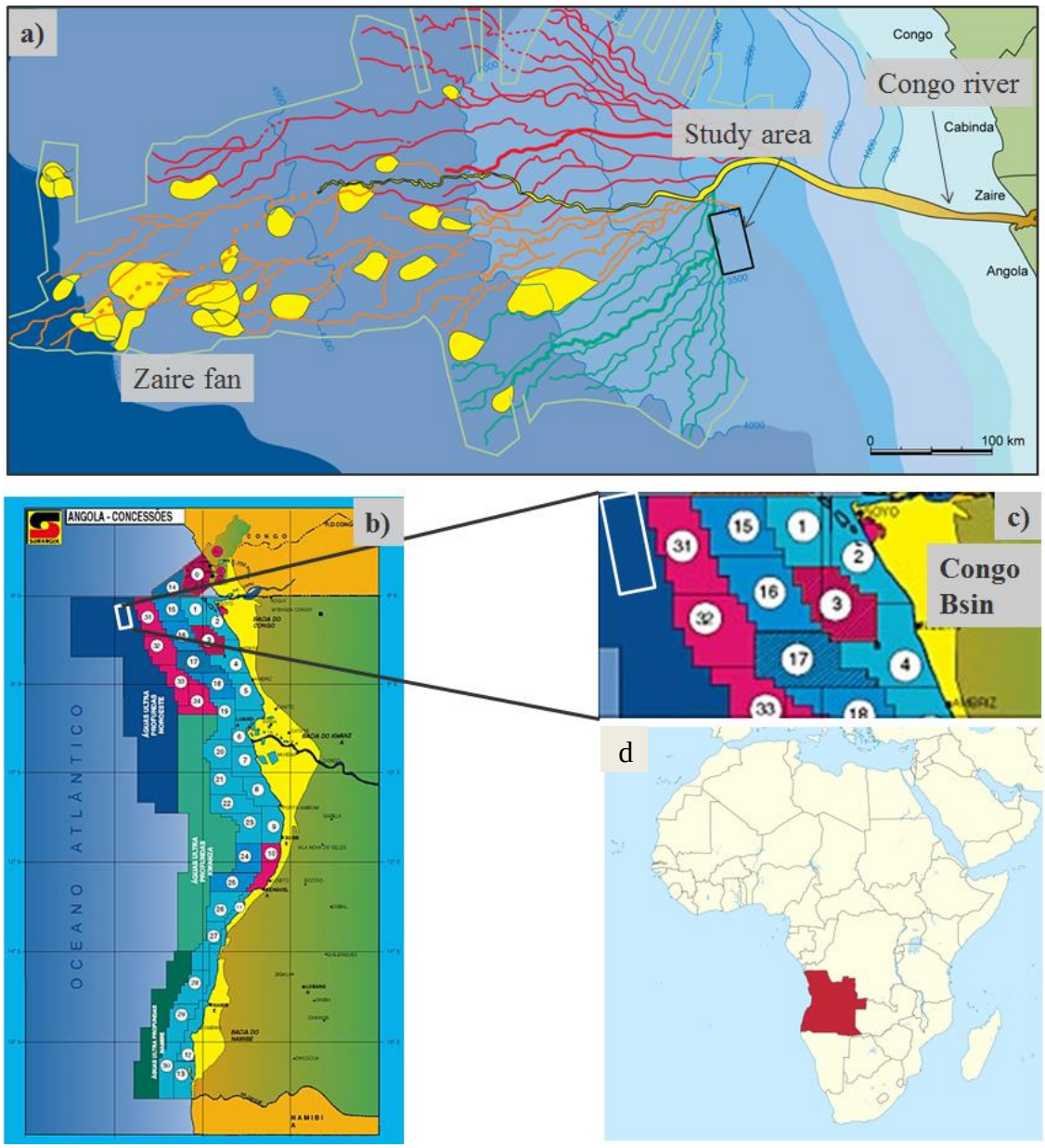

Figure 1.1: Location of study area in Lower Congo Basin offshore Angola. a) showing bathymetric maps of the study area, offshore the Congo–Angola passive margin, with interpreted channels of Zaire Fan (Modified from Droz et al. 2003). b) showing the coast of Angola and the license blocks. c) showing the study area, which is marked in the square. d) showing the African continent and Angola. (Modified from Sonangol report, 2003)

Chapter 2 : Regional geology of the Congo Basin and study area.

This chapter is mainly based on Stark (1991) in explaining the origin and evolution of the Angola margin. I use the stratigraphy of the Congo Basin, as described by Gjelberg and Valle, (2003) and Valle et al., (2001).

2.1 Geological Setting

The lower Congo Basin comprises six groups: Presalt Group, which corresponds to the syn-rift phase. Lome Group, correspond to the transition phase. The Pinda, Iabe, Landana and Malembo groups, which correspond to post-rift phases.

2.1.1 Origin and evolution of the Angolan margin

The tectonic, geological and sedimentary basin evolution of the Angolan margin evolved during the Mesozoic and Cenozoic. It is the result of early Cretaceous rifting of Gondwanaland. This process led to opening and formation of oceanic crust between the South American and African continents in mid Cretaceous time.

Angolan margin can be subdivided in four different phases: (i) pre-rift, (ii) syn-rift, (iii) transition and (iv) post-rift. See Figure 2.1 and description below.

The pre-rift phase (late Proterozoic to Jurassic) is characterized by extreme peneplanation in most part of the central and southern Africa and eastern South America. The sediments deposited during the pre- rift are alluvial, fluvial and lacustrine sediments (Stark, 1991).

The syn-rift phase (late Jurassic to early Cretaceous), is identified by extension on both the South American and African margins. During this period the continental lithosphere and crust were extended and became very thin, with formation of rift grabens (Figure 2.1). The sediments deposited during this phase consist mainly of lacustrine black shale and turbidity deposits (Stark, 1991).

The transition phase (Aptian to early Albian) is characterized by marine incursion. Evaporation led to the formation of a salt sequence mainly composed of Halite which make up the Loeme Group (Stark, 1991) (Figure 2.1). The post-rift phase (early Albian to present) started with a breakup unconformity just above salt (Gjelberg and Valle, 2003).

During the Cenozoic, huge loads of sediments were transported to the Angolan margin. The sediment supply, especially from the Congo River during the Cenozoic resulted in deposition of the submarine Zaire fan (Figure 1.1) (Amaral et al., 1998; Serqueira et al., 1998; Mateus., 2009).

The activity of extensional faulting extended until early-Aptian and ceased after development of final break-up unconformity in early – mid Aptian time (Figure 2.1 and Figure 2.2). The

cessation of rifting and basement involved fault activity coincided with the onset of oceanic spreading in the South Atlantic and transition to a passive margin (Valle et al, 2001).

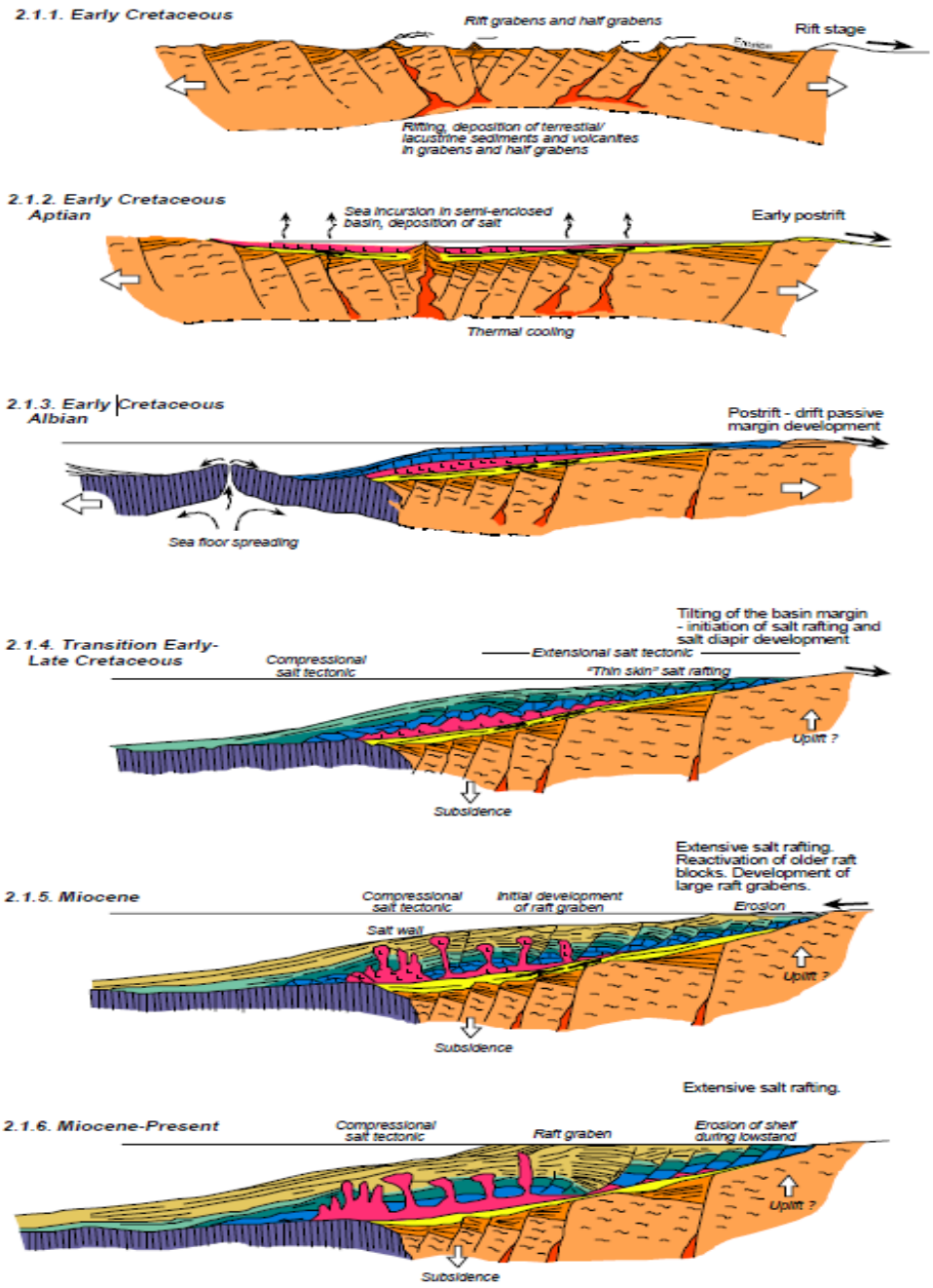

Figure 2.1: Stages of rift evolution. Illustrating the evolution of syn rift and post rift (Gjelberg and Valle, 2003).

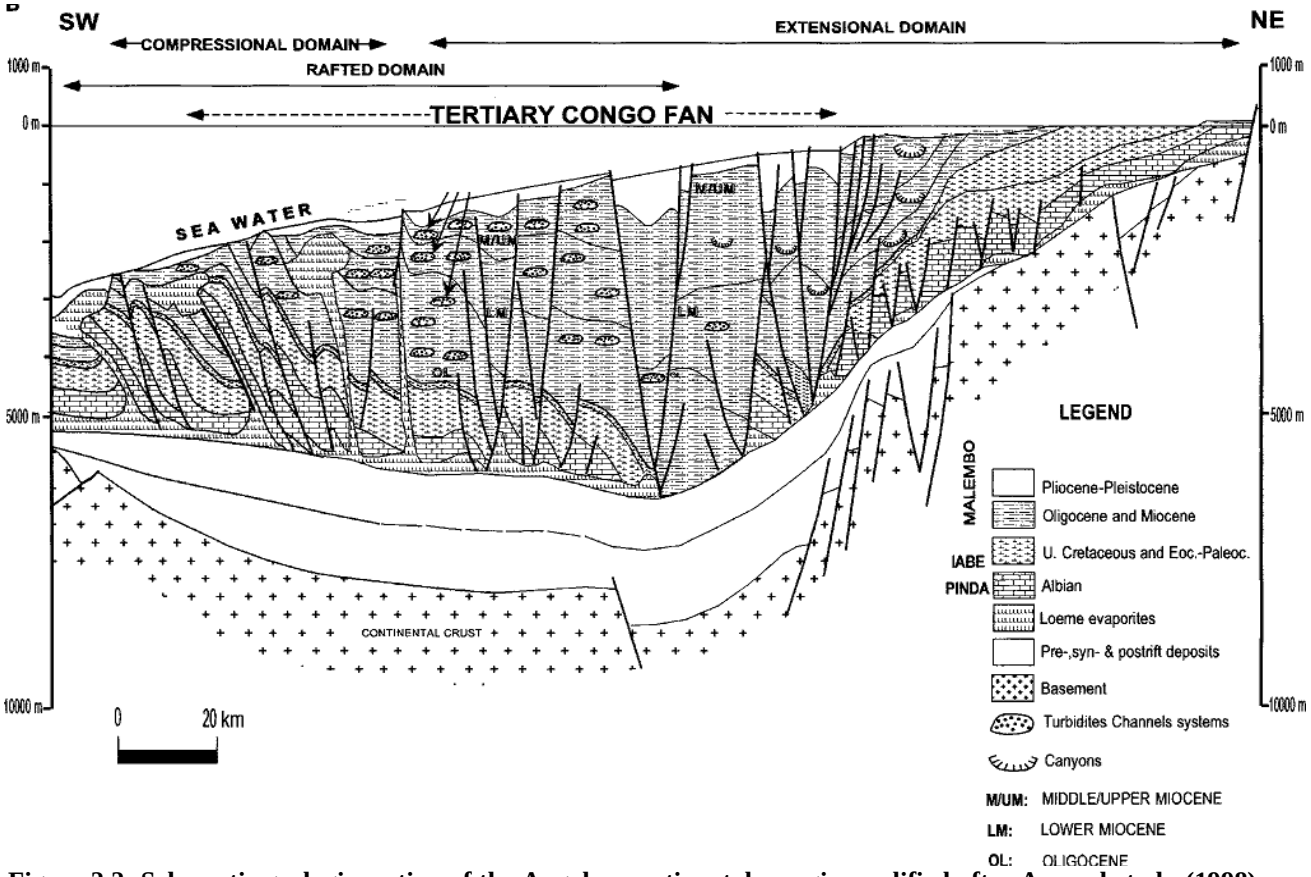

Figure 2.2: Schematic geologic section of the Angolan continental margin modified after Amaral et al., (1998) and Serqueira et al., (1998).

2.1.2 Stratigraphic framework of the Congo Basin

The sedimentary infill of the Congo Basin is subdivided into three main units: (i) Pre salt sequence that corresponds to the Syn-rift phase, (ii) Salt unit corresponding to the Transitional phase and (iii) Post-salt unit corresponding to Post-rift unit.

Syn-rift phase /sequence

The pre salt sequence comprises Neocomian to early Aptian sediments. It was deposited before the salt. The sediments consist mainly of volcanic, evaporitic, lacustrine and fluvial sediments like siltstone, sandstone, conglomerate, and carbonates. Previous studies describe the main source rock in syn-rift sequence, the Bucomazi and Chela formations. The maximum thickness of the syn-rift sediments is 1,500 m (Brice et al., 1982).

Transition phase /sequence

The Loeme Group covers the transitional phase /sequence with deposits of Aptian and Albian age. These deposits correspond to an overall transgressive phase. The evaporate sediments are predominantly composed of halite. These sediments represent a transitional sequence that shifts

from continental to marine environment. The sediment layer below the Loeme Group is represented by the Chela Formation (Gjelberg and Valle, 2003).

Post-rift phase /sequence

The post salt sequence (Albian to present) was deposited above the mobile substrate of the salt. The lower part consists of a sequence of clastics and marine carbonates. These deposits were strongly deformed due to salt tectonic. This unit ranges in thickness up to 6,000 m. It is thin in the east and thickens rapidly to the west (Brice et al., 1982). The post-rift sequence is divided into the Pinda, Iabe, Landana and Malembo Formations (Figure 2.3).

The Pinda Group, which was defined by Abilio (1986), is of Albian age. It lies above the Loeme Formation. The lithofacies varies from continental fluvio-alluvial to deep marine facies. The depositional environment varies from fluvio-continental to outer platform. The lithology consists of sand, silt, anhydrite, dolomite and clay. These sediments have very good reservoir and source potential.

The Iabe Formation was defined by Abilio (1986) and lies between the Pinda and Landana Group. It shows a relatively abrupt transition from limestones to argillaceous limestones, marls and shales.

The Landana Formation is bounded by the Malembo and Iabe groups. It consists of marls and carbonates (Gjelberg and Valle, 2003).

The Malembo Formation is separated from Landana Group by an extensive regional/sub regional unconformity at the transition between Eocene and Lower Oligocene. This formation also contains less marls and carbonates than the Landana Group. The Malembo Formation contains three formations such as Quifangondo, Landa/Bento, Areias cinzentas and Quelo Formation.

The major source rock sequence occurs in the upper Cretaceous post salt section, the Iabe Group from Cenomanian to Turoian. Other contributing source rock may be the uppermost Albian-Cenomanian Moita Seca Formation and the lower Tertiary Landana (Cole et al., 2000).

The Malembo Formation is progradational (Figure 2.3). Deltaic sediments prograding westwards with time into deep marine environments. The depositional environment recorded by the Malembo Formation, reflect the complex interaction between open marine sedimentation in the Lower Congo Basin and ancestral Congo River. Sandy turbidities were deposited in the Congo Fan, offshore of the delta (Anderson et al., 2000).

The canyon-fed turbidite systems of the Congo Fan were deposited in pro-delta slope and basin floor settings (Anderson, 1998). The canyon can be traced as far back as the Oligocene and Miocene (Anderson et al., 2000).

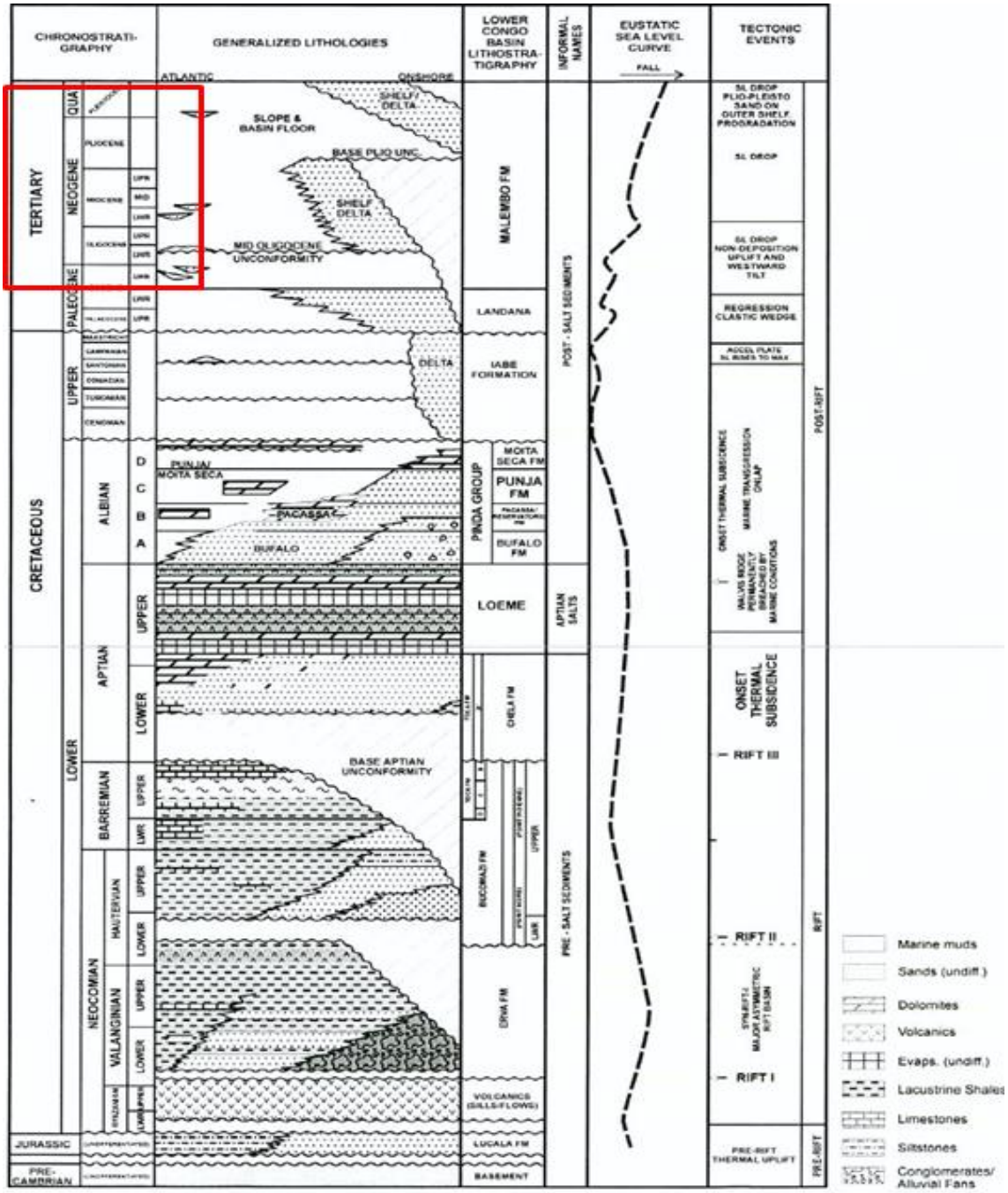

Figure 2.3: Stratigraphy of the Congo Basin, showing progradation of the Malembo Formation, which is studied in the present project. The approximate location of the study area is marked in red color. Modified from Anderson et al., (2000).

2.1.3 Structural framework of the Congo Basin

The West African passive margin has experienced a complex history of structural deformation during the late Cretaceous and Cenozoic post-rift thermal subsidence. The post-rift (also generally referred to as the post-salt) structural stratigraphy history is related to tectonics and basin sedimentary processes. In the Lower Congo Basin, the post-rift sediments have undergone thin-skinned extension in the east, with diapiric salt structures and thin-skinned compressional structures dominating in the west (Anderson et al., 2000).

Figure 2.4 summarizes structural domains of the Congo Basin. The extensional domain is in the proximal part (upslope). It starts with formation of grabens, which develop into tilted bocks and diapirs. The extensional domain has following sub-domains: (i) sealed tilted blocks, (ii) synthetic growth faults and rollovers, (iii) extensional diapirs between the rifts (Fort et al., 2004).

The compressional domain is in the distal part (downslope). Because of increased thickness during the synchronous sedimentation, fold wavelength increase as well. Therefore it is subdivided by growth folds, thrust and compressional domain (Fort et al., 2004).

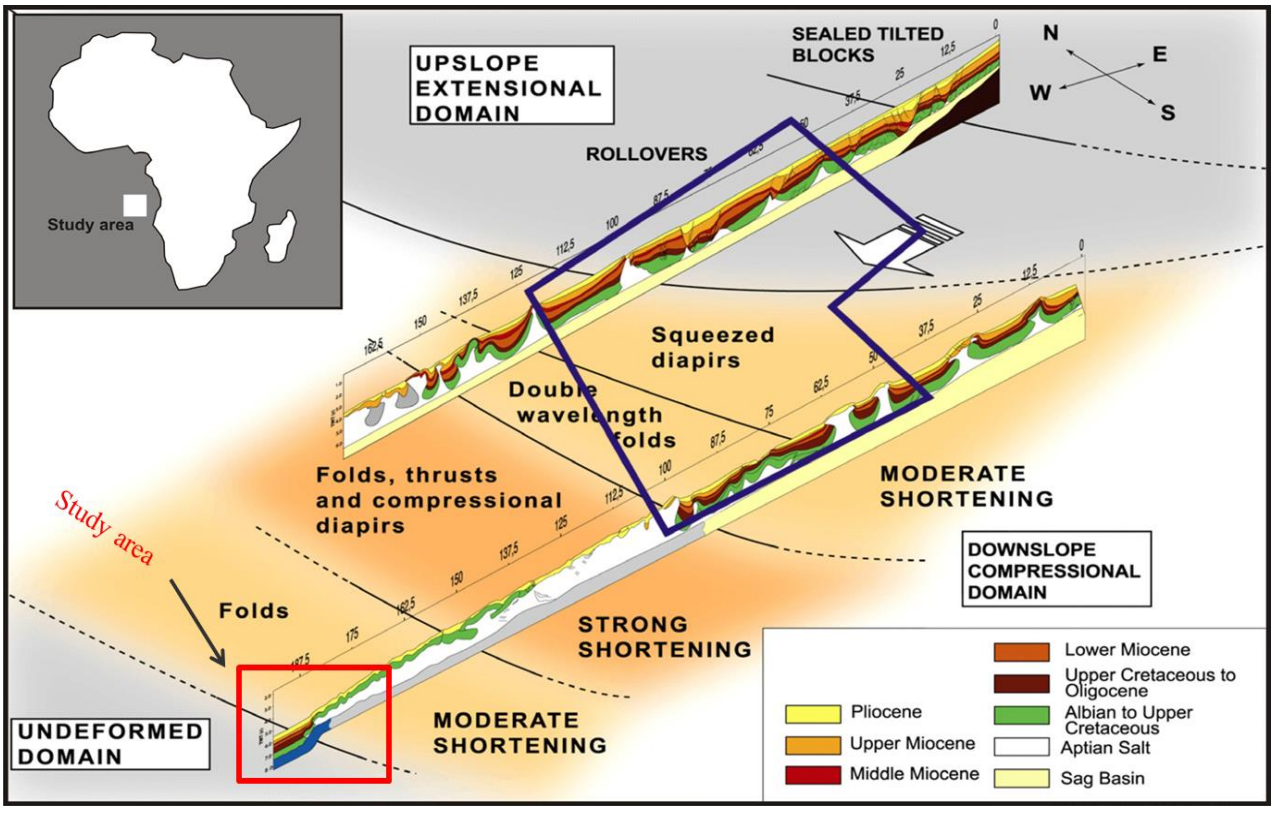

Figure 2.4: Post-salt section of the Lower Congo Basin illustrating the structures of extensional and compressional domains. The approximate location of the study area is marked with a red square (Modified from Fort et al., 2004).

2.2 The effect of salt tectonics in the basin

Salt tectonic is an interaction between salt body movements and sediments deposited. The Angolan basins are strongly affected by salt tectonics. At passive margin, the gravity driven deformation above salt commonly leads to the development of domains of upslope extension and downslope contraction (Fort et al., 2004), (Figure 2.5).

To have an accumulation of hydrocarbons there are some conditions that needs to be in place. A good source rock that generates hydrocarbons, good reservoir rocks with good porosity and permeability, a good trap for accumulation of hydrocarbons, migration path to permit the hydrocarbons to migrate from the source rock to the reservoir and a good seal to avoid that the hydrocarbons escape.

The salt deformation is very important in spatial and temporal distribution of sedimentary facies (reservoir) and the generation, migration and trapping of hydrocarbons (Rowan, 2008). Successful exploration for oil and gas in Angola thus requires a good understanding of the interaction between sediment deposition and salt movement, and many of the plays are related to salt tectonics.

Salt is very important for hydrocarbon exploration in the Congo Basin, and in others basins globally. The salt behaves very differently to other sedimentary rocks because of its physical properties such as density and viscosity. The salt has low density and high viscosity. Together with other sediments it tends to deform creating some geological structures that can be traps for hydrocarbon exploration (Figure 2.6).

The interaction between sediments deposited and salt movements can create diapirs. Because of the salt proprerties, the diapirs can be a seal. Reservoir rocks overlying a diapir can be folded by underlying salt, generating closures that may contain hydrocarbons (Figure 2.6). Below salt, others types of plays may develop. The salt can be important as the top seal, preventing hydrocarbons from leaking up (Figure 2.6).

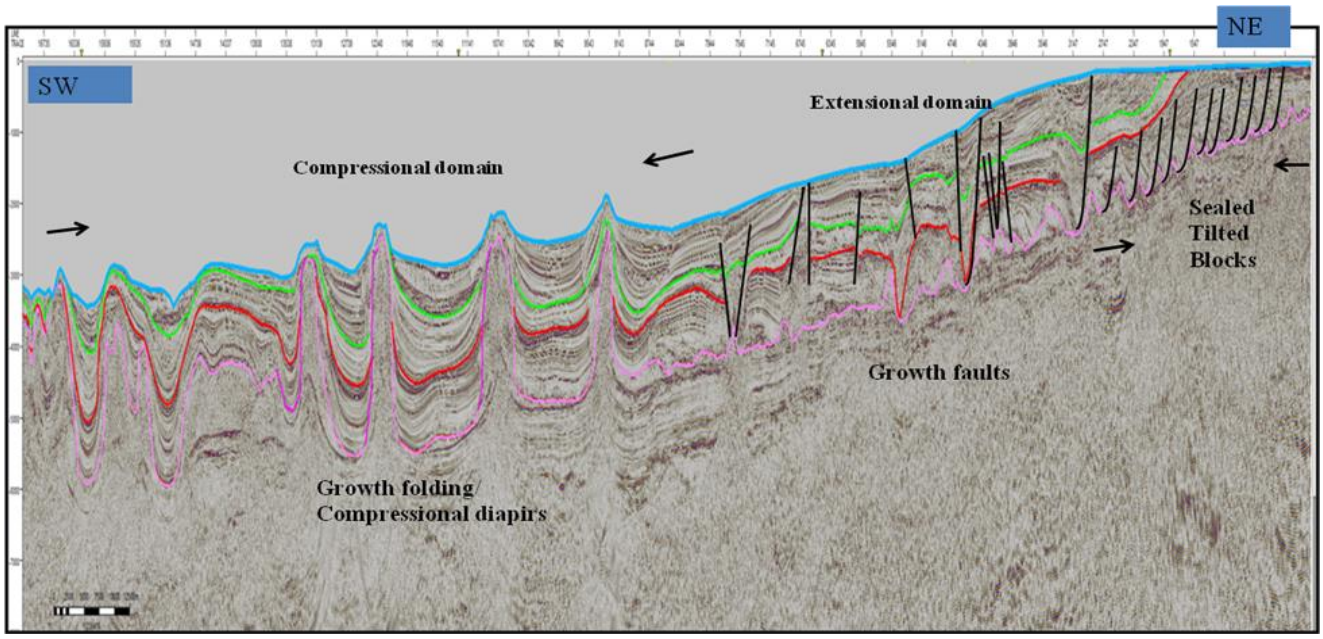

Figure 2.5 Seismic section from the Kwanza Basin illustrating two domains; The extensional domain comprises predominantly sealed tilted blocks and growth faults, whereas the compressional domain comprises mostly growth folding and compressional diapirs (Bartolomeu)

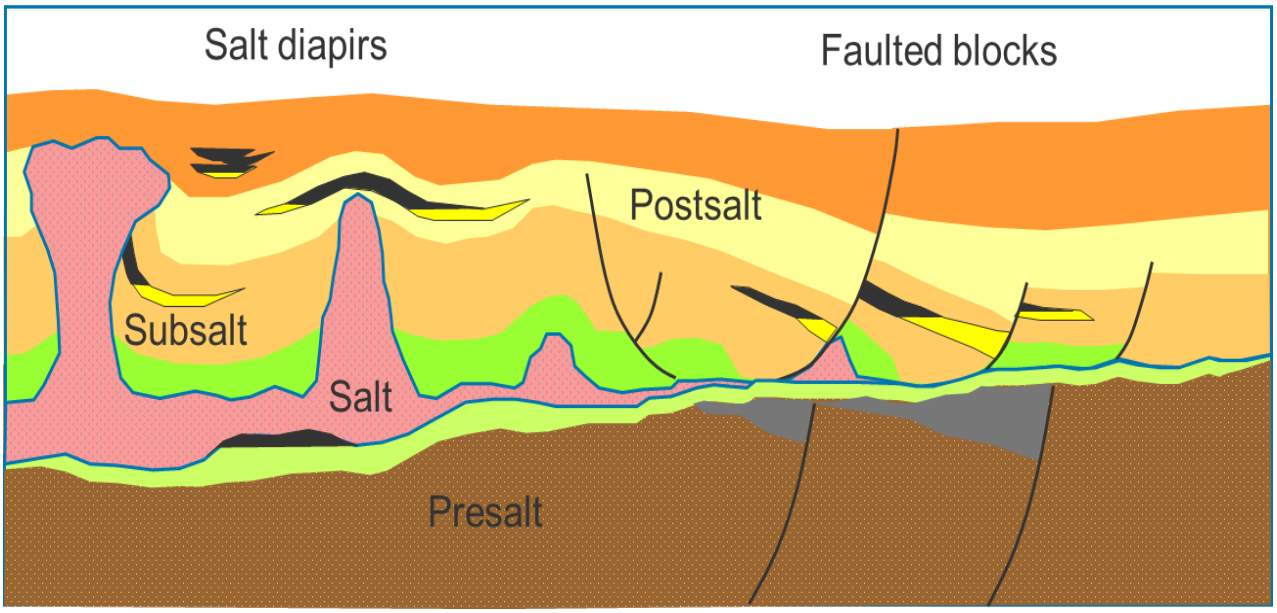

Figure 2.6 Geological structures resulting from salt deformation. These structures can create traps for hydrocarbon accumulation (Fejerskov et al., 2009

Chapter 3 : Literature review of channel systems and deep marine depositional environment.

3.1 Depositional system

To understand the depositional system, is important to know the principles of sequence stratigraphy.

3.1.1 Seismic sequence stratigraphy

Seismic sequence stratigraphy is key to understanding how the sediment packages are developed. It provides a tool for determining the presence of source rocks and distribution of reservoirs and seals.

Seismic stratigraphy can also provide information critical to understanding sea-level fluctuations, combinations of eustatic relative sea level change and tectonic subsidence (Gluyas and Swarbrick, 2004).

The accommodation space is created and destroyed by the interplay of tectonic subsidence or uplift and sea level, the sediments accumulate in accommodation space by sediment supply.

If **relative sea level is constant** the sediments will build up on the shelf and prograde into the basin (Figure 3.1 a).

If **relative sea level rises** the accommodation potential on the shelf will increase and most of the deposition will be confined with the shelf (Figure 3.1 b). It happens due to subsidence, compaction and/or eustatic sea level rise (Emery and Myers, 1996).When sea level rises, it calls transgression. The coastline migrates in land. Generally, the fine grains are on the top and coarse grains are on the base.

If **relative sea level fall** the accommodation potential will decrease and the sediment will be exposed and consequently eroded (Figure 3.1 c). It happens due to tectonic uplift and/or eustatic sea level fall (Emery and Myers, 1996). When sea level falls, the coastline migrates oceanwards.

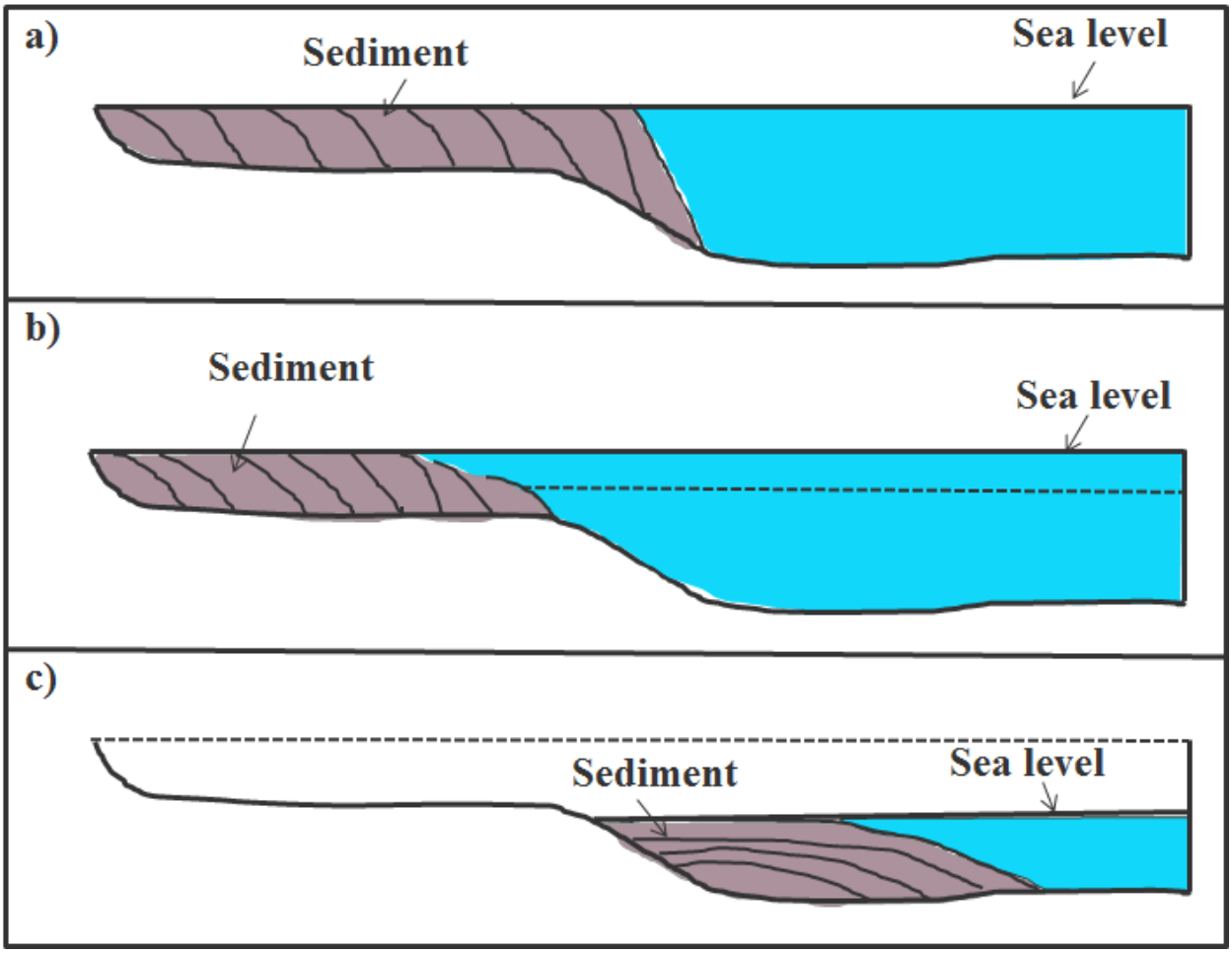

Figure 3.1: shows the effect of relative sea level changing. a) relative sea level is constant, b) relative sea level rise, c) relative sea level fall.

The Fundamental unit in sequence stratigraphy is the sequence. This has been defined as relatively conformable, genetically related succession of strata bounded by unconformities or their correlative conformities (Mitchum, 1977). A sequence can be subdivided into systems tracts. It is defined by their position within the sequence and by stacking patterns of parasequence sets and parasequences bounded by marine-flooding surfaces (Van Wagoner et al., 1988).

The system tract term is used to designate three subdivisions within each sequence: Lowstand, trangressive and highstand systems tracts (Van Wagoner et al., 1988) (Figure 3.2).

The lowstand system tract is most evident in this project, since I am working with deep marine depositional environments. Three elements are recognized within the lowstand-system track such as basin floor fans, slope fans and prograding complex.

The basin floor fan is characterized by deposition of submarine fans on the lower slope or basin floor (Van Wagoner et al., 1988). It is usually the highest net/gross of the deepwater system. The downdip portion of basin floor fans are equivalent to sheet sands (lobes). The updip portions are equivalent to amalgamated channels.

Slope fans are characterized by turbidite and debris-flow deposition on the middle or the base of the slope (Van Wagoner et al., 1988). The slope fan includes several elements: channel-fill, levee-overbank, extensive slides, debris flows and mass-transport deposits.

The prograding complex consists of prograding shallow marine deposits, slope and deep marine muds.

The trangressive system tract is in the middle system tract (Figure 3.2). It is characterized by one or more retrogradational parasequence set. The base of transgressive system tract is the trangressive surface at the top of lowstand or shelf margin system tracts. The top is the downlap suface (Van Wagoner et al., 1988).

The highstand system tract is the upper system tract (Figure 3.2). It is characterized by one or more aggradational parasequence sets that are succeeded by one or more progradational parasequence sets with prograding clinoform geometries (Van Wagoner et al., 1988).

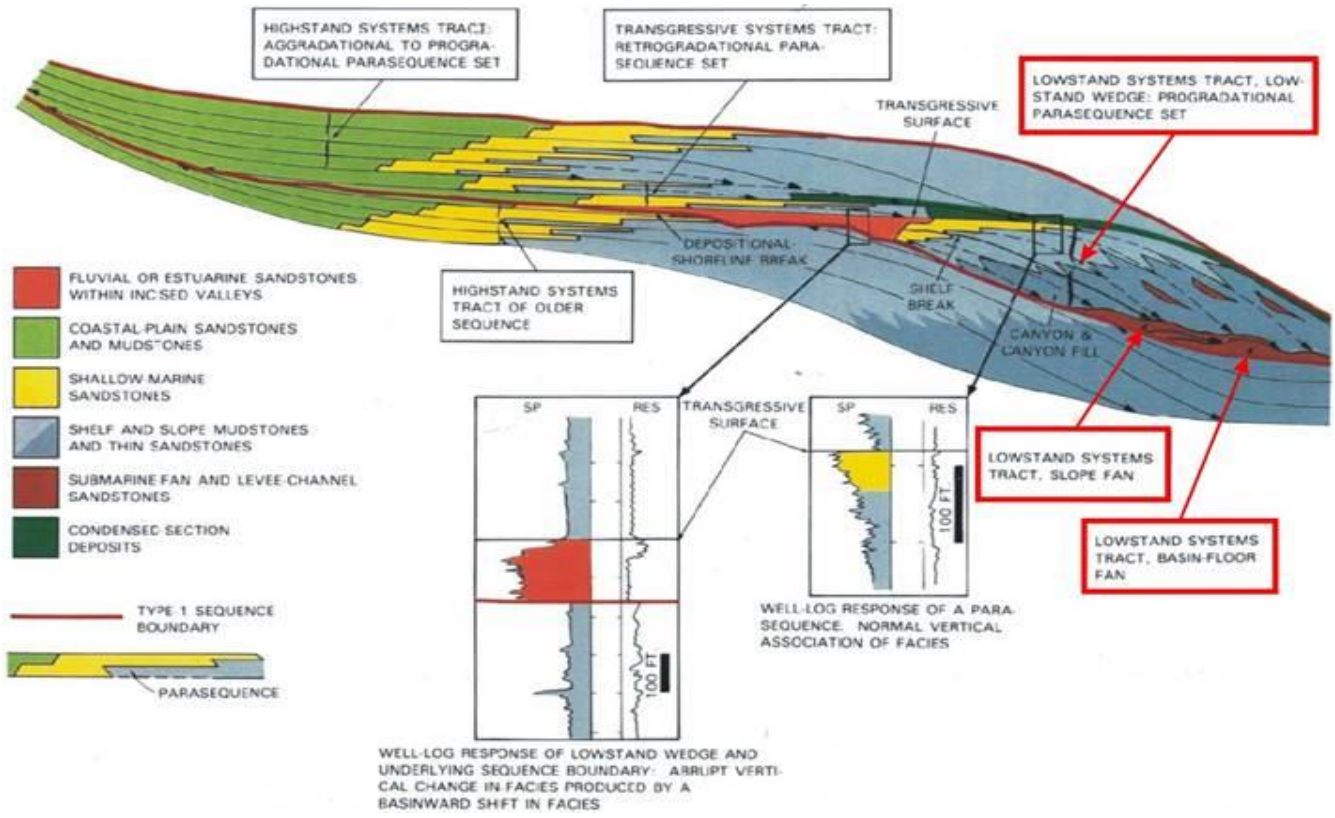

Figure 3.2: Stratal patterns in sequence deposited in a basin with a shelf break. It shows the lowstand, transgressive and highstand system tracts. The lowstand wedge, slope fan and basin-floor fan are marked in red color (Van Wagoner et al., 1988).

3.2 Deep water reservoirs

The deep water reservoirs provide many new technical challenges for hydrocarbon development and production. Therefore, it is important to understand the complex and elements in order to ensure optimal resource development and hydrocarbon recovery.

3.2.1 Deep water reservoir elements (architectural elements)

According to Funk et al. (2012), five reservoir elements have been recognized in the previous studies namely: (i) Channel elements (channel fill); (ii) Lobe elements; (iii) Levee elements (thin beds): (iv) Mass transport elements (slides); and (v) Mudstone sheet elements (amalgamated and layered).

i) Channel elements have erosional, concave-upward, lower bounding surfaces and flat, conformable, upper bounding surfaces. Strata are variable, but in most case coarsest grains in the axis and finer grain toward the lateral margin.

ii) Lobe elements have planar and conformable lower bounding surface and broadly convex-upward upper bounding surfaces. Strata are commonly coarsest in the axis, thin and become finer grained toward the lateral margin.

iii) Levee elements are located adjacent to some channel elements. They contain thin-bedded, fine-grained deposits that become thinner and finer grained with increased lateral distance from a channel. They are formed by overspilling of turbidity currents in channels.

iv) Mass transport elements are slumps and slides containing contorted bedding, internal faults and fluidization features.

v) Mudstone sheet elements have planar lower and upper bounding surfaces. They are entirely composed of pelagic and hemipelagic laminated mudstones

Figure 3.3 shows the static evolution of four categories of deep water architectural elements. Diagram A corresponds to architectural elements analysed above. Diagram B shows lateral and vertical stacking patterns common to deep-water settings. Diagram C shows three settings on the slope-to-basin profile such as:

Confined settings: This environment comprises strong erosional flows and is typically erosionally confined and/or levee-confined (Campion et al., 2000; Abreu et al., 2003). The deposits tend to be vertically stacked, with low aspect ratio discussed by (Sullivan et al., 2000). This reservoir type has commonly moderate net to gross and usually with good vertical and lateral connectivity.

Weakly confined settings: This environment has less erosion, and is characterized by laterally offset, compensationally stacked channel-fills mentioned by Beaubouef and Friedmann (2000). These reservoirs are high net-to-gross and have good to moderate with vertical connectivity (Sprague et al., 2005).

Unconfined- distributive settings: This environment is non to very weakly-erosional, and is characterized by unconfined flow on very low gradient slopes and basin floors (Sullivan et al., 2000; Beaubouef and Friedmann, 2000; Beaubouef et al., 2003). These reservoirs have high to very high net-to-gross, and high lateral continuity but poor vertical connectivity due to laterally extensive shale beds (Sprague et al., 2005).

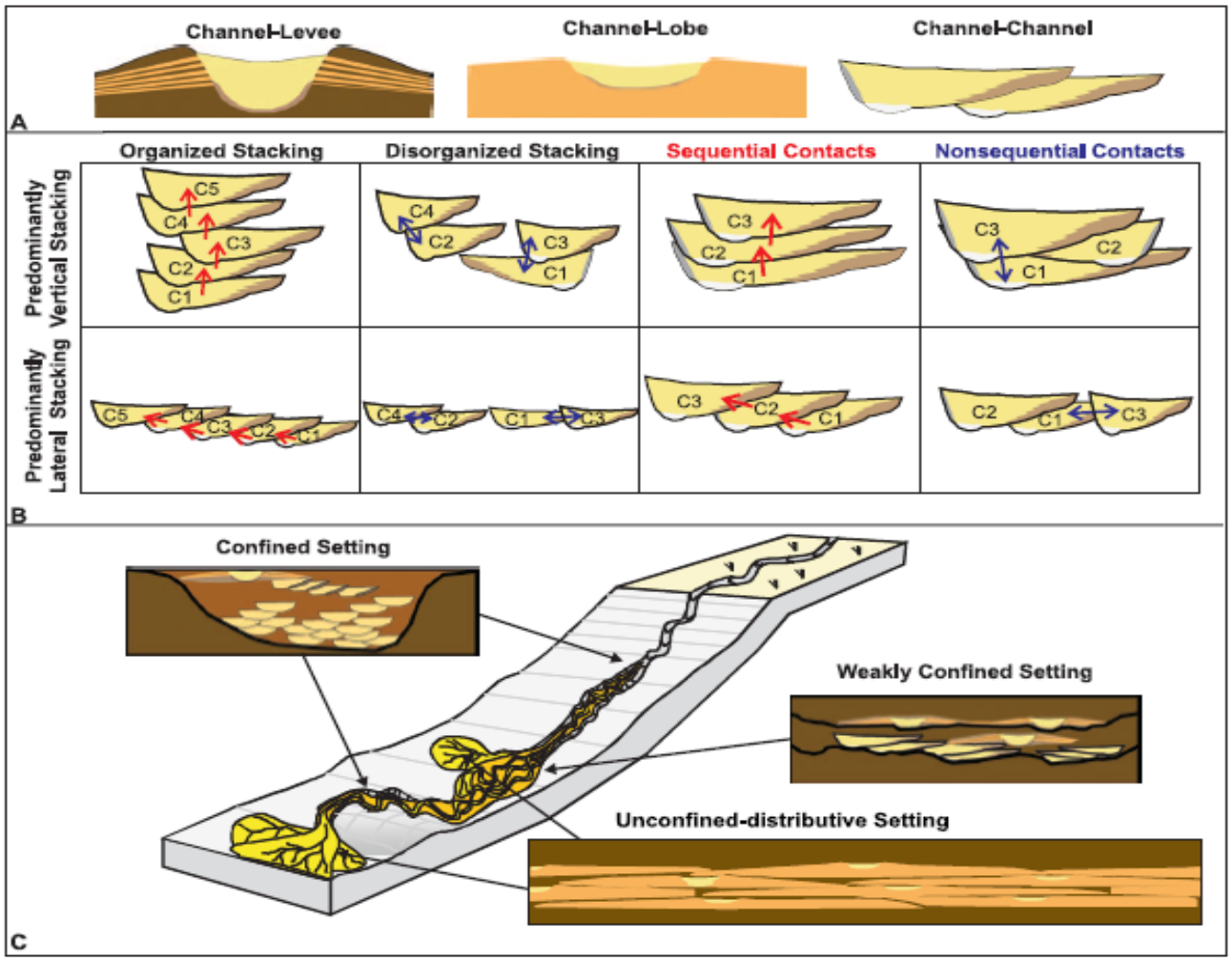

Figure 3.3 Deep water reservoir elements showing four categories. (A) Association of architectural elements analyzed: channel-levee, channel-lobe and channel-channel. (B) shows stacking patterns common to deep-water settings. (C) Shows three settings on the slope-

3.2.2 Deep water hierarchy

The deep-water stratigraphic hierarchy is based on the principles of sequence stratigraphy, which is the recognition of genetically-related strata packages and their bounding surfaces (Mitchum, 1977; Van Wagoner et al., 1988; Mitchum and Van Wagoner, 1991). It provides the framework and methodology to describe all strata deposited in deep water, slope to basin floor depositional environments (Sprague et al., 2005).

The deep water hierarchy is organized by channel story, channel elements and channel complex (Figure 3.4).This approach regards the channel element as the fundamental unit. Each channel element records an individual down cutting and filling succession and they are constructed of one or more stories. Each story contains bedsets that follow a similar facies association. The

stories are bounded by small-scale erosional features that do not scale to the depth of the channel element. Chanel elements of similar lithofacies type stack to build channel complex (Funk et al., 2012).

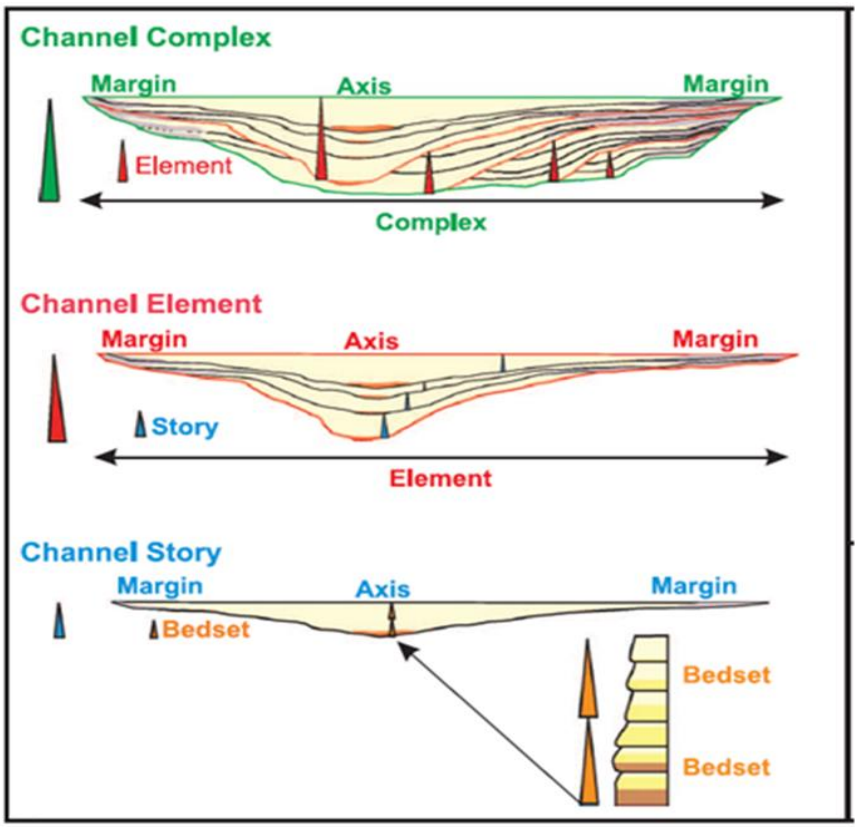

Figure 3.4: Schematic illustration of hierarchical, stratigraphic framework of channelized deep-water reservoir elements (Funk et al., 2012).

Chapter 4 : Seismic interpretational techniques in Petrel / workflow and methodologies

4.1 Workflow of interpretation

The interpretation has been done in the Petrel software. I used autotracking for continuous reflectors (Sea bed) and manual picking for discontinuous reflectors, with a grid size no larger than 50x50 lines m.

Petrel software has three window types (Figure 4.1):

- 2D windows

- 3D windows

- Interpretation window

The 2D window shows maps. The window also shows the direction of seismic sections and the color scale of the visualized map (Figure 4.1a).

The seismic 3D window was used to perform visualization and also to interpret seismic lines. It also provided the basis for performing quality control of the interpretation. For example, inline, crossline, time slice and random lines can be displayed in the 3D window (Figure 4.1b)

The interpretation window shows seismic sections and it is the platform where the actual seismic interpretations of horizons are done (Figure 4.1c).

According to the Society of Exploration Geophysics (SEG) standard there are two types of polarity, normal (American) and reverse (European) polarity. The normal polarity represents positive amplitude when the acoustic impedance increases, normally displayed as a peak in the wiggle trace and displayed as red color in the seismic section. The reverse polarity represents negative amplitude when the acoustic impedance increases. Normally, it displays as a trough in the wiggle trace and blue color displayed in seismic section. The reverse polarity is used in this project as it is shown in Figure 4.2 a and b and Figure 4.3.

The peak wiggle trace represents the positive amplitude and the white trough represents the negative amplitude as it is seen in Figure 4.2 a. It shows increasing acoustic impedance giving by negative amplitude. I have interpreted the horizons in trough. The blue color represents the negative amplitude and the red color represents the positive amplitude showing in Figure 4.2 b. The seismic section shows also increasing acoustic impedance giving by negative amplitude. I have picked the seafloor horizons in blue color.

We were two students working with the same data set. In order to subdivide tasks, the data set was divided into two intervals. The shallow interval goes from Sea bed to Horizon A, and the deep part, goes from the Horizon A to Horizon D (Figure 4.4). My focus is in deep interval (Figure 4.4).The interval is between 5430 to 6600 ms which corresponds to 1170 ms thickness.

The quality of the data is good. It is difficult to pick the reflectors in deep parts of the section and in steeply dipping areas which were formed by salt movements.

The salt movement leads to changes in the sediment in terms of their position, structures and disposition as shown in Figure 4.4 and Figure 4.5b. Some reflectors are also observed with depositional layers onlapping the flanks of salt diapirs. They are discontinuous in some parts, which become difficult to pick during interpretation.

Figure 4.5 illustrates a common problem in the area, which is syn depositional salt movement. Initially it was flat, the salt was deposited and others layers above it (Figure 4.5a). When the salt starts moving (Figure 4.5b), the sediments were deposited in the depression in the submarine environment. Turbidity channels are part of depositional system.

The interpretation started by mapping the most important horizons in order to delimitate the architectural elements (channel), and geological structure in the basin. The interpretation methodology divides the channel into several intervals, which are imaged by both variance and RMS amplitude maps.

I have picked five horizons; 1) Sea bed (SB), 2) Horizon A (HA), 3) Horizon B (HB), 4) Horizon C (HC), 5) Horizon D (HD). My interpretation was concentrated between horizon A and D (Figure 5.2 and Figure 5.3). Horizon A was the top and Horizon D was the lowest of the interpreted horizons.

I describe the strength of the amplitude and continuity of the reflection as shows in Figure 4.6. Different seismic features can be found on the seismic units within each of the interpreted horizons.

Seabed was the first horizon to be picked. The Seabed interpretation was selected as trough reflection. The velocity normally increases with increasing depth. The acoustic impedance of sea water is lower compared to the sediments on the sea bottom. Consequently the amplitude is very strong because the acoustic impedance increases when entering the sediments. The others interpreted horizons are shown in Figure 5.2 and Figure 5.3.

Surface maps, isopach and attribute maps were generated after finishing all the horizons interpretation (Figure 4.7, Figure 4.8, Figure 4.9, Figure 4.18, and Figure 4.19).

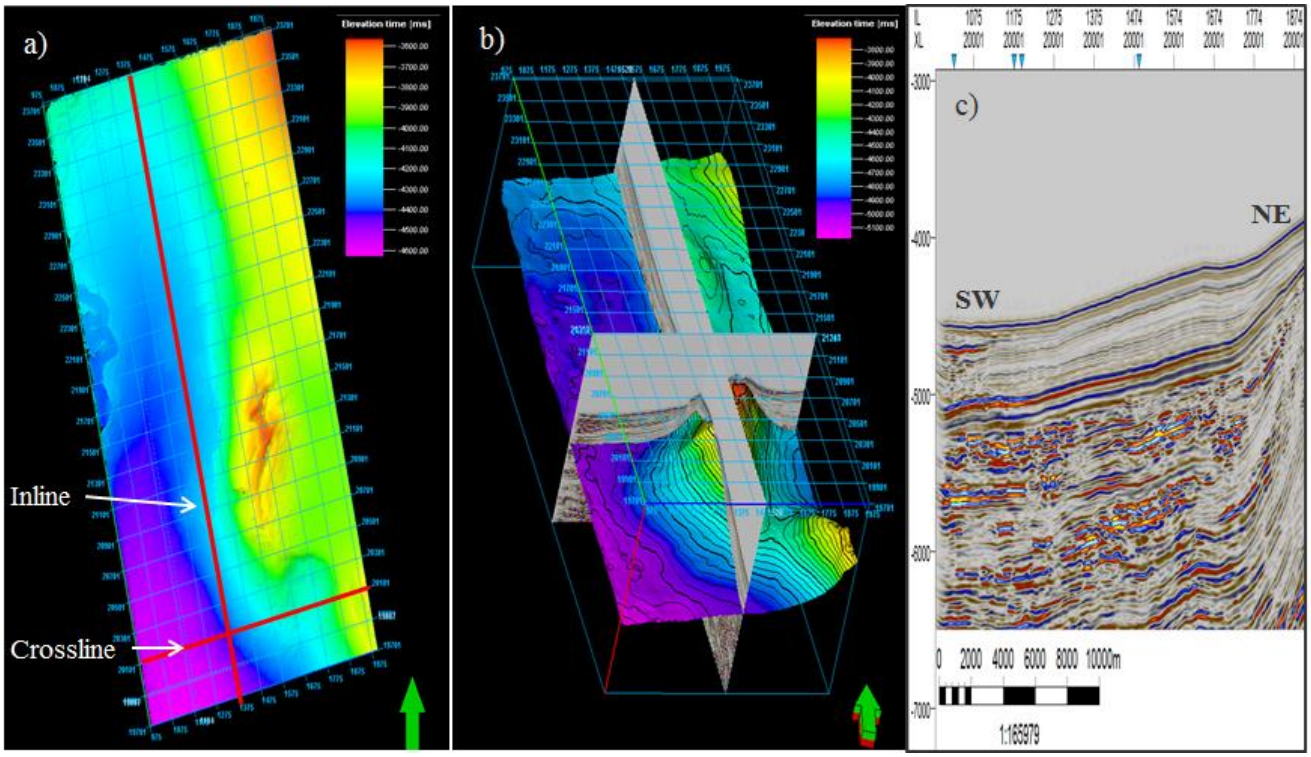

Figure 4.1 shows the windows of Petrel software. a) illustrates 2D window, where the base maps are displayed. b) illustrates 3D window, where the surface and attribute maps are displayed and visualized. c) illustrates the interpretation window, where the reflectors are interpreted.

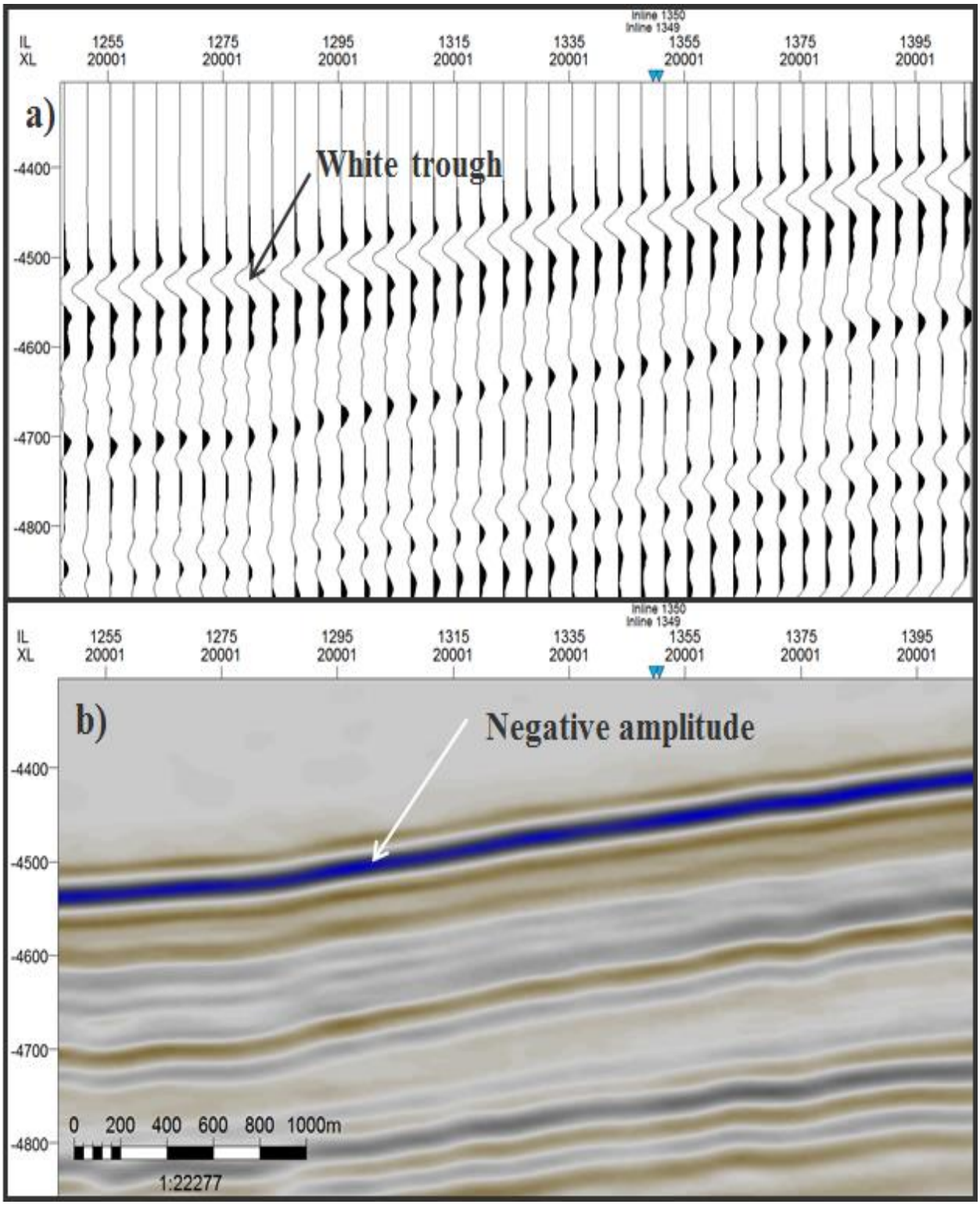

Figure 4.2 illustrates the polarity displayed in this project. a) shows the wiggle trace. b) shows the seismic amplitude display.

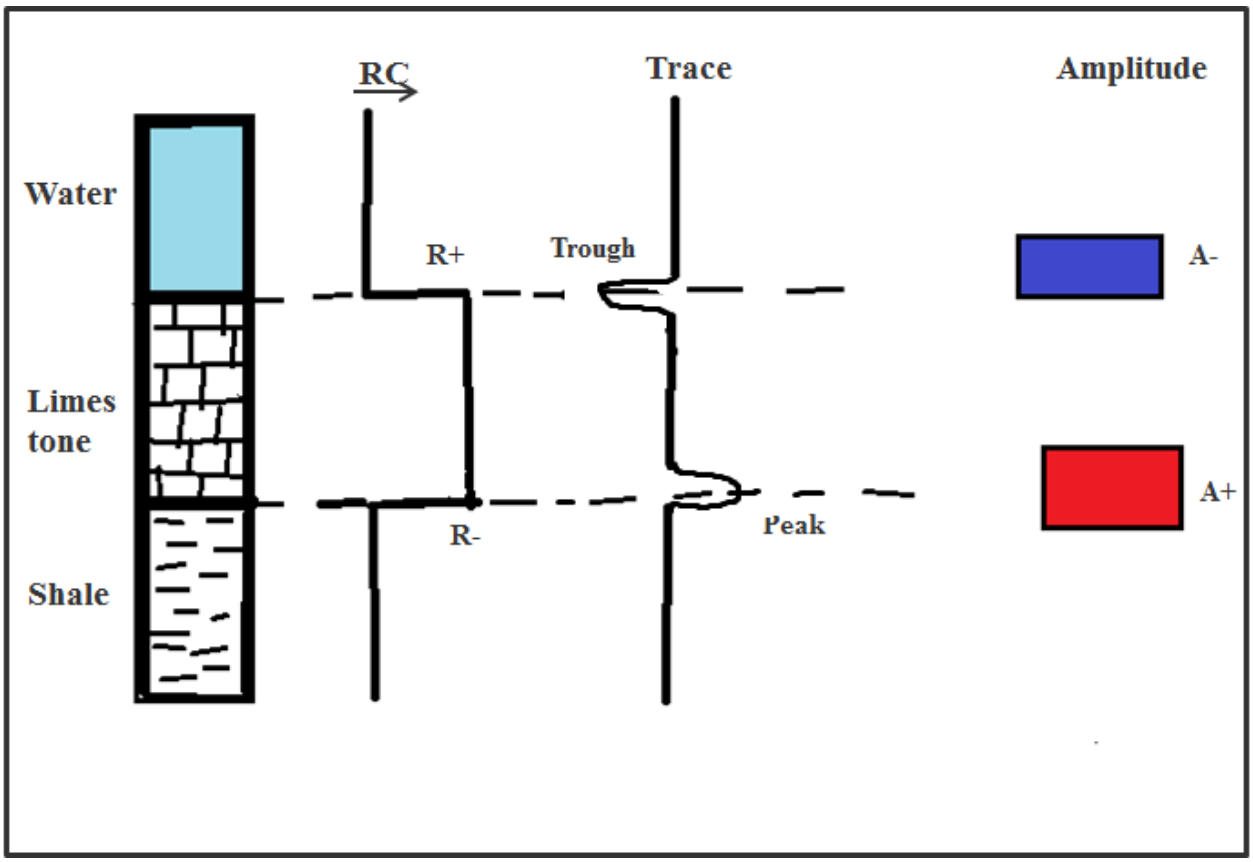

Figure 4.3: shows a sketch of polarity used in the project. Increase in acoustic impedance was interpreted as a trough. It was represented by negative amplitude with blue colour. It corresponds to reverse polarity (used in this project). Decrease in acoustic impedance was interpreted as a peak. It was represented by positive amplitude with red color. It corresponds to normal polarity.

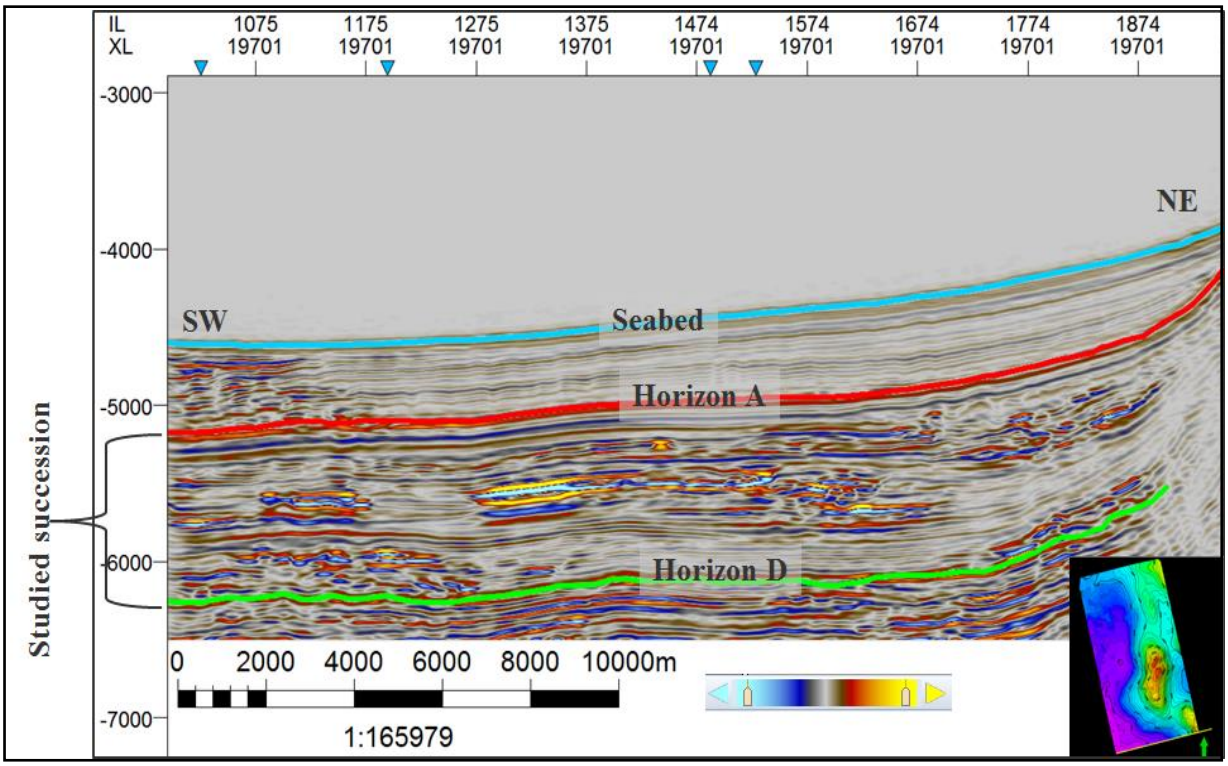

Figure 4.4 Seismic section showing the interpreted interval in this thesis.

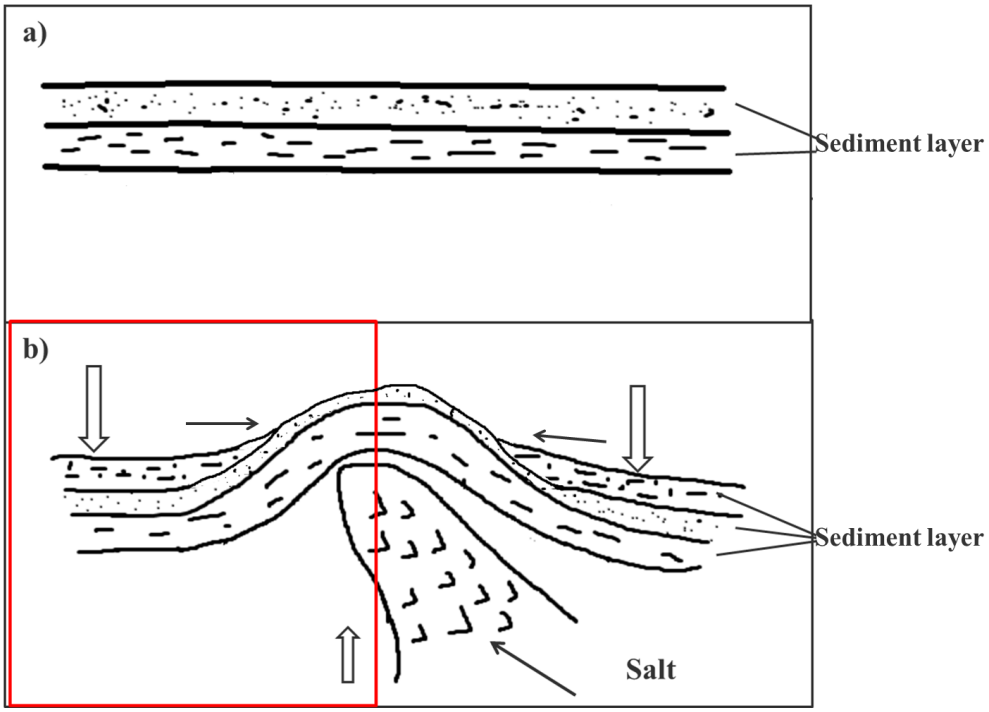

Figure 4.5 Sketch of salt movements. a) Illustrates the initial condition of salt and sediments deposited. b) Illustrate an advanced phase of salt movements. The position of Figure 3 is marked with red square

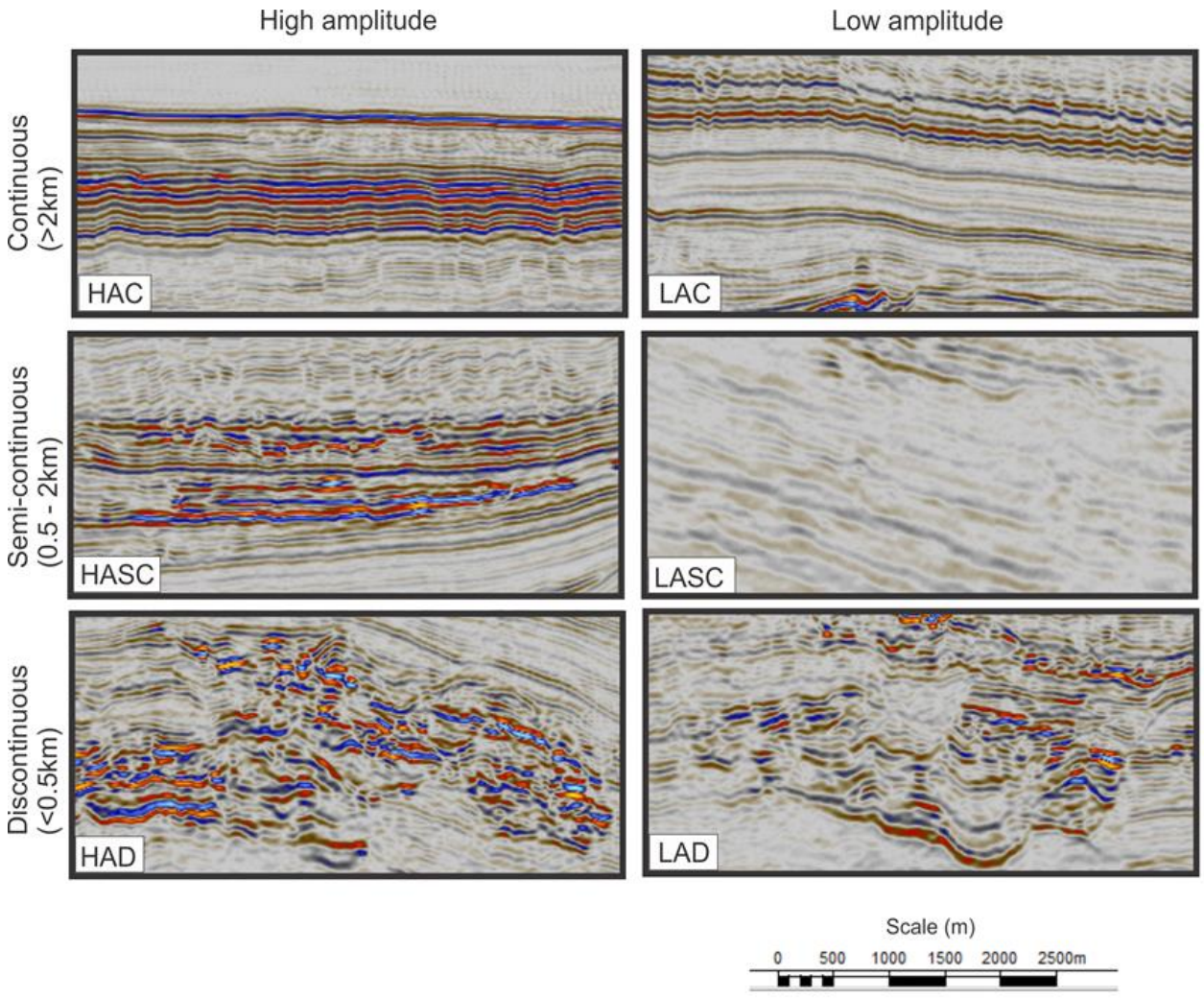

Figure 4.6: shows examples of seismic facies. HCA: High amplitude, LAC: Low amplitude continuous, HASC: High amplitude semi continuous, LASC: Low amplitude semi continuous, HAD: High amplitude discontinuous, LAD: Low amplitude discontinuous.

4.1.1 Surface map extraction

The surface maps were generated from seismic interpretation horizon SB, HA, HB, HC and HD. These maps are represented by contour lines which correspondent to time (TWT). The surface maps were generated in order to see the shape of the horizons and identify some structural and stratigraphic trap / possible hydrocarbon traps. Anticlines are located above salt diapirs.

The maps were also used to quality control for areas where the automatic interpretation had gone wrong. The deep parts are coloured with purple and blue colour. Orange colour show shallow areas.

The SB and HA maps, are continuous seismic horizons. They were easy to interpret through the studies area. A channel in the west was easily identified in the seabed map, as the western part

was more gently dipping. However, the eastern section shows an anticlinal feature, with a four way closures. This area are possible areas where structural and stratigraphic traps could be located alongside the anticlinal features identified with the salt movement (Figure 4.7 a and b).

The HB, HC and HD are discontinuous horizons Figure 4.8a, b and c. They are not interpreted above the anticlines. Due to salt movements, the sedimentation above pushed up and this leads to discontinuity of reflectors. The horizons are therefore not interpreted here. Due to non-interpreted areas, I made some polygons in order to delimitate my interpretation to make these maps.

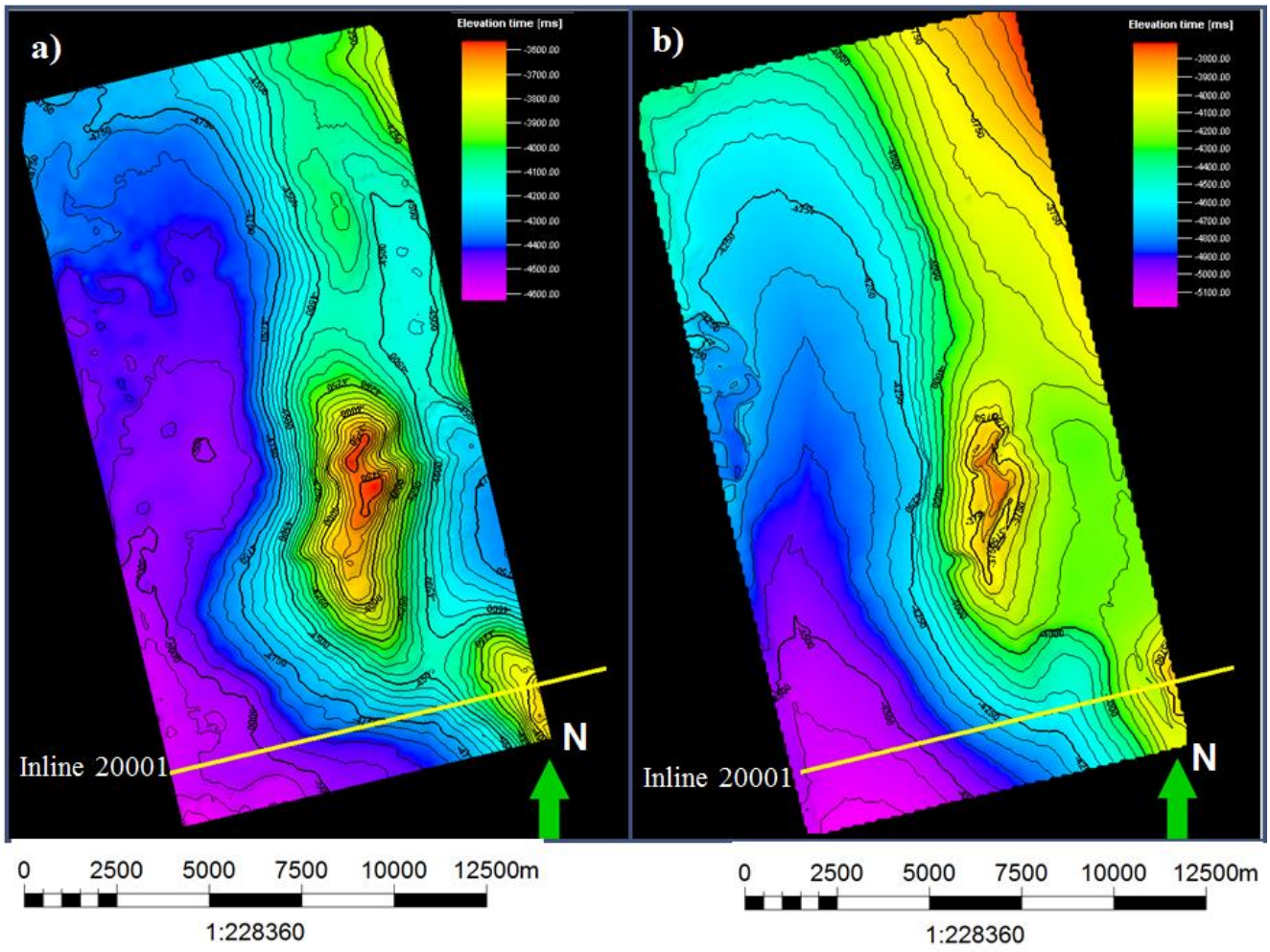

Figure 4.7: Surface maps for horizons interpreted. The yellow line represents the seismic section 20001 shown in Figure 4.4 and Figure 5.2. a) shows the Seabed (SB). b) shows the Horizon A (HA).

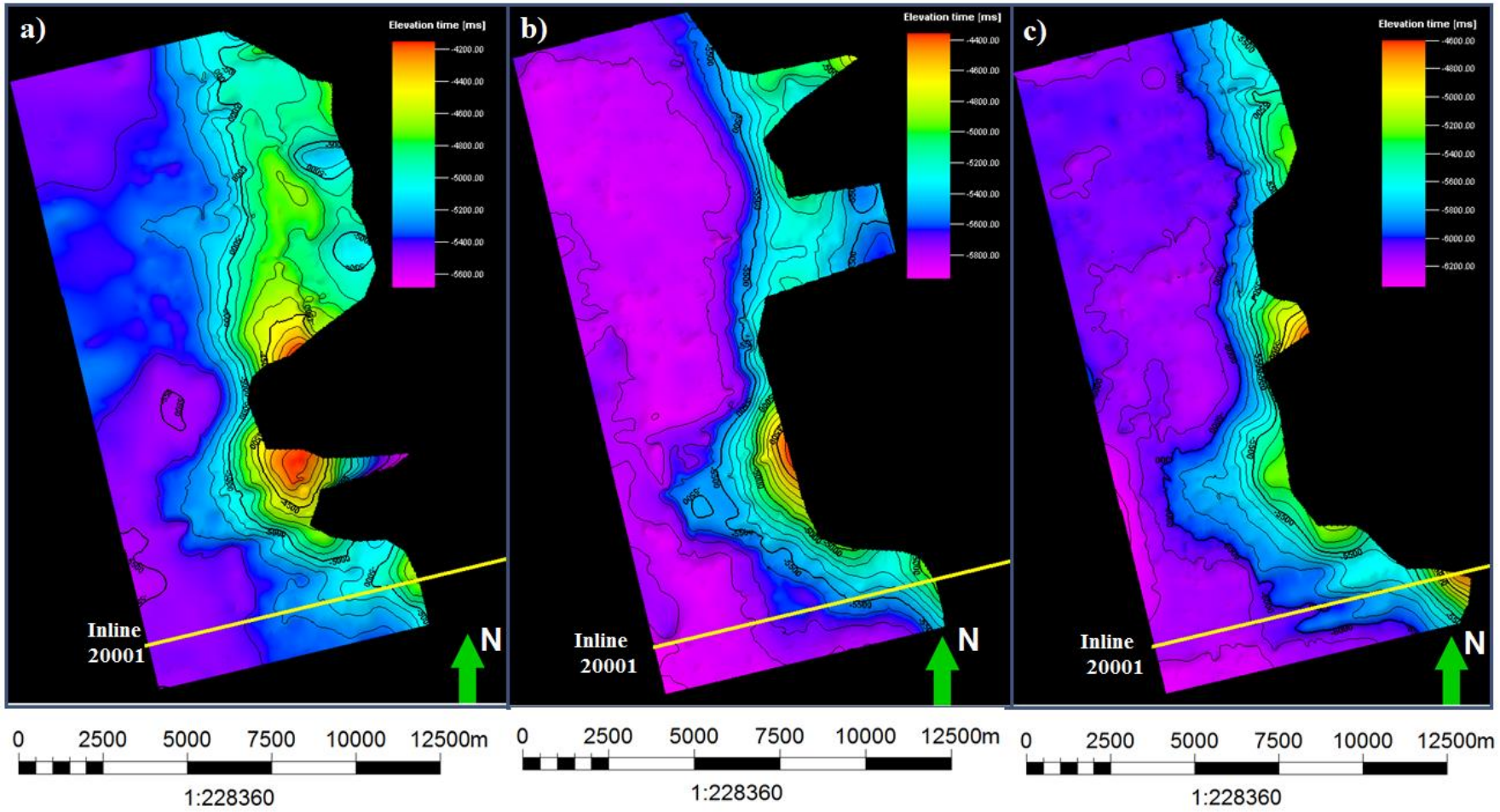

Figure 4.8: Surface maps for interpreted horizons. The yellow line represents the seismic section 20001 shown in Figure 4.4 and Figure 5.2. a) Shows Horizon B (HB). b) shows e Horizon C (HC). c) shows Horizon D (HD).

4.1.2 Isopach maps extraction

An isopach map is a map showing contour lines connecting points of equal formation thickness of a given stratigraphy unit. Isopach maps can help you understand how a rock layer formed, to see how the structure is, and other features such as the size and extent of ore deposits and oil fields.

The isopach map is important for determination of the main tectonic and structural characteristics of a particular type of sediment accumulation or basin. This implies that the shape of a basin, the position of the shoreline, areas of uplift, and under some circumstances the amount of vertical uplift and erosion can be recognized by mapping the variations in thickness of a given stratigraphic interval (Bishop, 1960).

In this project, three isopach maps were generated, between interpreted horizons. The thin layers are coloured with purple and blue colour. Orange colour show thick layers (Figure 4.9).

My maps display thickness variation that can be explained by salt movements. The non-interpreted part represents the uplift area. Here the layers are confined by salt dome and consequently tend to be thin due to the movement of salt.

The yellow lines represent the seismic sectional lines as represented in Figure 4.10a, b and c. Figure 4.10 is an example to show how the thickness varies between the horizons units, which is also a reflection of the thickness variation as shown in the isopach map (Figure 4.9).

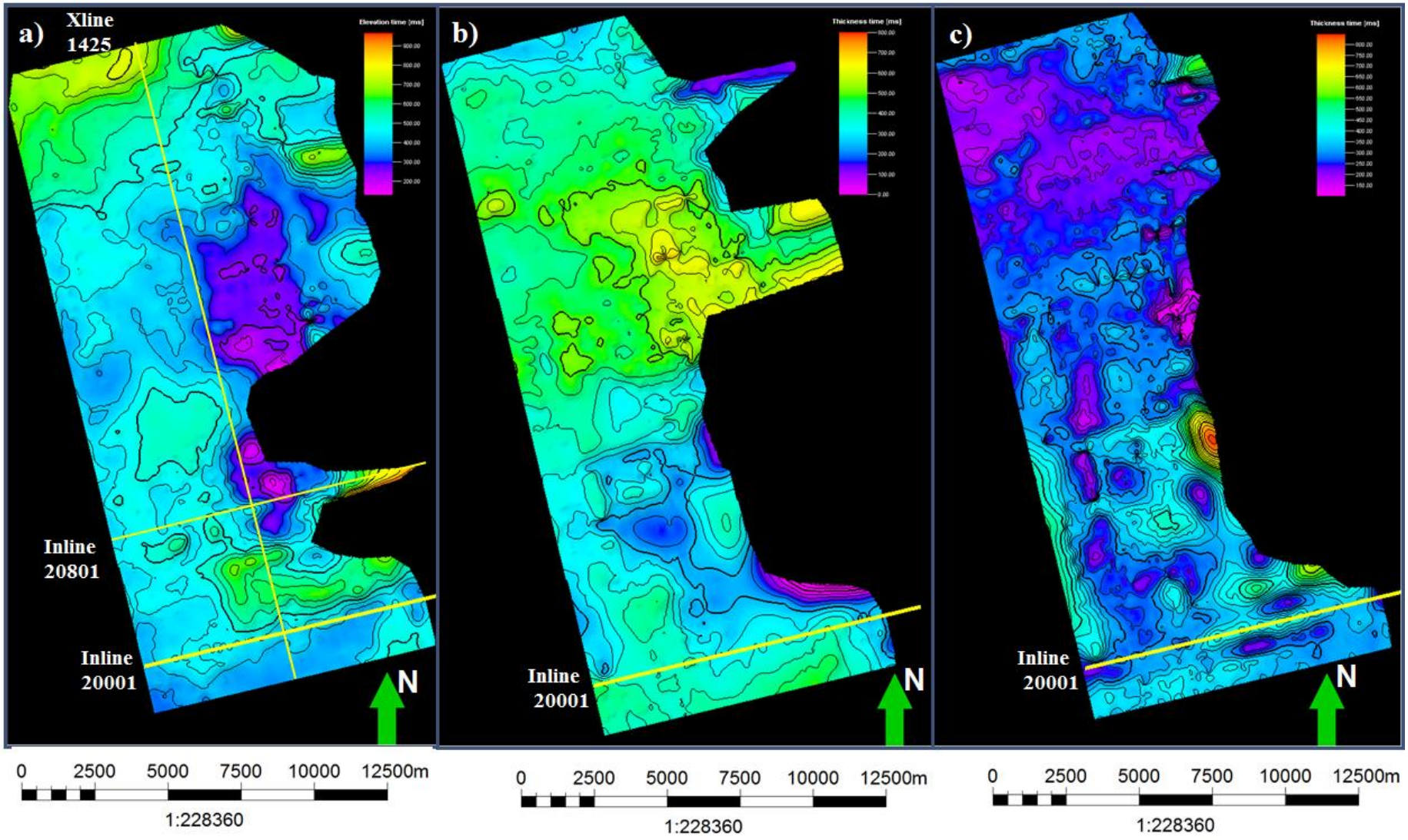

Figure 4.9: Illustrates isopach maps between interpreted horizons. The yellow lines represent the seismic section shown in figure Figure 4.10 a, b and c. a) represent the isopach between HB and HA (unit III). b) represent the isopach between HC and HB (unit II). c) represent the isopach between HD and HC (unit I).

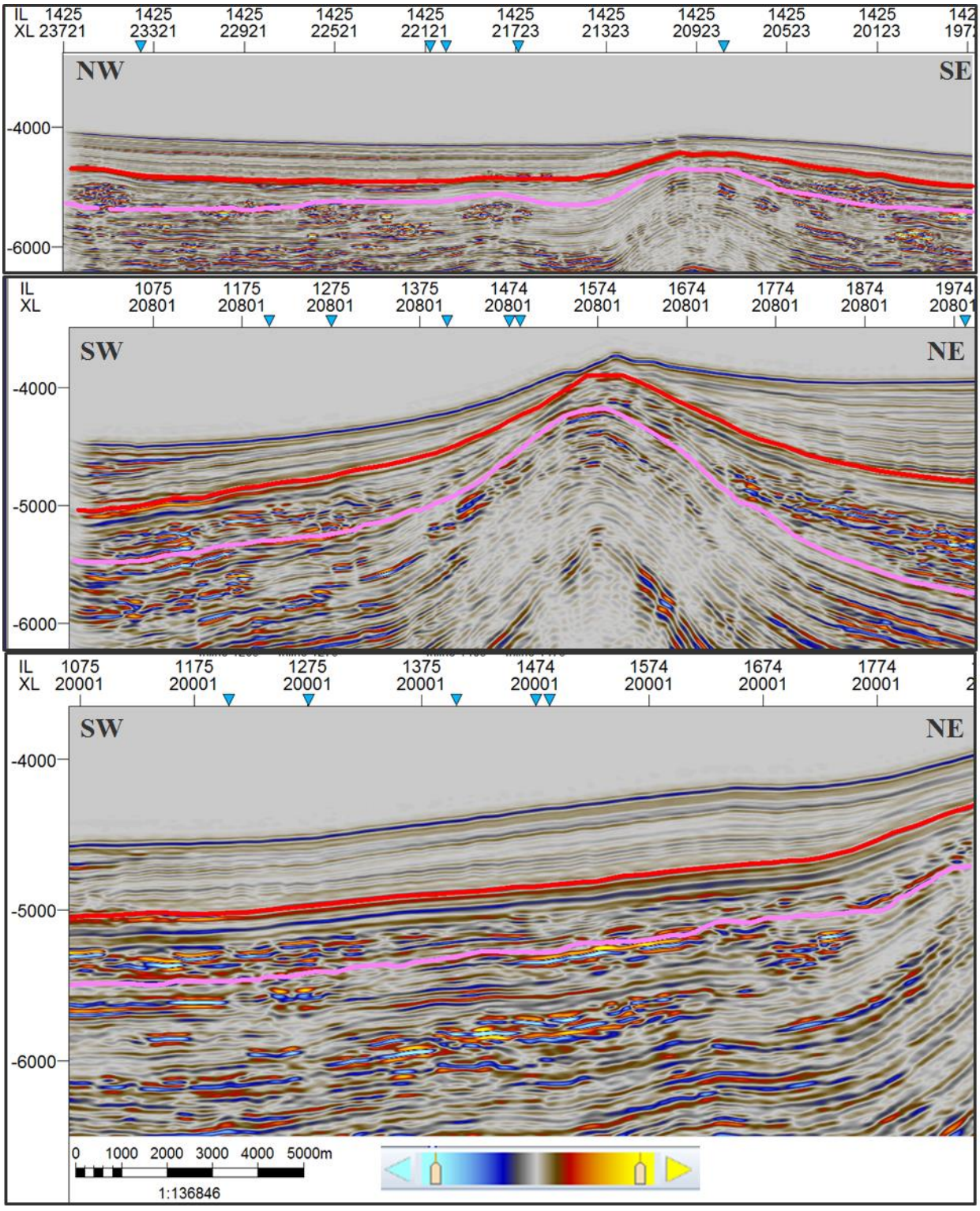

Figure 4.10: Cross section correspondent to yellow line in Isopach map seen in Figure 4.9.

4.1.3 RMS Attribute map extraction

Seismic attributes are obtained from seismic data. The study and interpretation of seismic attribute gives some qualitative information of the geometry and physical parameters of the subsurface (Taner, 2001).

The principal objective of the attributes are to provide accurate and detailed information to the interpreter on structural, stratigraphic, and lithological parameters of the seismic prospect (Taner, 2001). A seismic attribute map displays the amplitude values along an interpreted seismic horizon.

In this project, the attribute maps were extracted to analyze submarine channel architectures, geomorphologies and the sinuosity (Figure 4.14) and (Figure 4.15). I made three types of maps: i) RMS of seismic amplitude (Figure 4.16a), ii) RMS of variance (Figure 4.16b) and iii) Blended amplitude and variance (Figure 4.16c), which was combined with the RMS of seismic amplitude and variance.

I extracted several attribute maps for different times, within my interval of interpretation (Figure 4.4) in order to visualize the sinuosity of channels. To give a reference time interpretation of each of the attribute maps, interpreted horizons were used as key reference markers in Petrel. The best interval selected to extract the attribute map, in order to describe the channels within the units is showing in Figure 4.11, Figure 4.12 and Figure 4.13.

Figure 4.17 shows an example of amplitude maps in different time, within unit II. In 40ms, the channels were not well developed. In 60ms the channels were developed, was easier to follow the channels. In 90ms the channels were developed but the amplitude were too strong, and was difficult to interpret it.

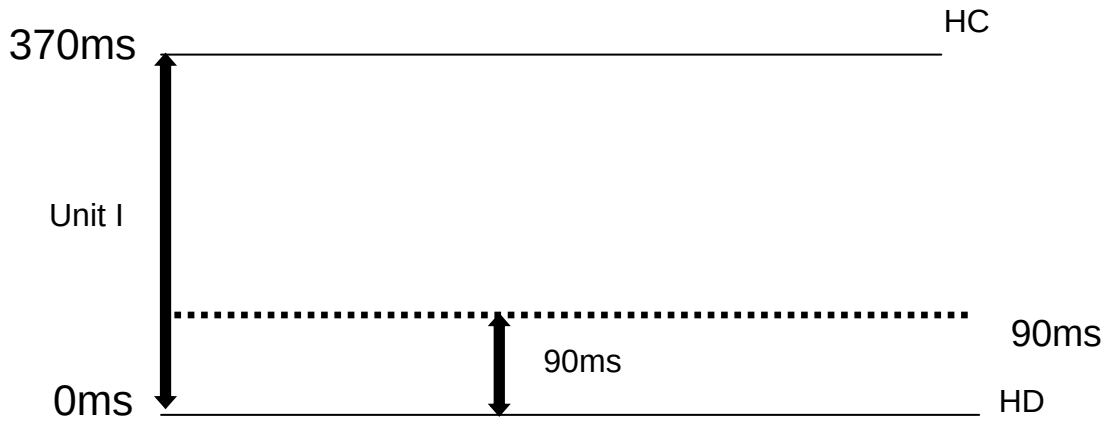

Figure 4.11: Sketch showing the best interval selected to extract the attribute map within unit I. The best interval was 90ms. To define the time, horizons D was used as reference. From Horizon D, I added 90ms up compared to the top interval and Horizon D is the base interval.

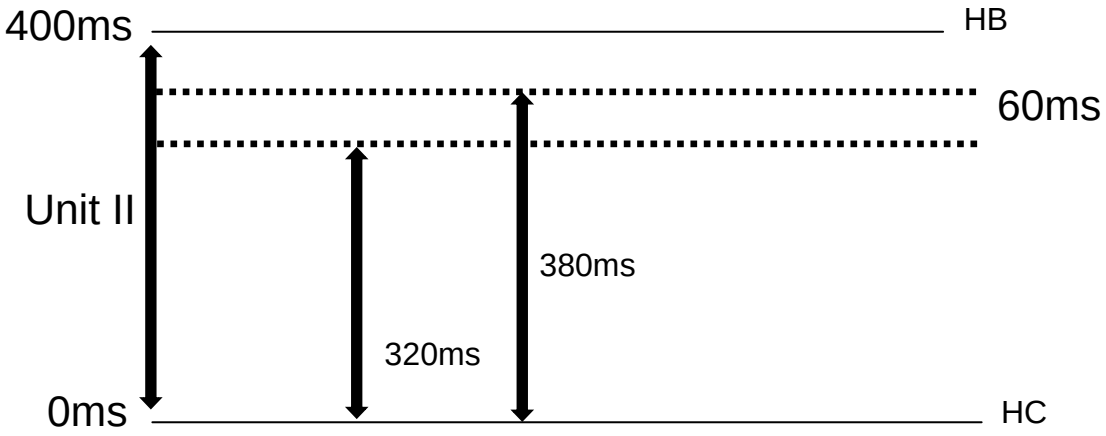

Figure 4.12: Sketch showing the best interval selected to extract the attribute map within unit II. The best interval was 60ms. To define the time, horizon C was used as reference. From Horizon C, I added 380ms above considering to the top interval and 320ms as base interval.

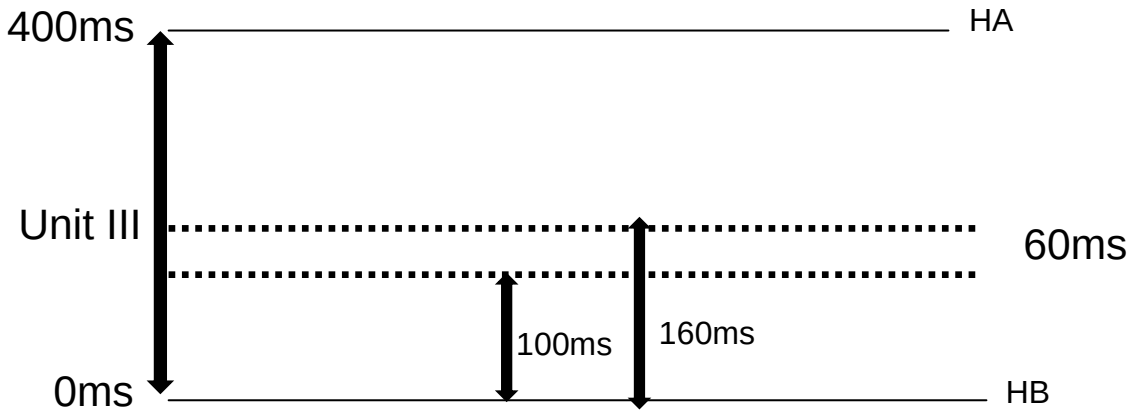

Figure 4.13: Sketch showing the best interval selected to extract the attribute map within unit III. The best interval was 60ms. To define the time, horizon B was used as reference. From Horizon B, I added 160 ms above considering to the top interval and 100ms as base interval.

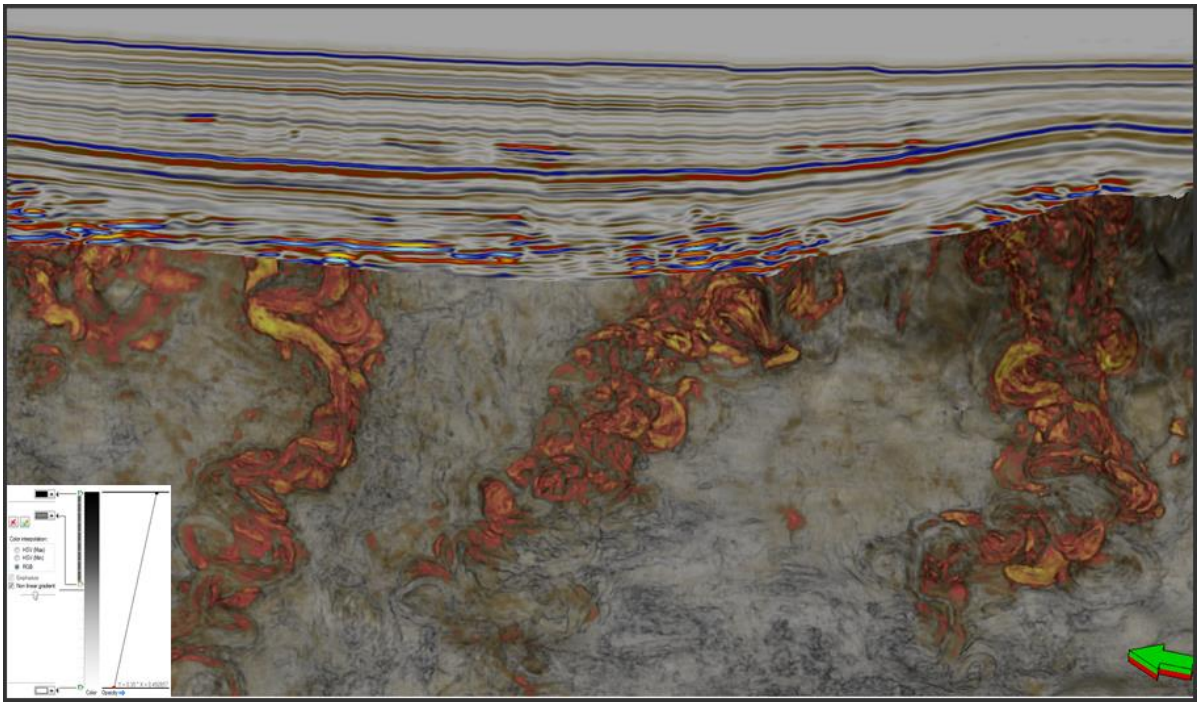

Figure 4.14: Combination of seismic section inline 1502 with attribute seismic of 60ms within unit II

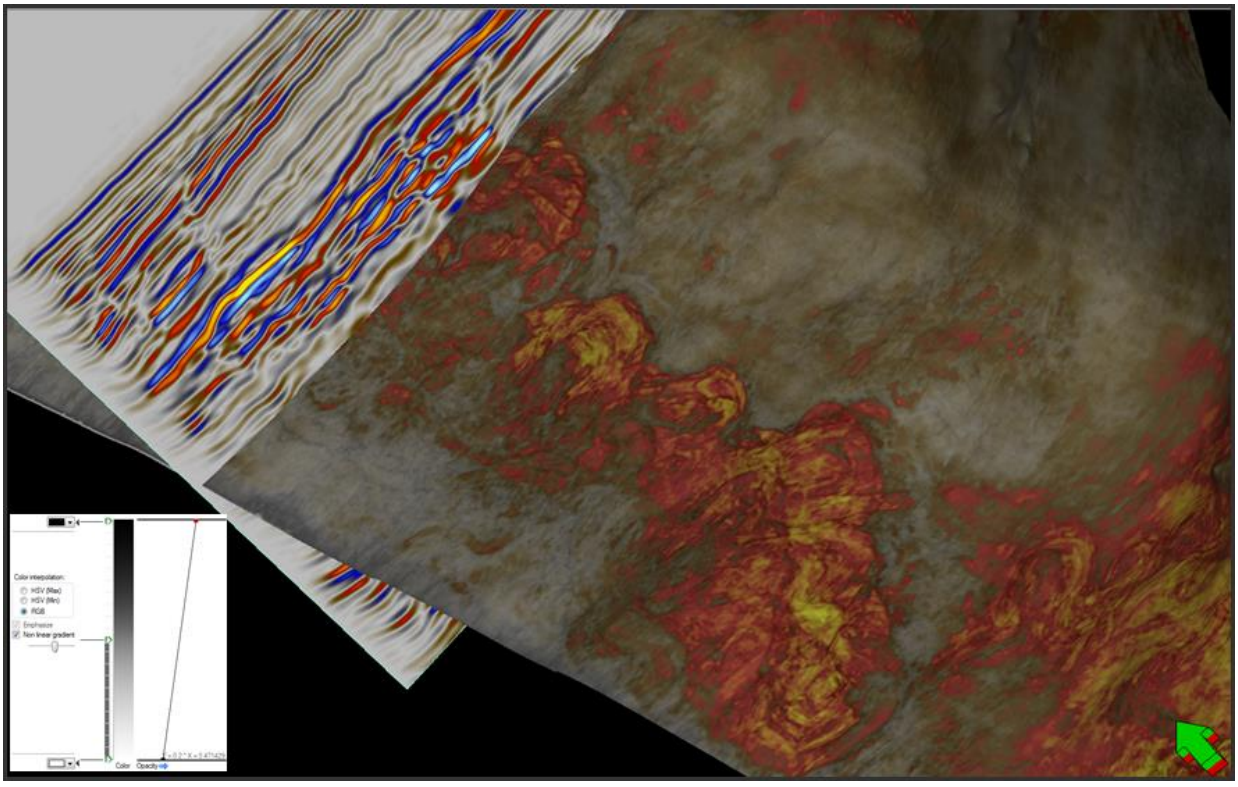

Figure 4.15: Combination of seismic section Xline 22655 with atrtribute seismic of 60ms within unit III.

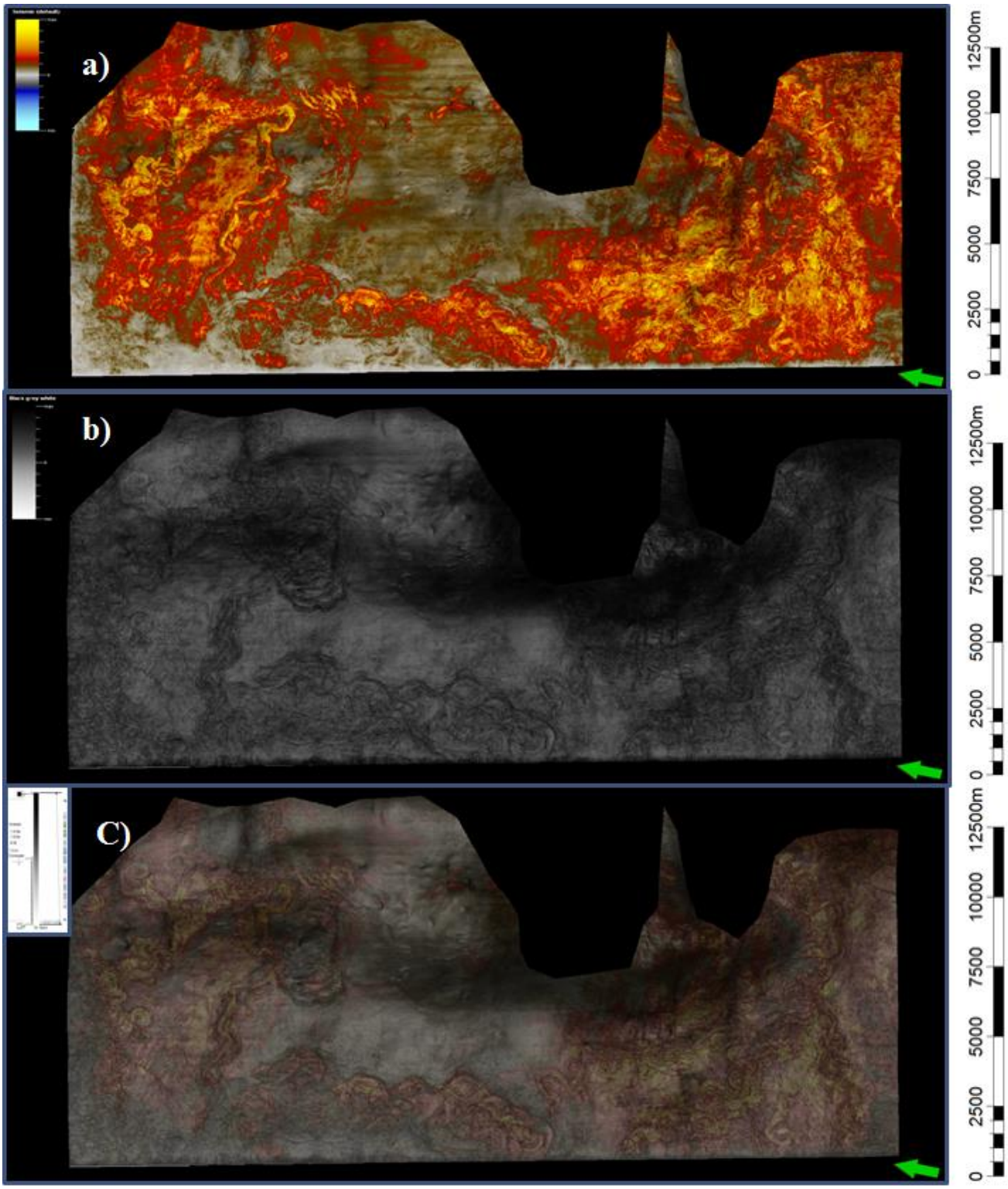

Figure 4.16: Illustrates the attribute seismic corresponding to unit III, 60ms. a) represents the RMS amplitude map. b) represent the RMS variance map. c) represents the blended amplitude and variance map

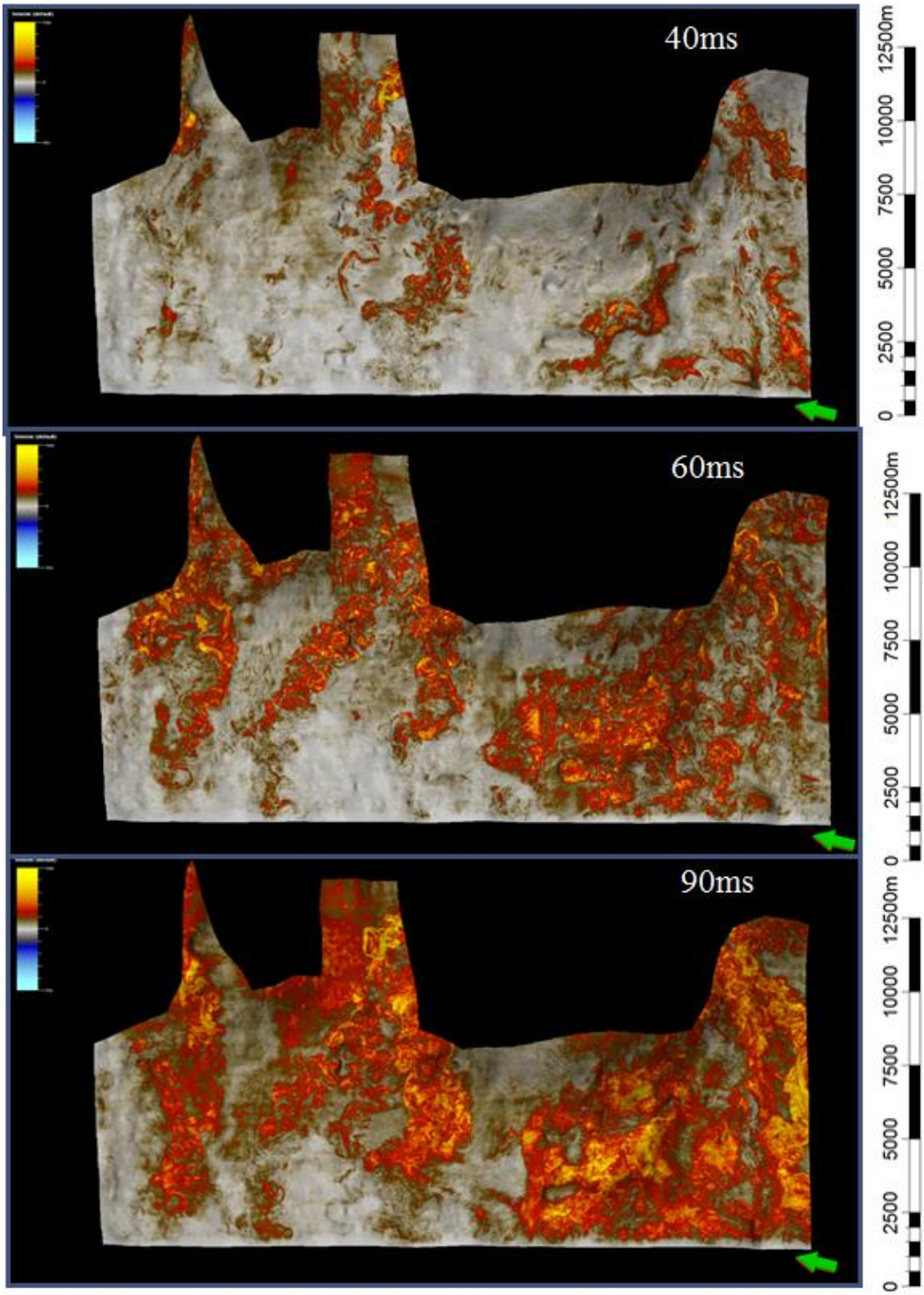

Figure 4.17: Example of amplitude maps extracted with different time intervals (40,60 and 90 ms), within the unit II.

4.1.4 Time slice extraction of flattened cube

According to Schlumberger glossary seismic time slice (with non-flattened cube) is a map view of 3D seismic data, having a certain arrival time. A time slice is a quick, convenient way to evaluate changes in amplitude of seismic data.

I used the time slice, to visualize the deep–marine channels and strike through time to understand the channels evolution trough time, space and directions.

The time slice was extracted between my interval interpretation chosen (Figure 4.4). It was flattened at Horizon A (HA) to Horizon B (HB). The flattening time was done to avoid cutting the geology. The geology evolution and the features in the interval were well expressed on time slices of the flattened cubes.

Figure 4.18 shows the time slice map flattened at HA. The bright color represents very strong amplitude, which is interpreted as uplift area. The light color represents low amplitude. The map displays evidence of salt diapiric growth influence, channels distribution coming from the north, and slump features. Figure 4.19 shows time slice map flattened at HA, which is intercepted by inline 1371. It also reveals more about the nature of the channels when both the seismic section and time slices are combined. Also others feature like faults are picked out using this combined display.

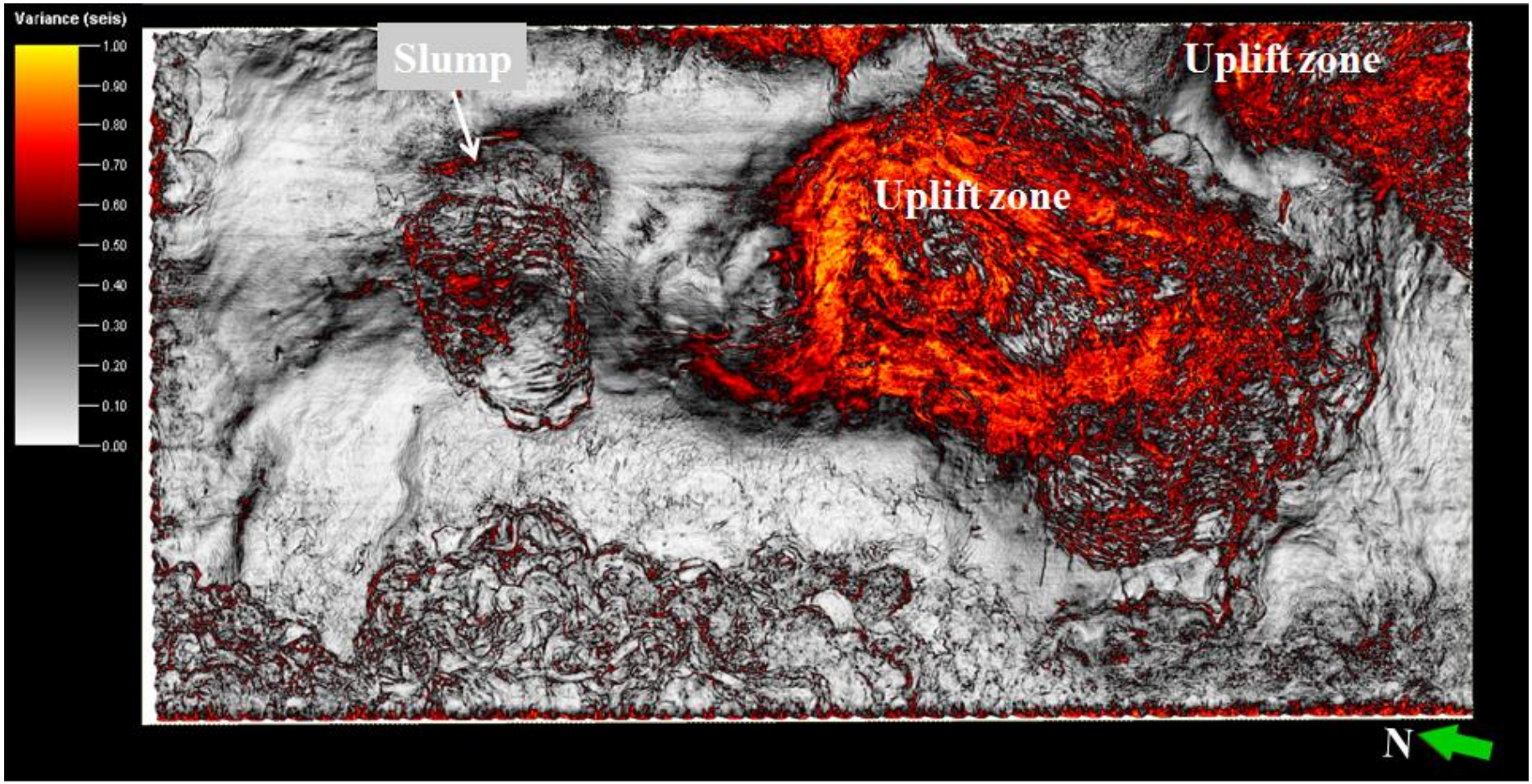

Figure 4.18: Time slice map flattened at horizon A (HA). It shows an uplifted area with high amplitude and a slump. The channels are coming from the north.

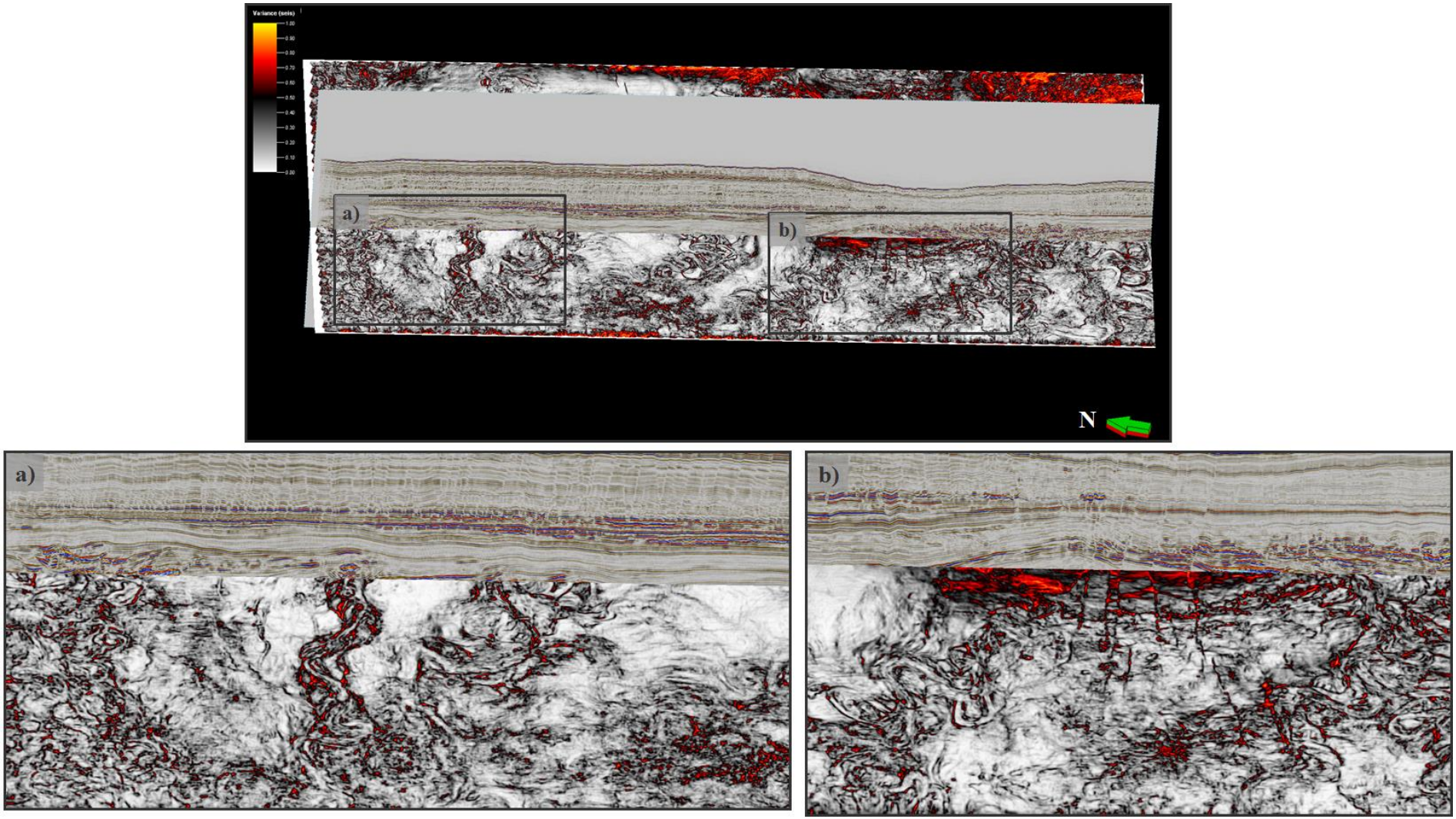

Figure 4.19: Time slice map at flattened horizon (HA) intersected by a seismic section corresponding to inline 1371. a) close-up of the channels shown in the seimic section combined by the time slice. b) close-up of the faults shown in the seismic section combined by the time slice.

Chapter 5 : Seismic evaluation of stratigraphic units and characterizations of features

I have identified three stratigraphic units (Figure 5.2 and Figure 5.3). The seismic units are bounded by the horizons interpreted. Their seismic facies, thickness variation, spatial reflection patterns is also described and interpreted.

5.1 Unit I (UI)

5.1.1 Description

UI is bounded by Horizon D (HD) at the base and Horizon C (HC) at the top (Figure 5.2 and Figure 5.3). These horizons (HD and HC) were difficult to interpret, as the reflectors were discontinuous on some seismic lines, due to influence of salt movements and the presence of incised channels in the area.

HD is the lowest interpreted horizon. It was interpreted on a trough with positive acoustic impedance. The amplitude varies from low to high. It consists of gently dipping continuous seismic reflection. The topography shows large local elevation variation due to salt movements. I did not interpreted horizon D in the east where the dips are large (Figure 4.8 c).

HC was interpreted on troughs with positive acoustic impedance. The amplitude is low. HC consists of continuous seismic reflection but the dips are lower than HD. It is only interpreted in parts of the 3D survey and not in the east where the dips are high (Figure 4.8 b).

The UI is the oldest unit. The reflectors internally are discontinuous to transparent low amplitude reflections in some of the seismic sections. The isopach of this unit suggest that it is relatively constant in the western sections of the seismic inlines (Figure 5.3) but it thins out within the section to the east in areas of salt diapirs. It is identified that the main features of interest within this unit internally is the chaotic discontinuous reflections of the channel reflections which is identified in both inline and crossline seismic within this interval (Figure 5.2 and Figure 5.3). The inline section suggest that the channels are more confined in the eastern part and unconfined in the west, with the channel development cutting across this unit into other interpreted units of the seismic section.

Also, the unit description is based on attribute maps. Figure 5.4 shows an amplitude map within this unit of 90ms, based on surface Horizon D (Figure 5.4 a). To define the time, I added 90ms up from horizon D and it was also considering as base interval. This is intentionally done to pick out areas of channelized reflections within the unit. The map shows variation in amplitude. The bright color represents the high amplitude and light color represents the low amplitude (Figure 5.4 a and b).

Finally, the attribute maps show the direction of channel development as mainly from eastern sections of the seismic (Figure 5.4 a and b). The attribute maps, isopach maps and seismic based

interpretation of the units together tells much of the unit development to horizon positions, structures and reflections characteristics, which would be further developed in subsequent chapters of characterizing the main channelized features.

5.1.2 Interpretation

The channels identified in Unit I are interpreted as confined and weekly confined channel systems. The channels have a stronger mounded boundary or levee ridges that confines the main channel flow axis (Figure 5.4 b). The channels are striking E-W in the attribute maps which are in the main flow direction of the channel. The E-W striking channels are complex with laterally stack migration of the channels and corresponding vertical stack of channelized successions as observed with several time sliced of the main channel b1. The channels are interpreted to contain sand with the channel axis and interpreted point bars, with amplitude contrast of shale to sand intervals identified within the channel axis (Figure 5.6).

These reservoirs channels are moderate to high net gross as commonly identified with high sinuosity channels (Chapter 3) and the amplitude profile of the sands within the aggraded channel axis. According to the sinuosity calculation, the channels described in this unit are interpreted as meander channel with sinuosity index greater than 1.5 (Chapter 5).

The channel b1 is highly sinuous with flat strong amplitude reflection areas identified as floodplains. They are more confined in the eastern part and unconfined in the west. The accreted sediments in the inner bends of the channel are interpreted as point bar, which has mostly strong positive amplitude reflections within parts of the channels, this also suggest area of interest as the channels since the ‘lithologic ‘reflections are similar to the channel axis. The sediments in the outer parts of the channel are interpreted as crevasse splay deposits, with ‘strong positive amplitude reflections’, this might have resulted to period of higher sediment influxes that overflood the channel and shedding sediment within adjacent areas of the channel axis.

The channel b2 is lower sinuous compared to the channel b2. The channel and valley side are almost the same. They can have also any sediment incise them, but has more coarse sand than channel b1 as seen with the ‘typical sandy strong positive reflections’. The sediments in the outer of this channel are interpreted as crevasse splay. The strong positive amplitude showing in Figure 5.4 a and b can be interpreted as sand fill sediments while, the low amplitude can be fine grained materials.

5.2 Unit II (UII)

5.2.1 Description

The UII is bounded by Horizon C (HC) in the base and Horizon B (HB) in the top (Figure 5.2 and Figure 5.3). These horizons (HC and HB) were also discontinuous and challenging to interpret. Salt movements and the presence of incised channel is the main reason for the discontinuous reflection in that area.

The HB was interpreted on troughs with positive acoustic impedance. The amplitudes vary from low to high. On seismic section it appears as discontinuous seismic reflection with gently dipping. The topography shows large local elevation variation due to salt movements. I did not interpreted horizon D in the east where the dips are large (Figure 4.8 a).

Unit II is the second oldest unit. Internally, this unit consists of discontinuous and low amplitude reflection. The isopach of this unit suggest that it is relatively constant in the western sections of the seismic inlines (Figure 5.2) but it thins out within section due east in areas of salt diapirs. The inline and cross section, suggest that the channels development is cutting across this unit into other interpreted units of the seismic section (Figure 5.2 and Figure 5.3).

The unit description is also based on attribute maps. Figure 5.7 shows an amplitude map within this unit of 60ms, based on surface Horizon C (Figure 5.7 a). To define the time, I added 380ms up considering the top interval and 320ms as base interval. This is intentionally done to pick out areas of channelized reflections within the unit. The map shows variation of amplitude. The redish color represents the high amplitude and bluish color represents the low amplitude (Figure 5.7 a and b). Finally, the attribute maps show the direction of channel development as mainly from eastern (Figure 5.7 a and b).

5.2.2 Interpretation

Unit II is interpreted as unconfined deep marine channel system. The strike of the channels is between E-W showed in the attribute maps which are in the main flow direction of the channel. The channels are complex with laterally stack migration as observed with several time sliced of the main channel described in this unit.

The channels are interpreted to contain sand with amplitude contrast of shale to sand intervals identified within the channel axis. (Figure 5.9). These reservoirs channels are high net gross (Chapter 3) as commonly identified with low sinuosity channels and the amplitude profile of the sands within the aggraded channel axis. According to the sinuosity calculation, the channels b1 and b2 are interpreted as sinuous channels. They are less than 1.5.while channel b3 is interpreted as meander channel. It is higher than 1.5 (Chapter 5).

The channel b1 and b2 (Figure 5.7) is lower sinuous comparing to the channel b3. They can have any sediment incise them, but has more sand than channel b3 as seen with the ‘typical sandy strong positive reflections’. The sediments in the outer parts of the channel are interpreted as crevasse splay deposits, with ‘strong positive amplitude reflections’, this might have resulted to period of higher sediment influxes that over flood the channel and shedding sediment within adjacent areas of the channel axis.

The channel b3 is highly sinuous. They can have any sediment incise them, but sands are typically in this channel. They can have also any sediment incise them, but has less coarse sand than channel b1and b3. The sediments in the outer of this channel are interpreted as crevasse

splay. The red amplitude showing in Figure 5.7 a and b can be interpreted as sand fill sediments while, the low amplitude can be fine grained materials.

5.3 Unit III (UIII)

5.3.1 Description

The unit III is bounded by Horizon A (HA) in the base and Horizon B (HB) in the top (Figure 5.2 and Figure 5.3).

HA is the top of the interpreted interval. It was interpreted on troughs a reflection which corresponds to positive acoustic impedance. The amplitude is high and continuous gently dipping. The topography does not show large elevation variation. It was possible to interpret all the area (Figure 4.7 b).

Unit III is the youngest unit. The unit consist in continuous, medium to high amplitude reflection. It is identified that the main features of interest within this unit internally is the chaotic continuous reflections of the channel reflections which is identified in both inline and crossline seismic within this interval (Figure 5.2 and Figure 5.3). The isopach of this unit suggest that it is relatively constant in the western sections of the seismic inlines (Figure 5.3) but it thins out within section due east in areas of salt diapirs.

The unit description is based on attribute maps. Figure 5.10 shows an amplitude map for 60ms, based on the surface of Horizon B (Figure 5.10a). To define the time, I add 160ms up considering the top interval and 100ms as base interval. This is intentionally done to pick out areas of channelized reflections within the unit. The map images the variation of reflection amplitudes. The bright color represents the high amplitude and the light color represents low amplitude (Figure 5.10 a and b). It is more confined in the northern part and unconfined in west. Finally, the attribute maps show the direction of channel development as mainly from north (Figure 5.10 a and b).

5.3.2 Interpretation

Unit III is interpreted as confined and weekly confined channel system. The channels have a stronger mounded boundary or levee ridges that confines the main channel flow axis. The channels are striking N-W showing in the attribute maps which are in the main flow direction of the channel. The N-W striking channels are complex with vertically stack aggradation as observed with several time sliced of the main channel. The channels are interpreted to contain sand, with amplitude contrast of shale to sand intervals identified within the channel axis (Figure 5.12). These reservoirs channels are moderate to high net gross (Chapter 3) as commonly identified with high sinuosity channels and the amplitude profile of the sands within the aggraded channel axis.

The main channel described in this unit is highly sinuous with floodplains many times. They can have any sediment incise them, but clays and fine sands are typically in this channel. The sediments in the outer parts of the channel are interpreted as overbank deposits, with 'strong positive to light amplitude colour reflections'.

The high amplitude displayed in map (Figure 5.10 a) can be interpreted as sand fill sediments deposited. The low amplitude as overbank deposits. The confined part can be interpreted as low net gross comparing to unconfined part.

5.4 Sinuosity channel measurement

The sinuosity ratio is the distance measured along the channel divided by the straight line distance between the two points (Figure 5.1). This methodology was used to calculate the sinuosity of the channels described within the units.

According to previous studies, the sinuosity value ranges from 1 to 4 (Leopold et al., 1964). The straight line channels have a sinuosity value of 1. The channels less or approximate of 1.5 are considered as low sinuosity. The channels higher than 1.5 are considered as high sinuosity (Leopold et al., 1964).

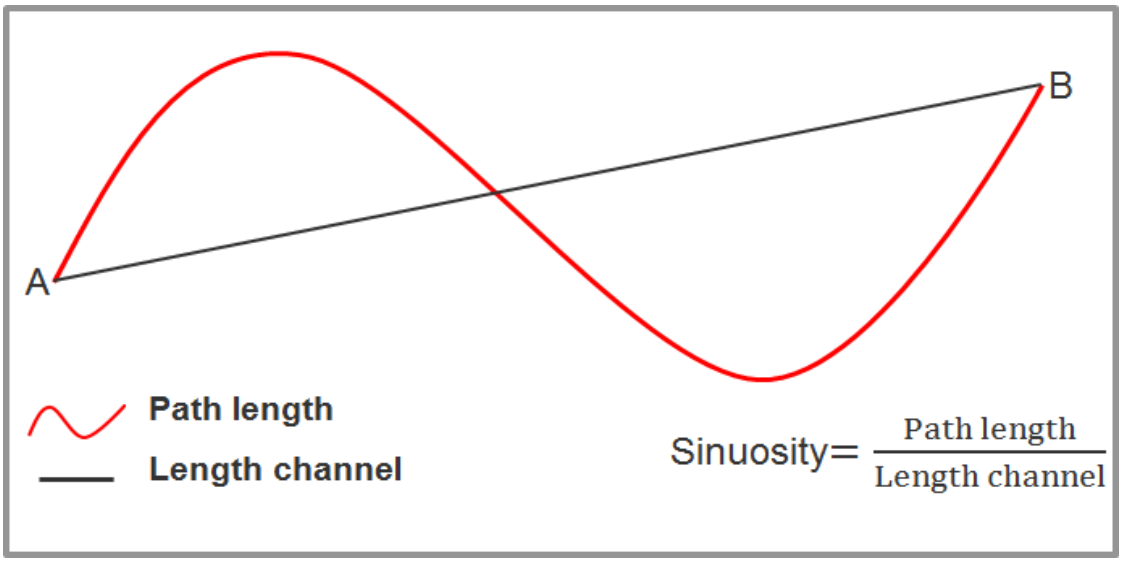

Figure 5.1: Definition of sinuosity

According to the sinuosity definition (Figure 5.1), I have calculated the sinuosity of channels described within units defined in this project. To make this calculation, I have used petrel software. First I made a polygon, in order to measure the path length. Then I measured the distance from point A to B.

Unit I has identified two main channels. The first channel has a sinuosity of approximately 1.9 (Figure 5.5a). The second channel has a sinuosity of 1.53 (Figure 5.5). According to the sinuosity values ranges, these two channel (Figure 5.5 a and b) are classified as high sinuosity channels.

In the **unit II**, three main channels have been identified. The first channel has sinuosity of approximately 1.4 (Figure 5.8 a). The second channel has sinuosity of 1.2 (Figure 5.8 b). The third channel is approximately of sinuosity 1.7 (Figure 5.8 c). According to the sinuosity values ranges, channel 1 and 2 (Figure 5.8 a and b) are classified as low sinuosity channels and channel 3 is classified as high sinuosity (Figure 5.8 c).

Unit III has one identified channel. The sinuosity is approximately 1.7 (Figure 5.11). According to the sinuosity values ranges, this channel (Figure 5.11) is classified as high sinuosity channel.

5.5 Seismic facies analysis of the channels in the units

5.5.1 Channels in seismic Unit I

It was discussed previously that the main channel of sections b1 and b2 in the eastern section of the seismic survey area, was mainly identified in this unit with lateral extensions of the channel broken as a result of salt halokinesis (Figure 5.3). It was also previously observed that the channel extension was more laterally extensive within this unit as it developed to the western sections of the seismic sections. Furthermore, using the attribute maps the geologic sub facies of the channel systems was described ranging from channel axis, levee, crevasse splay, point bars and flood plain deposits. It is important to confine this interpretation to the seismic reflections in terms of amplitude reflections and cross sections in other to characterize this channels on seismic, identify facies unit and analyze net to gross units of the channelized reflections.

Taking a cross section of the main channels b1 and b2 in this unit, main seismic facies were identified in Figure 5.6 namely channel axis – point bar reflections in cross sections AA', BB', CC' and DD'. Channel levee to axis in section EE', FF' and finally channelized axis of GG' and HH'.

The first cross section of channelized axis to point bar reflections has juxtaposed reflections of low amplitude with high amplitude patch reflections that are linearly sandwiched with the low brighter amplitudes. The seismic boundary is concave down-shaped feature on the base and on the top. It is represented by continuous, variable dipping and high amplitude reflections at the base and in the top. This suggests that the internal facies are amalgamated channel subfacies that are vertically stacked with a lateral migration of channel axis to point bar accretion centres with the strike direction of sediment flow. The higher amplitude areas are much suggestive of sands reflections in the channel (Figure 5.6 AA', BB', CC' and DD').

Secondly, cross section of channel levee to Channel axis in Figure 5.6 EE' and FF', also suggest a juxtaposed reflections of low amplitude with high amplitude patch reflections that are linearly sandwiched with the low brighter amplitudes. The difference from the formerly described facies is much in that the signatures are more shingled in geometry, with the amplitude streaks not much lateral when compared. This I interpret also a function of the stacked difference of the

channel migration with facies stacked at different time intervals within each of the complex channelized areas (Figure 5.6 EE' and FF').

The last facies classification is the main channelized reflections of cross section GG' and HH' shown in Figure 5.6. It is mainly known to have more of lighter amplitude reflections with little streaks higher amplitudes observed. This section suggests more sandy reflections when compared to the previous earlier described facies classification. The reflection is also shingled or ribbon like with clay drapes of other subfacies identified with the channel complex. It must be said that the section showed little faults within part of the reflection, which might be suggestive that the channel facies or deposits have been affected by later salt intrusives. Finally, it can be said that the net gross of this classified facies section and with the first is much higher when compared the second facies class.

5.4.1 Channels in Seismic Unit II

Taking a cross section of the main channels b1, b2 and b3 in this unit, main seismic facies were identified in Figure 5.12namely channel axis – point bar reflections in cross sections AA' and BB', channel levee to axis in section CC' and DD' and finally channelized axis of EE' and FF'.

The first cross section of channel axis - point bar in reflections (Figure 5.9 AA' and BB') consists of low amplitude reflections and high amplitude patch reflections. The seismic boundary is parallel internal pattern. It is represented by continuous, variable dipping and high amplitude reflections at the base and in the top. This suggests that the internal facies are channel vertically stacked with a lateral migration. The higher amplitude areas are much suggestive of sands reflections in the channel (Figure 5.9 AA' and BB').

The cross section of channel levee to Channel axis in Figure 5.9 CC' and DD', consists of juxtaposed reflections of low amplitude reflections and high amplitude patch reflections. This I interpret also a function of the stacked difference of the channel migration with facies stacked at different time intervals within each of the complex channelized areas. The cross section CC' suggests shale intervals of the levee suspensions, which means that the presence of net gross reduces with this section of the channel complex (Figure 5.9 CC'). While the cross section DD' suggest having higher presence of the net gross.

The last facies classification is the main channelized reflections of cross section EE' and FF'. It consists of low amplitude reflections and high amplitude patch reflections. The section shows little faults within part of the reflection, which might be suggestive that the channel facies have been affected by salt intrusive. This section suggests more sandy reflections when compared to the previous earlier described facies classification. The net gross of this classified facies section and with the first is much higher when compared the second facies class.

5.4.1 Channels in Seismic Unit III

Taking a cross section of the main channel this unit, main seismic facies were identified in Figure 5.12 namely channel axis – overbank-flood plain reflections in cross sections AA'. Channel levee to axis in section BB', CC' and DD'.

The cross section of channel axis to overbank-flood plain in Figure 5.12 AA'. It suggest of low amplitude reflections and high amplitude patch reflections. The seismic boundary is concave up-shaped feature on the base and on the top. It is represented by continuous, variable dipping and low amplitude reflections at the base and in the top. This suggests that the internal facies are vertically stacked with a lateral migration of channel. The higher amplitude areas are much suggestive of sands reflections in the channel. It can suggest that the net gross in this facies is high.

The cross section of channel levee to Channel axis in Figure 5.12 BB', CC' and DD'. It suggest of low amplitude reflections and high amplitude patch reflections. The cross sections suggests shale intervals of the levee suspensions, which means that the presence of net to gross value estimate reduces with this sections of the channel complex.

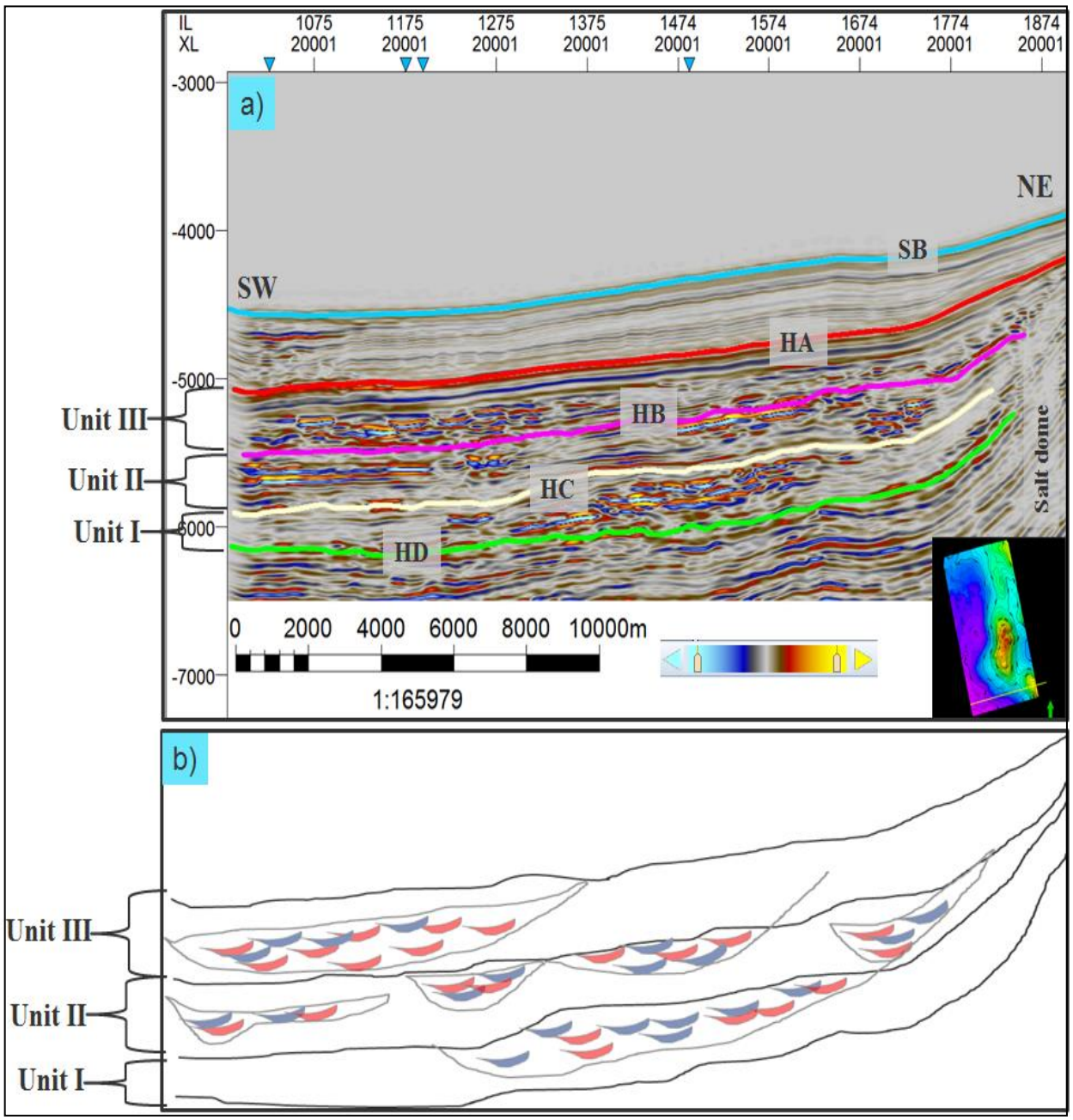

Figure 5.2: Seismic section interpreted and sketch of this seismic. a) cross line showing all interpreted horizons. Seabed (SB), Horizon A (HA), Horizon B (HB) and Horizon C (HC). b) schematic line of the image showing the channels in the area.

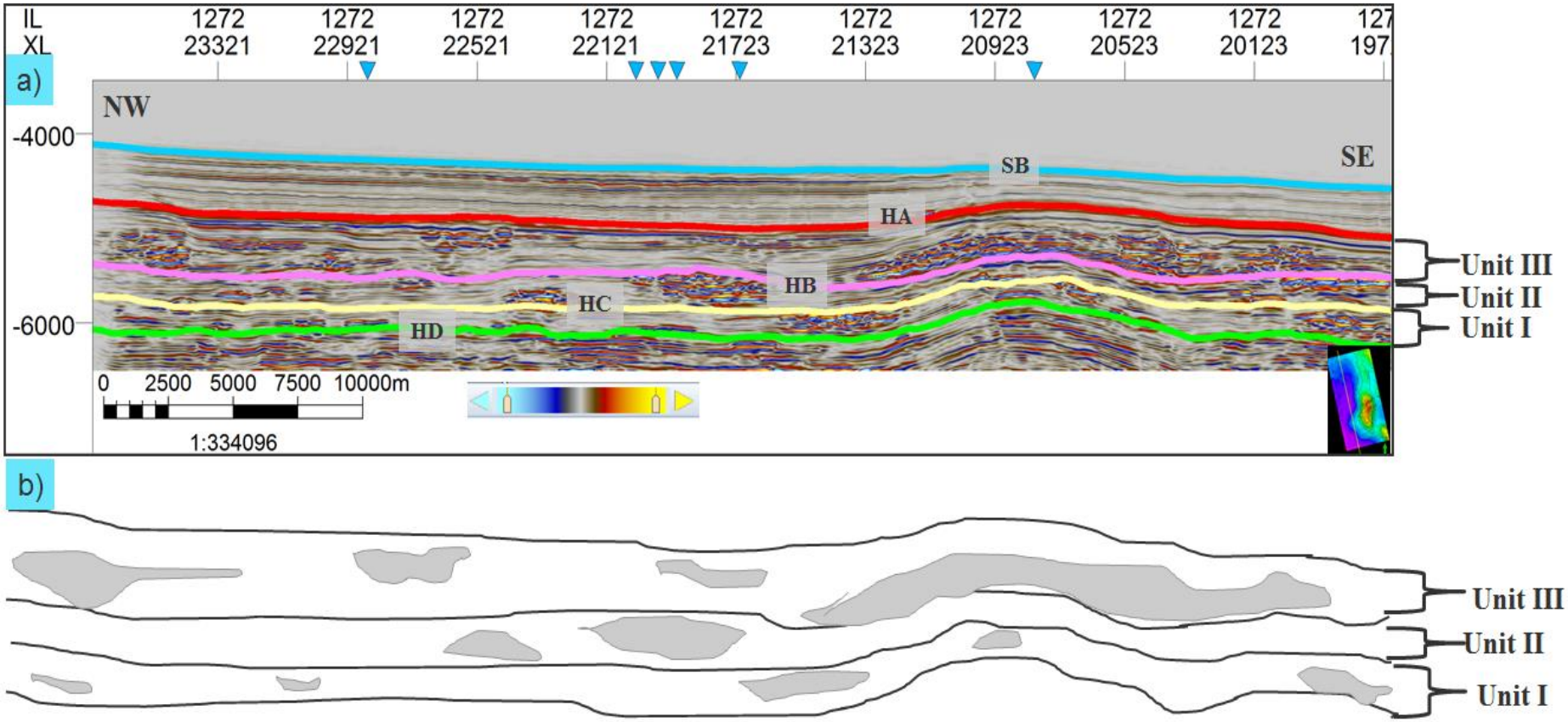

Figure 5.3: Seismic section interpreted and sketch of this seismic. a) Inline showing all interpreted horizons. Seabed (SB), Horizon A (HA), Horizon B (HB) and Horizon C (HC). b) schematic line of the image showing the channels in the area.

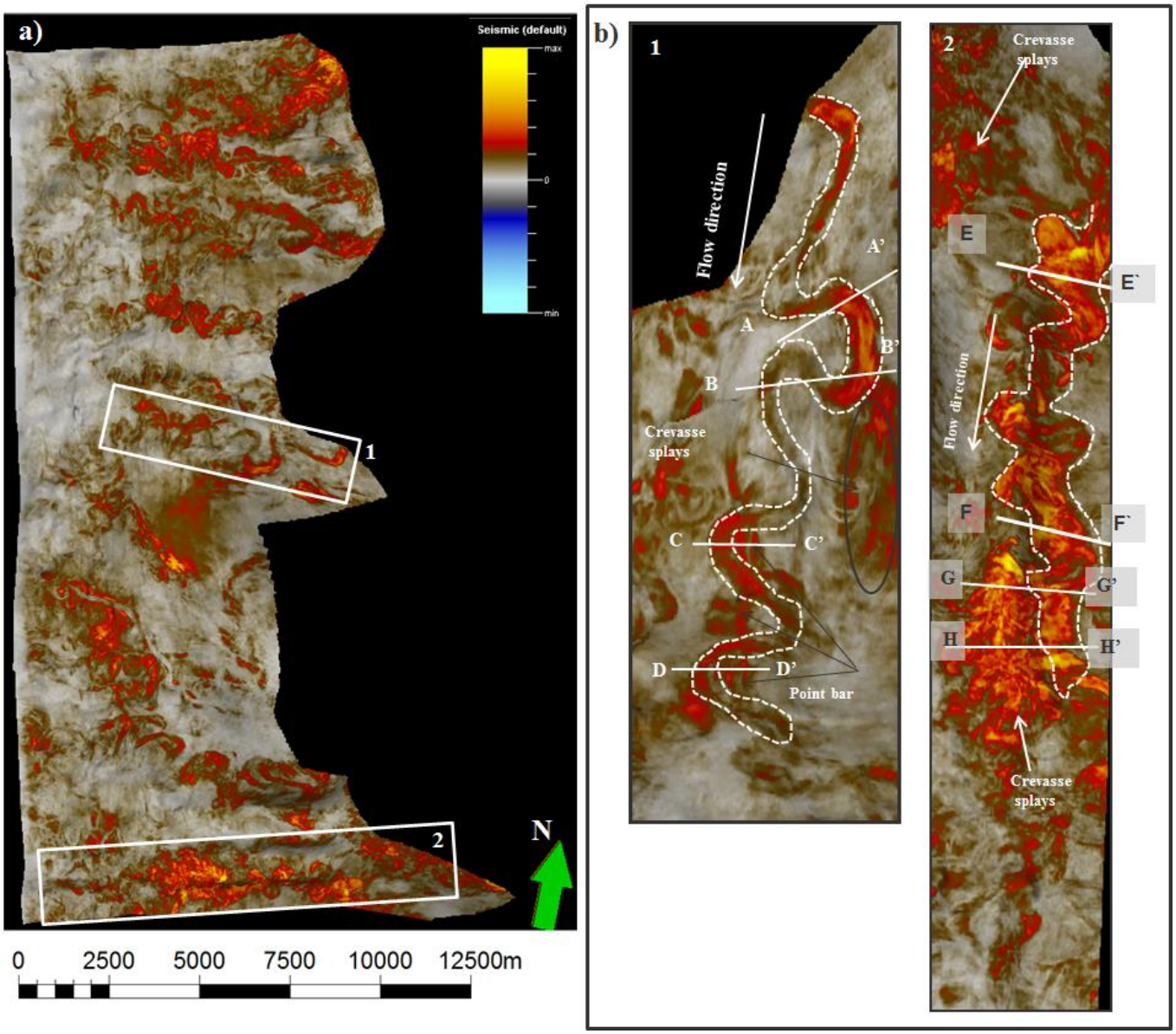

Figure 5.4: Illustrates attribute maps. a) shows seismic attribute map within Unit I corresponding to 90ms. b) shows meander sinuous taken from image a.

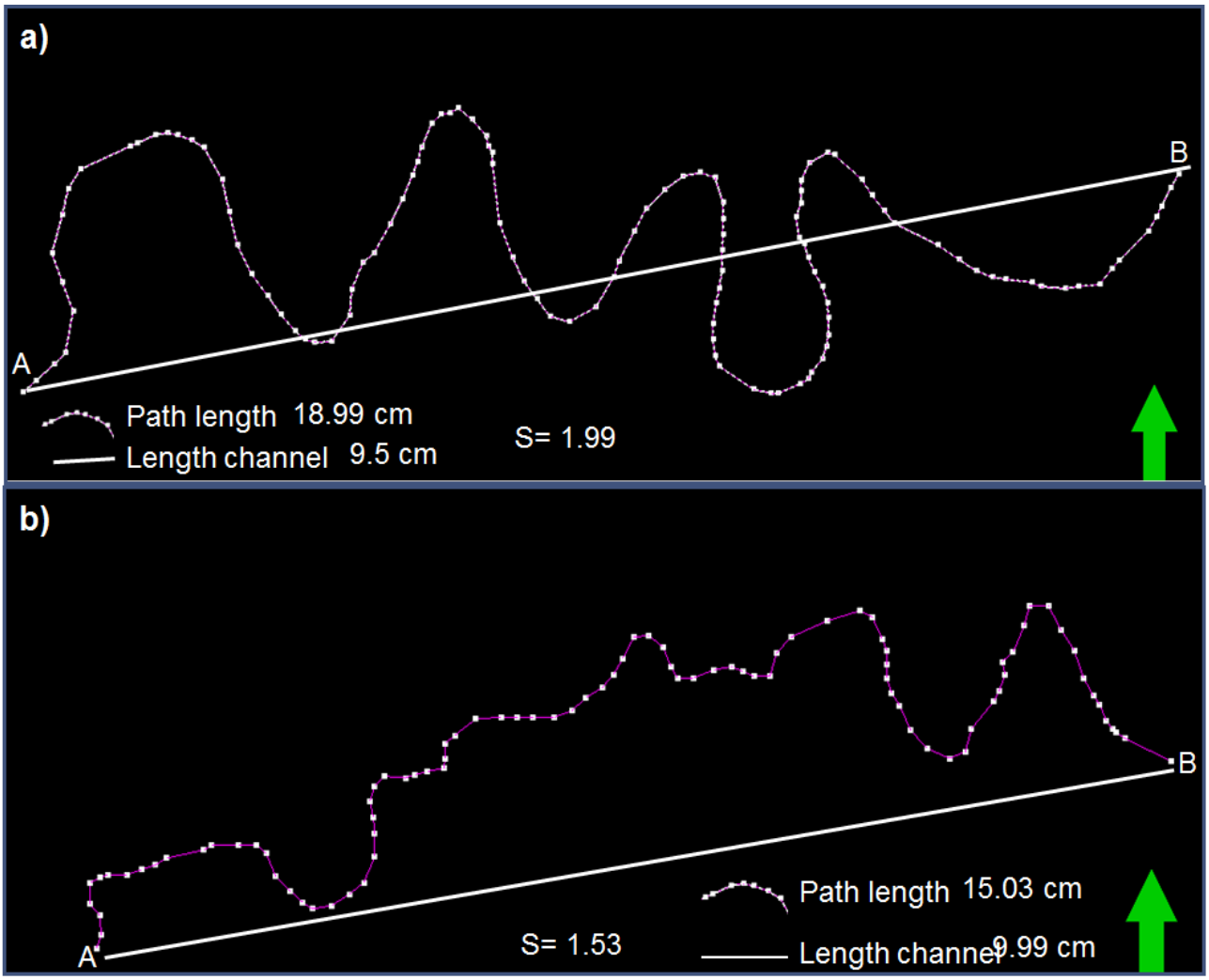

Figure 5.5: Calculation of channel sinuosity within Unit I showed in Figure 5.4 b1 and b2. a) shows sinuosity calculation of channel b1 showed in Figure 5.4 b1 (S=1.9). b) shows sinuosity calculation of channel b2 in Figure 5.4 b2 (S=1.4).

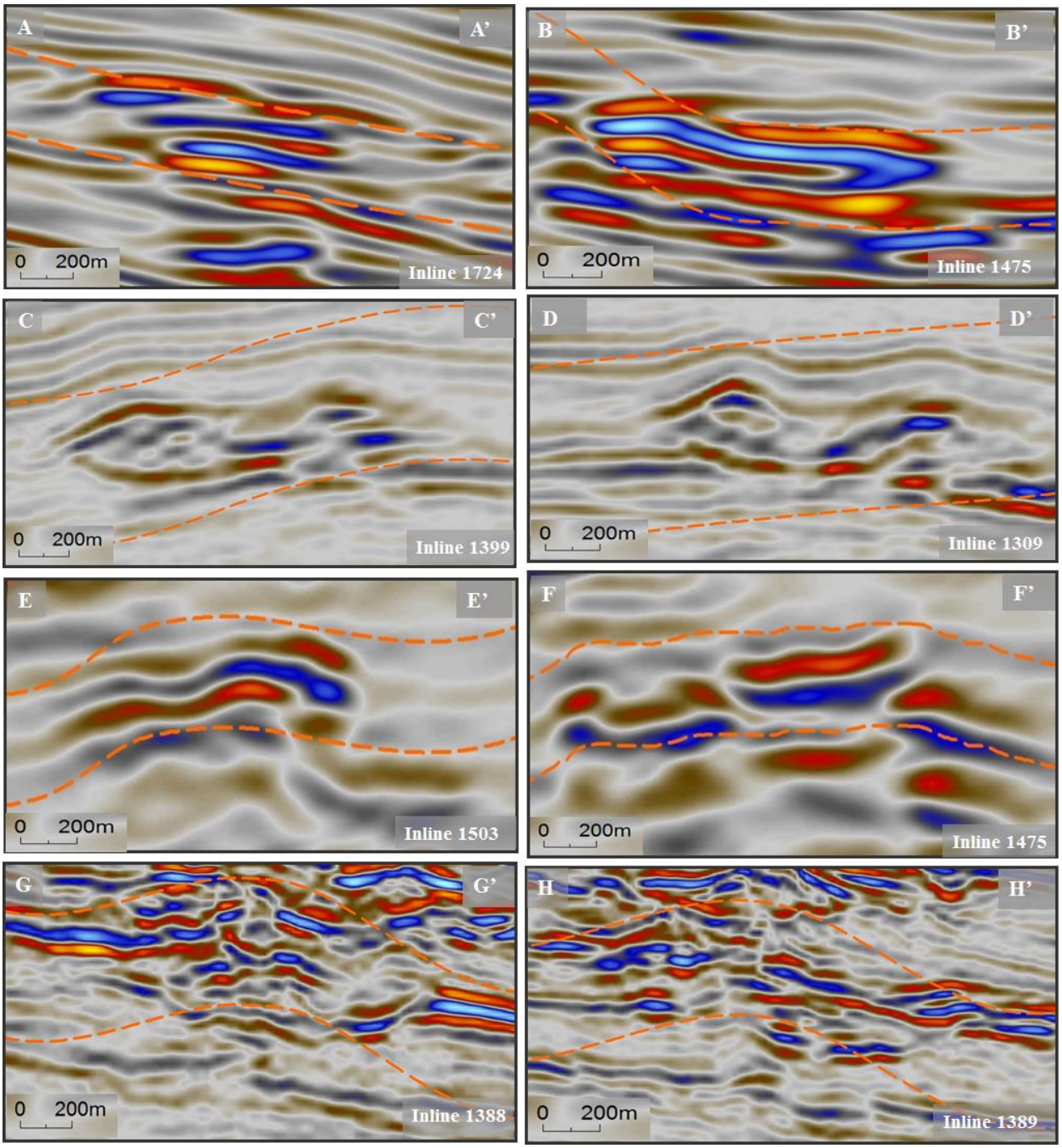

Figure 5.6: Shows different cross section taking from Figure 5.4 b, which is characterized by seismic facies analyzed within Unit I.

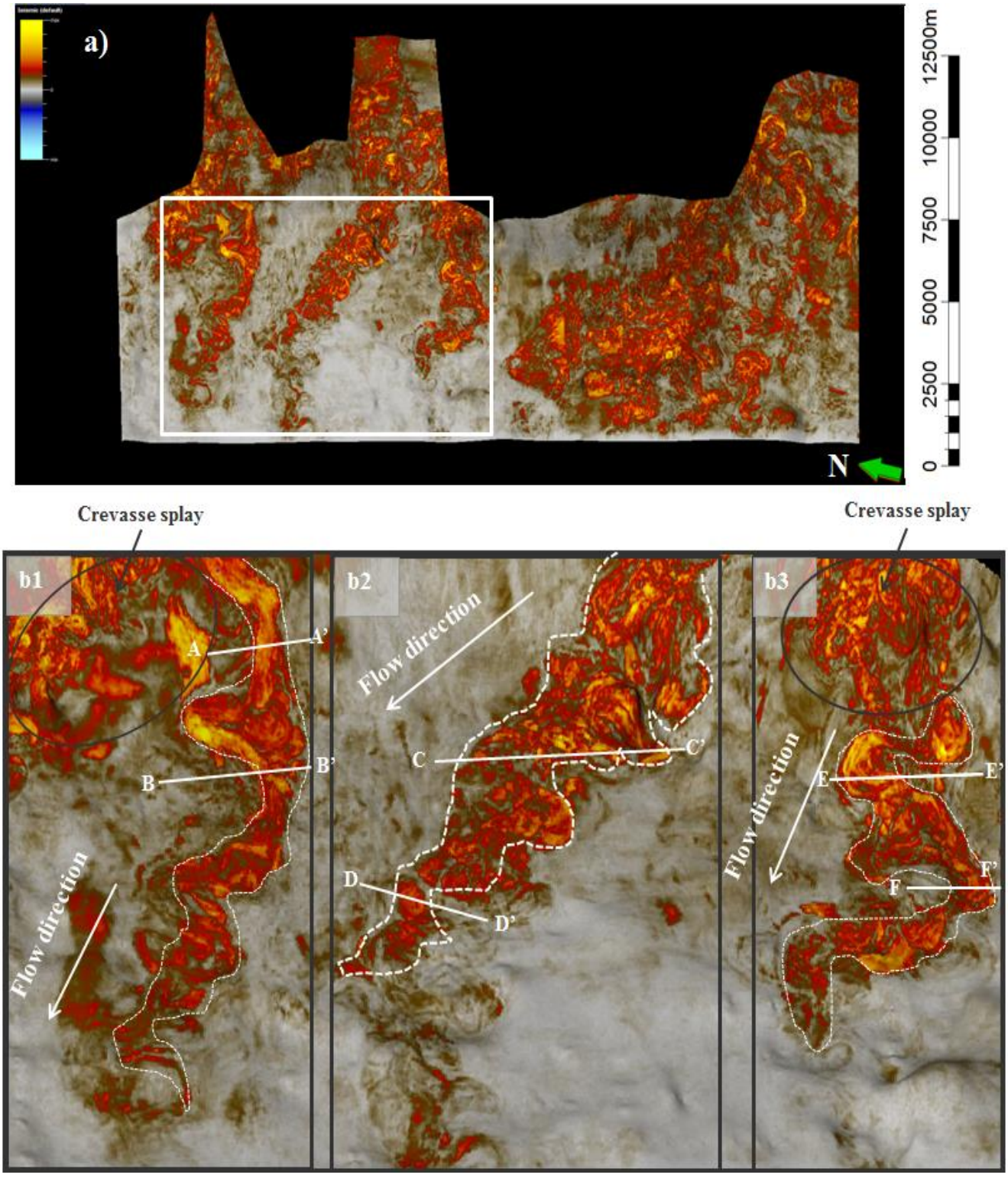

Figure 5.7: Illustrates attribute maps. a) shows seismic attribute map within Unit II correspondent to 60ms. b1, b2 and b3 show meander sinuous channel taken from image a.

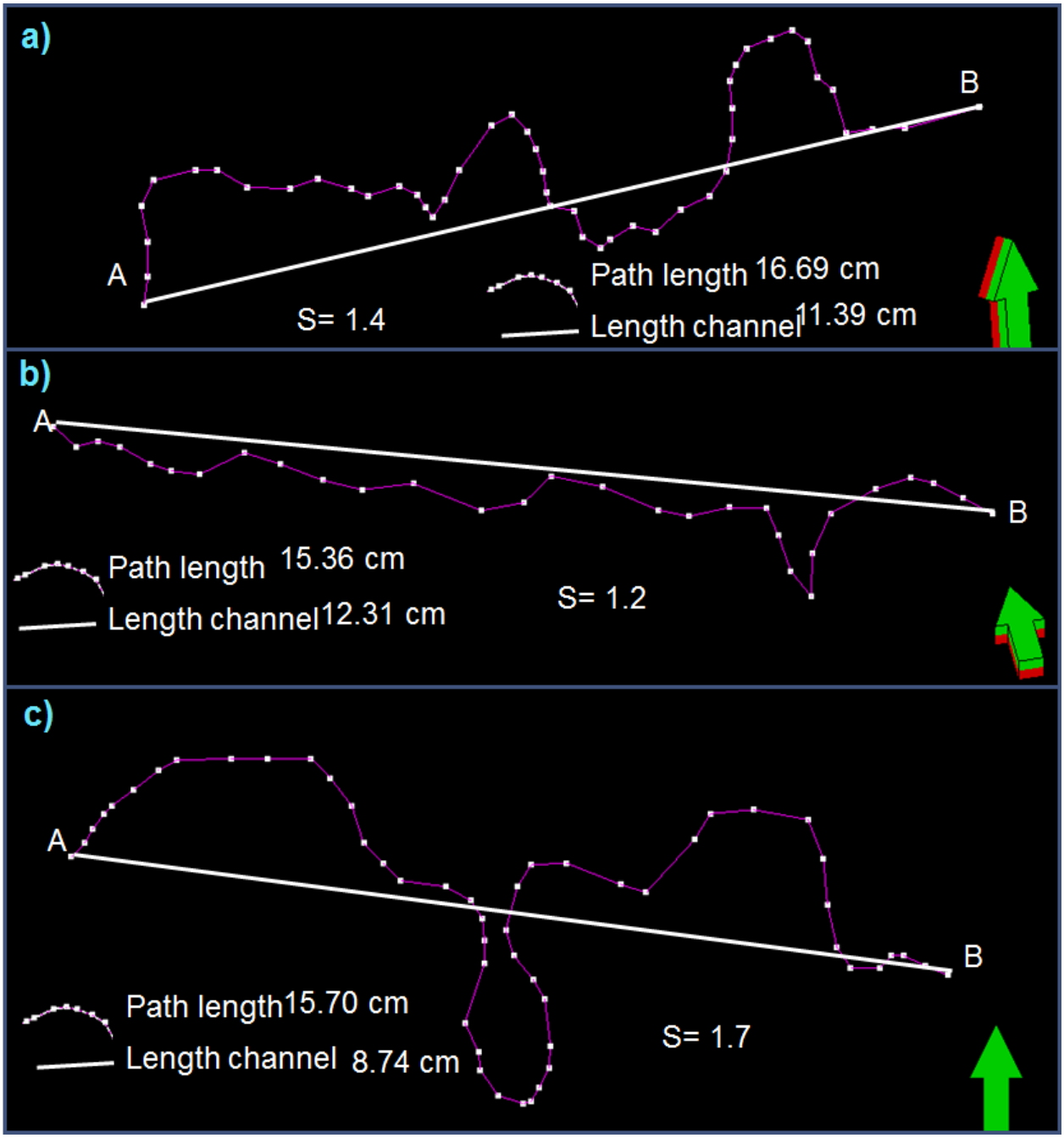

Figure 5.8: Calculation of channel sinuosity within Unit II showing in Figure 5.7b1, b2 and b3. a) shows sinuosity calculation of channel b1 in Figure 5.7 (S=1.4). b) shows sinuosity calculation of channel b2 in Figure 5.7 (S=1.2). b) shows sinuosity calculation of channel b3 in Figure 5.7 (S=1.7).

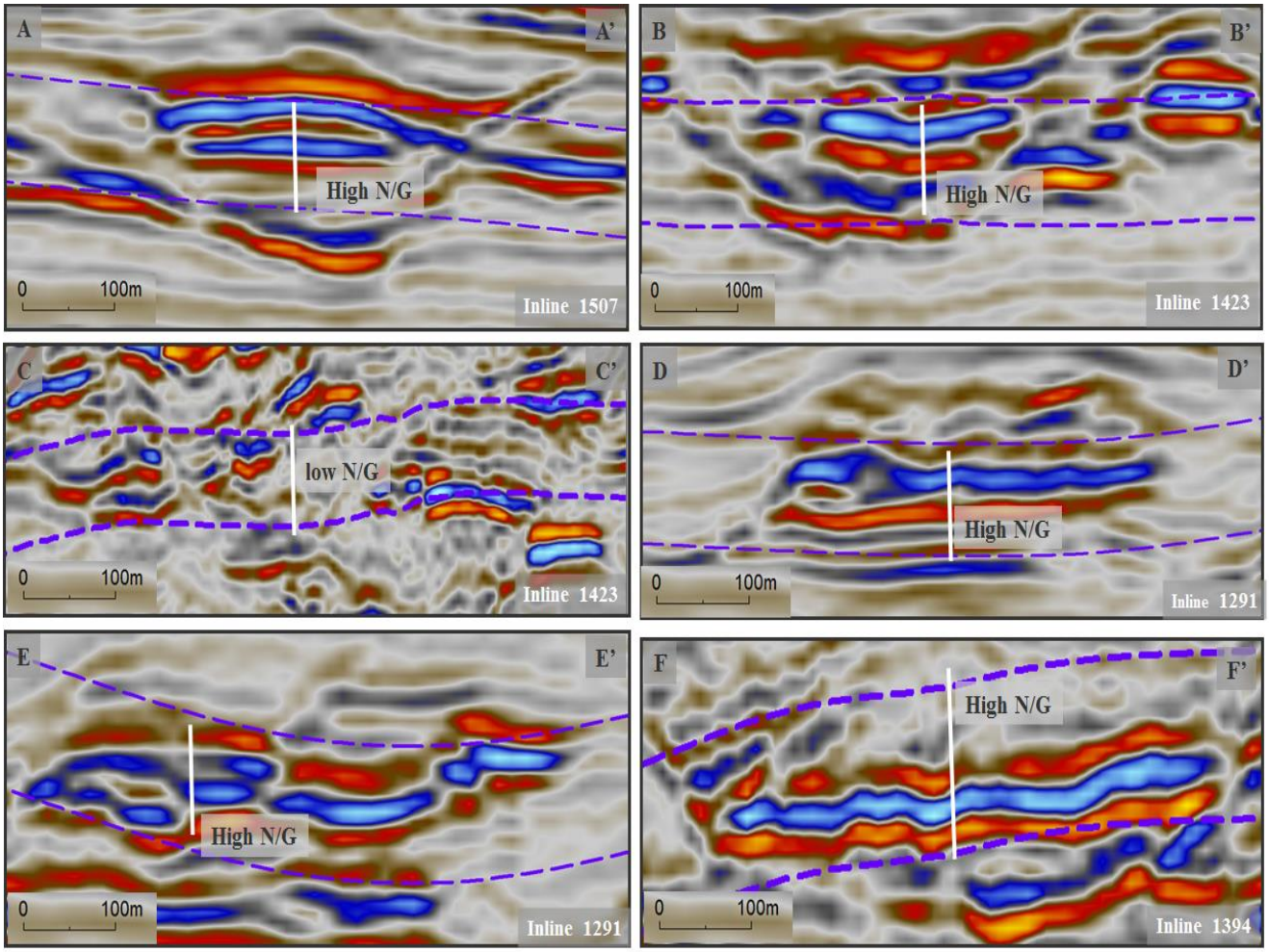

Figure 5.9 Shows different cross section taken from Figure 5.7 b, which is characterized by seismic facies analyzed within Unit II..

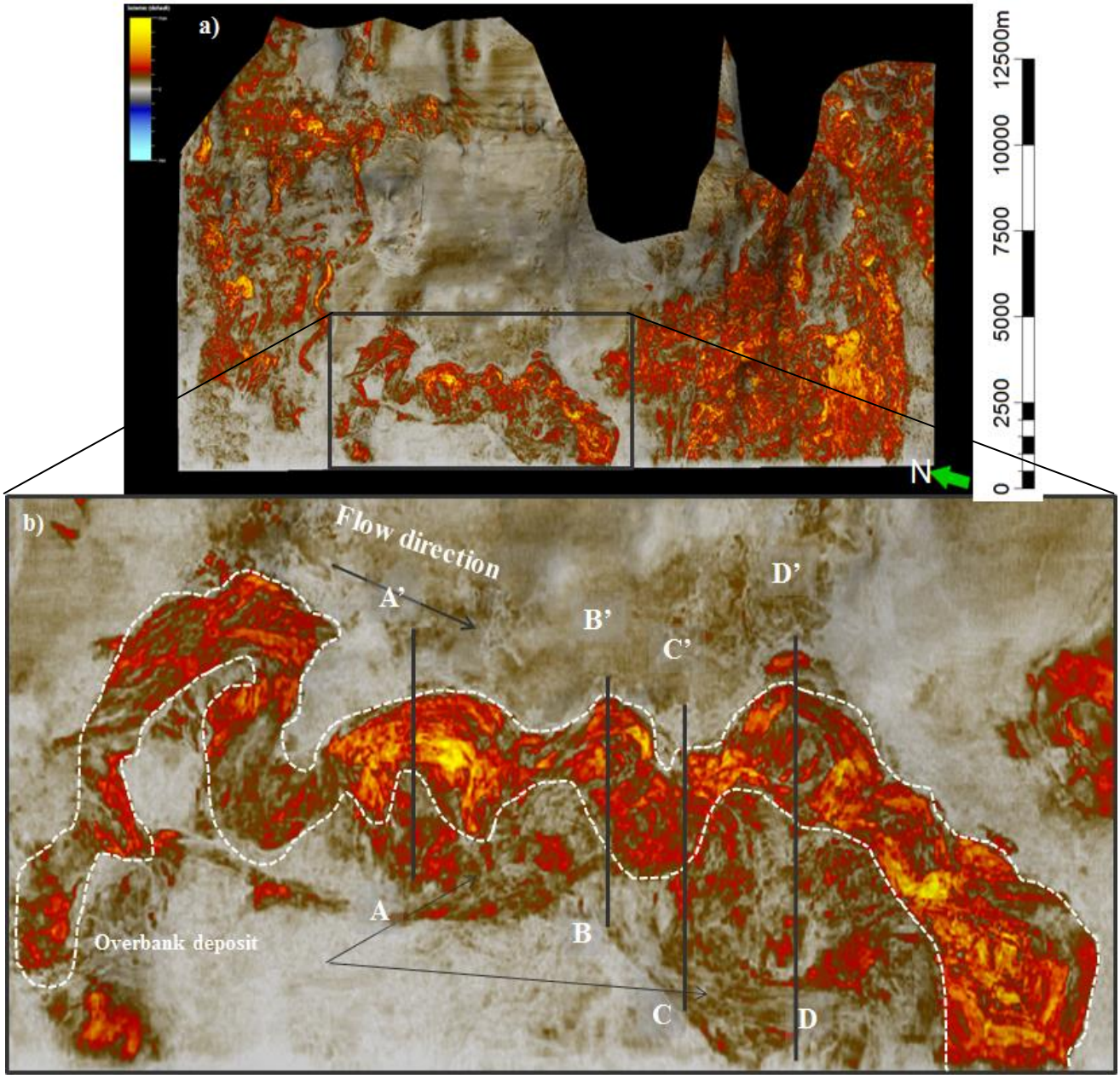

Figure 5.10 : Illustrates attribute maps. a) shows seismic attribute map within Unit III corresponding to 60ms. b) show meander sinuous channel taken from image a.

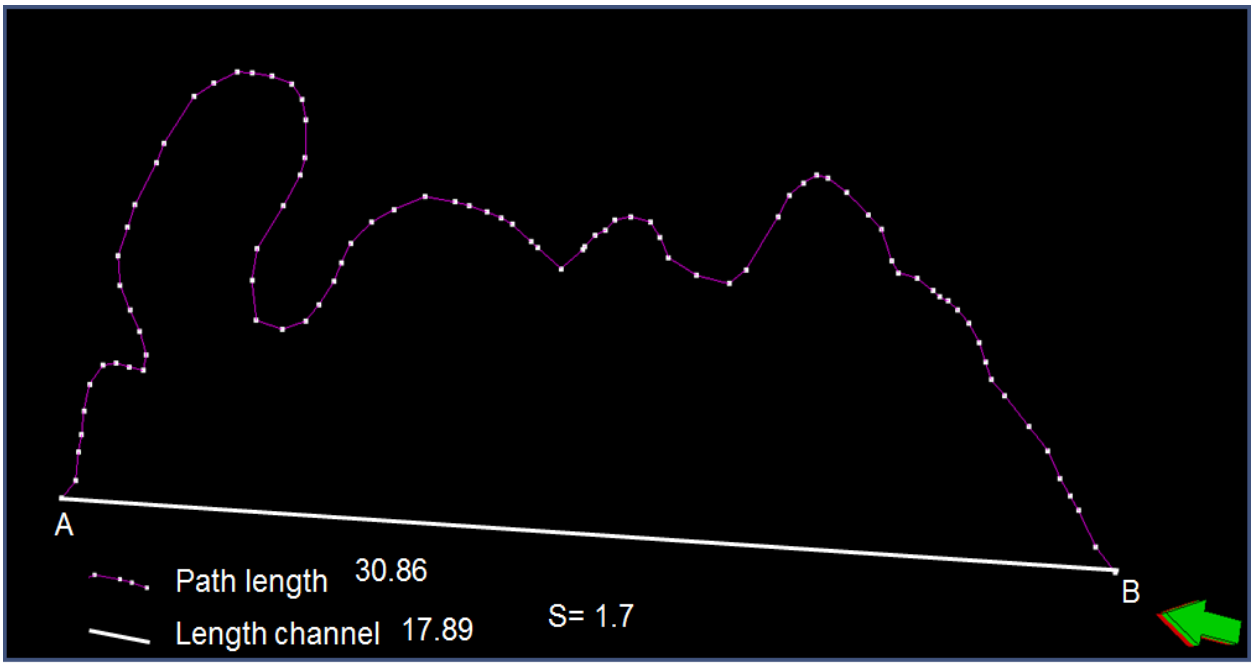

Figure 5.11: Calculation of channel sinuosity within Unit III shown in Figure 5.10 (S= 1.7).

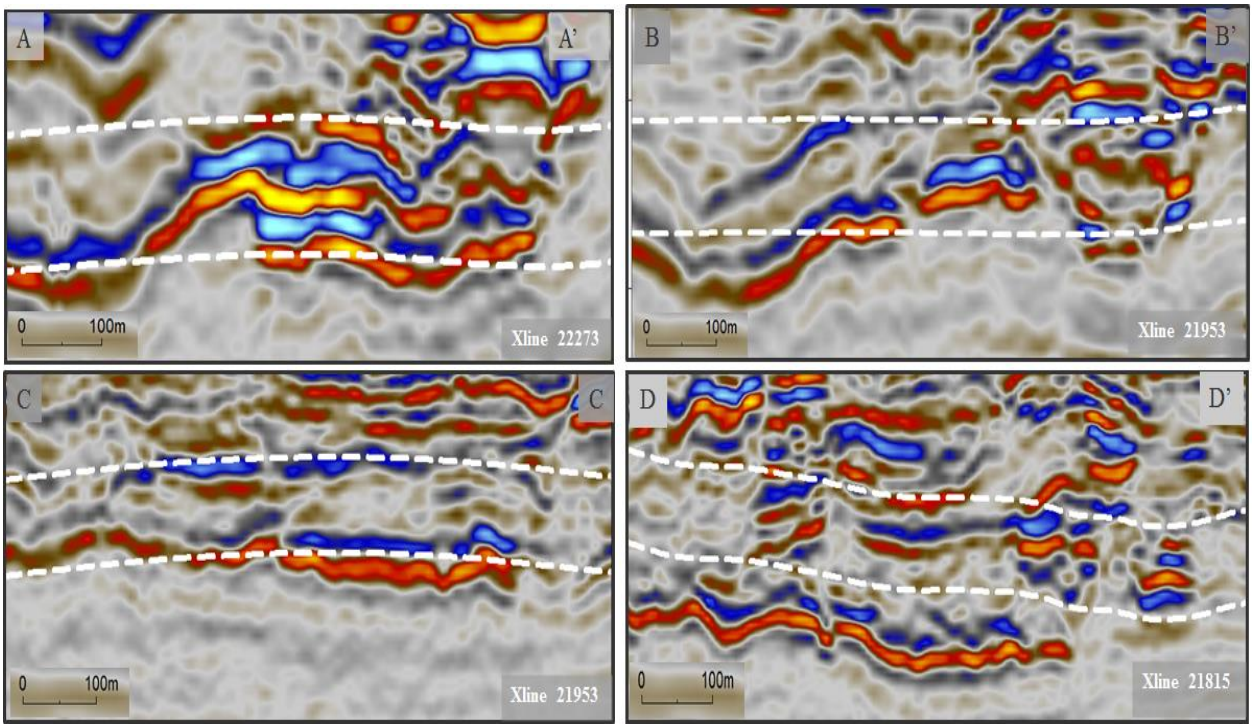

Figure 5.12: Shows different cross section taking from Figure 5.10 b, which is characterized by seismic facies analyzed within Unit III.

Chapter 6 : Seismic section overview and description of main events and other structural-stratigraphic features

The interpretation of the seismic data was mainly based on four selected seismic section in order to analyses the formation of channel, tectono-stratigraphy in the basin and the interaction between sediment deposited and salt movement.

6.1 Seismic section I

Taking the crossline 21905 in the central area of the Seismic section (Figure 6.1), located in the SW-NE direction with good quality data, gives another overview of the channel reflections within the units with discontinuous shingled reflections that forms laterally continuous bodies that are arched in parts by the salt and broken into sleeves discontinuous bodies in the seismic. It is also noticed that this channels tend to pinch out mostly as they form wedges to the salt bodies while some of the channels tend to be largely continuous, others appear to be broken due to the halokiness. In this section it is noticed that the channels tends to have cusp ends or at other points tapered to pinch outs. These cusps might suggest different regimes of channel development.

The seismic section (Figure 6.1a1 and a2) evidences the occurrence of two main features, which are channels in different style of deposition. Channel a1 shows high amplitude package. It is complex channel, with laterally migration and off-lapping reflection, in the lower part and vertically aggradations with on-lapping reelection, in the up part. Channel a2 shows high amplitude package. It is scallop-shape in the base and in the top. In the lateral parts are characterized by low thickness and in the middle by high thickness. In the low thickness can be interpreted as low net gross and the high thickness as high net gross.

6.2 Seismic section II

From Inline 1272 located NW-SE, it also confirms the channel interpretation to having lateral channelized bodies that pinch out and broken to form isolated channels and pockets (Figure 6.2). The seismic section describes the main channel feature. It is mounded channel, concave downward and convex upward channel, associated with relatively sharp bends. This is a complex and unconfined channel. It is a very high indicator of sand prone. In generally, their laterally continuous high amplitude indicates coarse grained deposited. In terms of reservoir, it is normally consider a very good.

6.3 Seismic section III

The cross line 1272 (Figure 6.3) located SW-NE shows good quality data. The areas within the western sections of the section, seems to have deeper channel incision and aggradational fill (Figure 6.3 a), the net gross tends to be higher. It therefore means that the net gross depends on how deep the channel incision is with the lateral subfacies connectivity and vertical aggradation stack.

6.4 Seismic section IV

On crossline 20757 (Figure 6.4), the wedge sediments were seen abutting the salt walls, with pinch out of sediments and the channel deposits. In the seismic sections, of the channels within the stratigraphic level of my interpretation, it was observed that the salt halokinesis has resulted in fault displacement within the channel axis (Figure 6.4). These faults vary from small faults that are hardly seen in the section to more pronounced displacements of the channel deposits. Relict or isolated channels were also observed that were probably broken from other main channels and cannibalized by the salt intrusive (Figure 6.4 a). This suggests that the salt event was a much earlier event that postdated the channels development, within these sections.

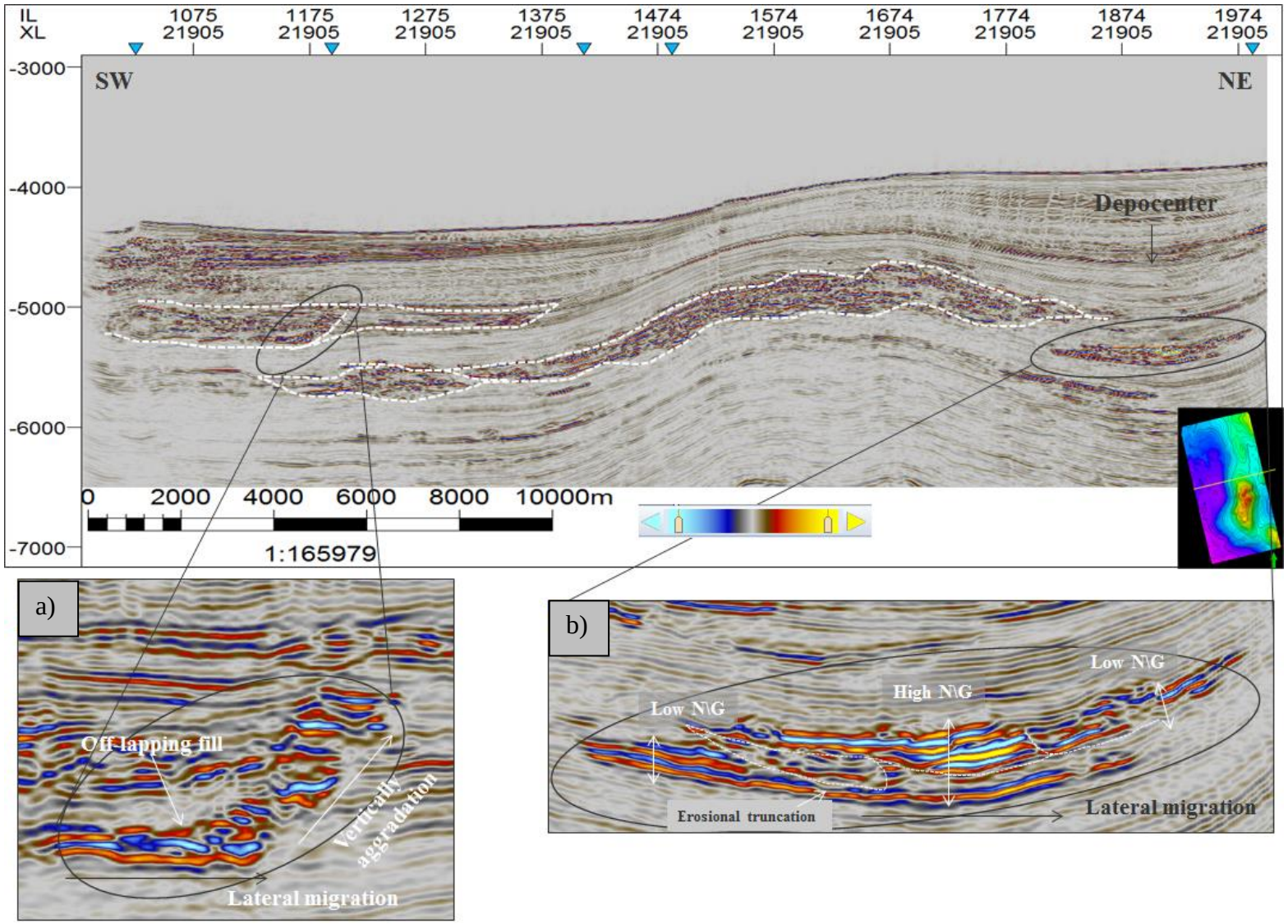

Figure 6.1: Seismic section I marked by two kinds of channels. a1 is complex channel with lateral migration and vertical aggradation. b) is a complex channel with lateral migration

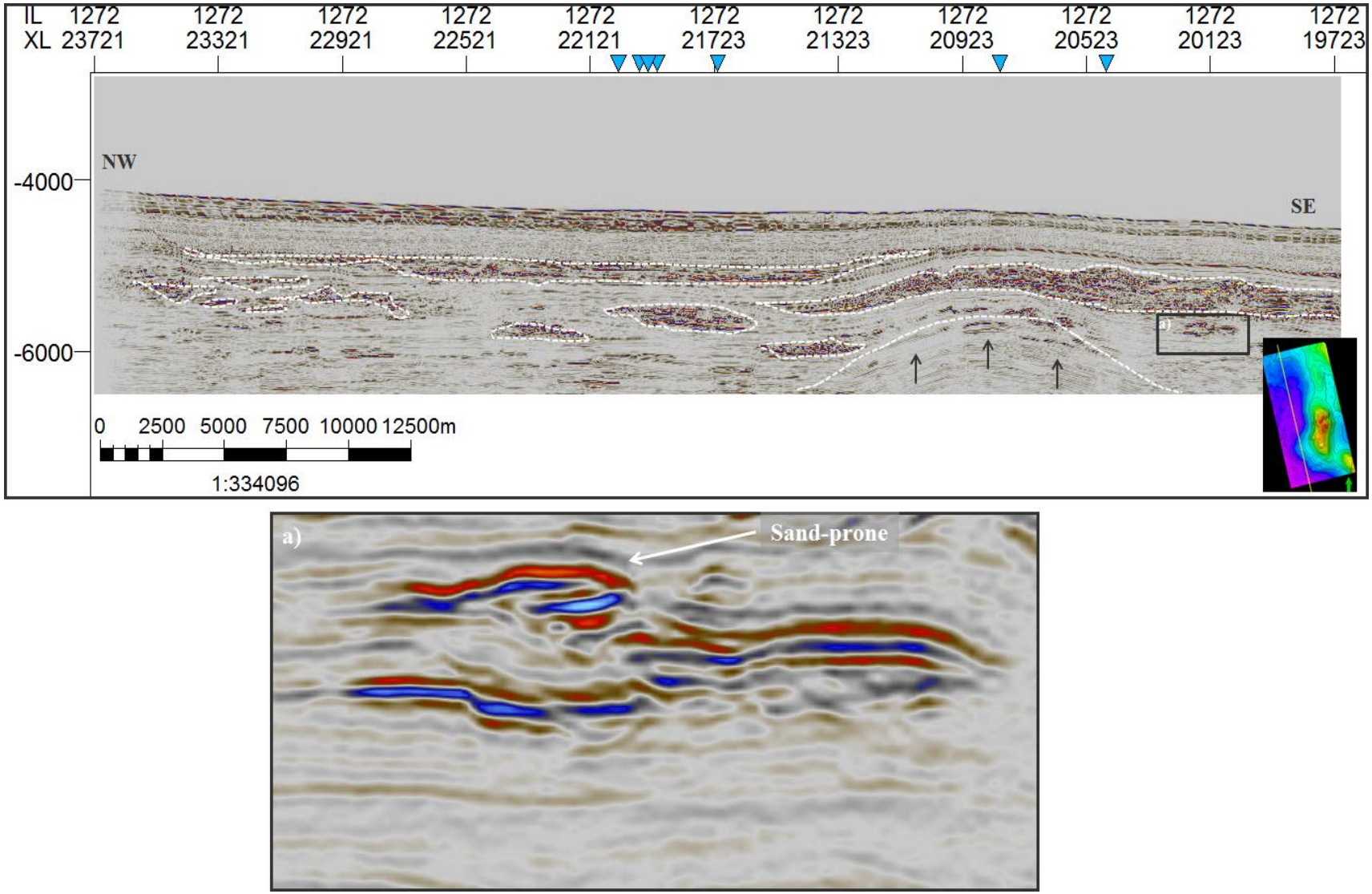

Figure 6.2: Seismic section II marked by a channel mounds a) is complex channel convex-up or hat shaped in the top with sand-prone fill.

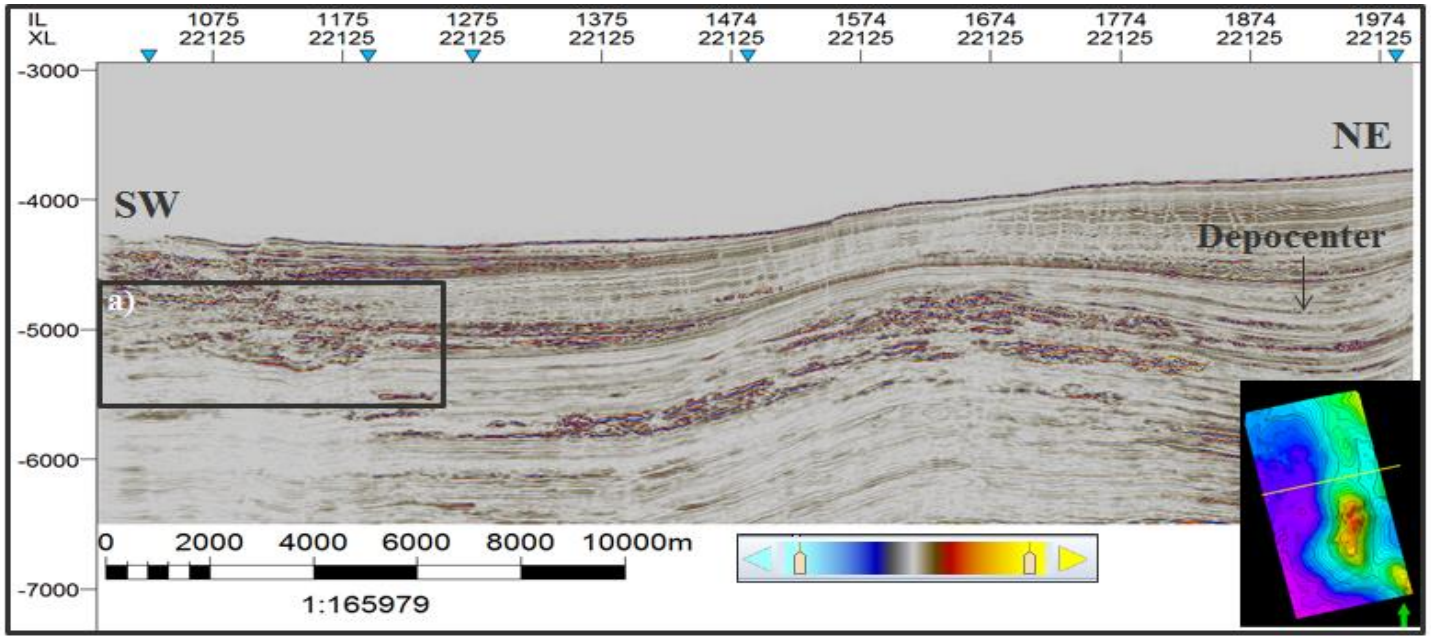

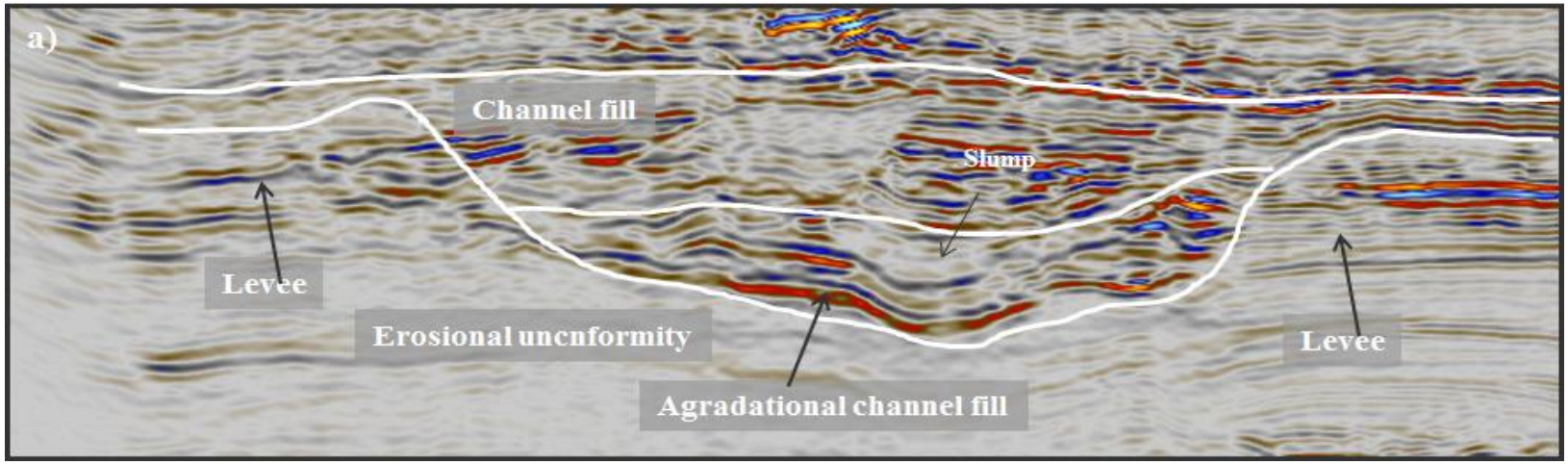

Figure 6.3 Seismic section III marked by a levee channels. a) is complex channel with levee sediments and aggradational to non-aggradational channel fill.

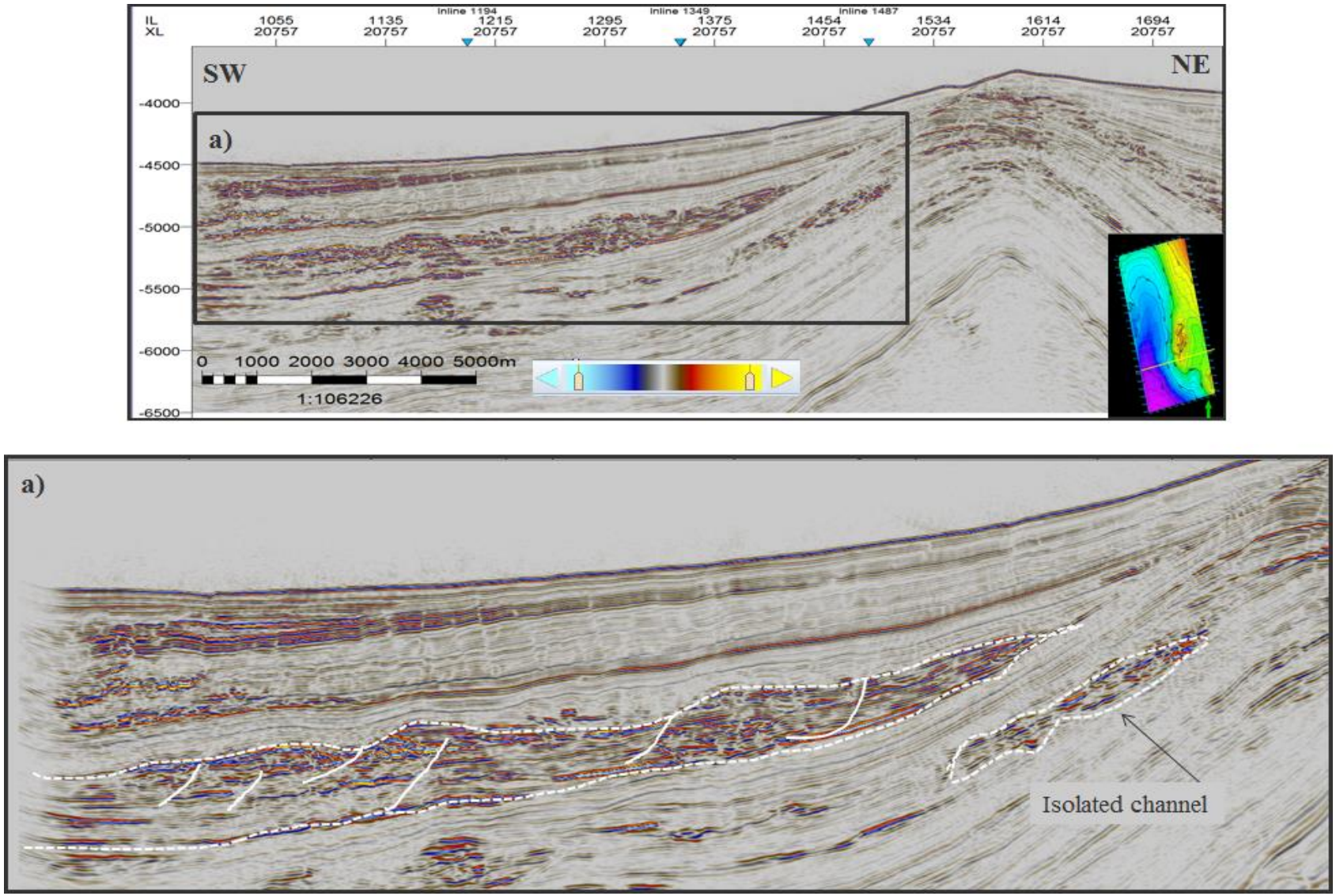

Figure 6.4: Seismic section IV marked by a stratigraphic trap. a) show the Pinch out feature.

Chapter 7 : Discussion

The sedimentary series of the lower Congo basin shows three main units: pre-rift continental deposits (Jurassic), syn-rift fluvio-lacustrine deposits, early post-rift thermal sag phase (Lower Cretaceous), and the post-rift unit with a large accumulation of salt (Middle Aptian) covered by thick marine successions (Albian to present) (Savoye et al., 2009).

The volume of sediment transported to the Angolan margin increased during the Cenozoic due to structural deformation and uplift of the hinterland that combined with a humid climate, increased river runoff and erosional processes resulted in increased bed-load transport in rivers in the drainage area (Savoye et al., 2009). These factors led to the initiation and development of the huge Congo system during the Oligocene, first on the slope and then in the Lower Congo Basin and the formation of the Congo deep-sea fan (Brice et al., 1982). The activity of the Congo turbidite system is directly linked to the behavior of the Congo River. This behavior has changed over time, in relation to relative sea-level variations, tectonic episodes and climatic changes (Savoye et al., 2009).

Salt tectonism has had a significant impact on basin formation and on the development of the studied deepwater channel systems. Because of the instability of the salt layer, the sedimentary cover on the continental slope is affected by syn- and post-sedimentary deformation due to gravity tectonics, which generated growth faults, salt sheets, diapir structures and compressional structures and increase of sediment load (Savoye et al., 2009).

The development and morphology of the channels in the study area is impacted by salt movements, which is summarized in Figure 7.1. A stratigraphic change in the orientation of the channel systems (and interpreted paleoflow) is observed between Unit I / Unit II and Unit III (dominantly E-W and N-W respectively). The orientation of the channel systems is interpreted to have been strongly influenced by salt tectonics, with their direction being impacted by variations in gradients due to salt movement causing a localized readjustment. The E-W direction reflects the regional flow direction and orientation of the paleoslope. Local perturbations resulting from salt diapirism led to a reorientation of the Unit III channel system and a switch to a northerly trend to the depositional system (especially in the areas adjacent the salt flanks).

The channels of unit I and II are relatively older than the channels of unit III and were deposited before the onset of salt movement (Figure 7.1a). The movement of salt altered the gradient of the substrate and consequently sediment dispersal patterns. In some instances the salt growth has resulted in the apparent truncation of the channel bodies. This observation supports the interpretation that the channelization of Units I and II commonly predates the growth of the salt. Channel bodies are observed to be tapered or pinch out against the edge of the salt, which

suggests that deposition is influenced by the salt movement and changes in useable accommodation (Figure 7.1c and d).

The overlying channels of unit III are the youngest channel system studied and are also impacted by salt tectonics and sediments derived from Congo River. The channels within unit III are interpreted to represent syn-depositional channels as their formation is concurrent with the accommodation generated by the movement of the salt. A critical look at the seismic section (Figure 5.2 and Figure 5.3) reveals a higher degree of continuity to the channels of Unit III relative to that observed in Units I and II. The lateral continuity of the channel also depends on the limit position of the salt, but much of the channels seem to be well developed within the depocenters. Therefore the salt halokiness occurred syn- or predeposition of the channel systems within the section (Figure 7.1e).

The channels in the units are interpreted to represent weakly confined to unconfined channel systems because it is disorganized and it is difficult to distinguish which one is young and older (Figure 7.2). The channel fill is interpreted to comprise relatively coarse-grained sediments within the channel axis. Channel systems that exhibit these morphologies are commonly characterized by high net gross and sections of interconnected or amalgamated sandy facies within the channel complex. And therefore, represent possible target intervals. The channel axis may also be associated with relatively higher porosity and permeability compared to the channel system as a whole. Point bars may also represent viable exploration targets. Potential reservoir targets within the channel system include sections of stronger amplitude reflections (interpreted to represent sands), related to reservoir quality and inferred higher porosity and good permeability (Sullivan et al., 2000; Beaubouef et al., 2000; Beaubouef et al., 2003; Sprague et al., 2005).

In deep water systems channel may exhibit lateral migration and vertical aggradation as seen in the channel belts across the interpreted seismic (Figure 7.3). According to Kola (2007), laterally migrating channel facies may be followed by thicker, increasingly vertically aggrading sinuous channel complex with varying degrees of lateral migration. Lateral migration and vertical aggradation may be either continuous or discrete and are due to cut and fill of various magnitudes. Lateral migrations and vertical aggradations can occur as a consequence of relatively continuous erosion, discrete cuts, or less deposition on the concave (outer) bank and more deposition on the convex (inner) bank (Imran et al., 1999); or as a result of episodes of distinct and discrete channel-wide cuts and fills. Both laterally migrating and vertically aggrading sequences might appear as off-lapping and on-lapping reflection shingles or strata, often filling closely spaced, subtle or discrete cuts. Inner channel banks that migrate with lateral channel shifts may or may not be of high amplitude and may or may not be sand-prone in deep water channels.

Furthermore, the channels show a varying sinuosity index ranging from highly sinuous channels to less sinuous channels as earlier described. This according to Kola (2007), suggests that many sinuous channel complexes, with associated banks and overbanks, are housed within larger

channels/valleys, flanked by large overbanks. These larger channels/valleys are designated as master valleys, and their overbanks as master overbanks (outer overbanks or outer levees). These features are characteristic of the channels within the sections of the seismic as ridge like levees confine the channel main flow axis with overbank deposits interpreted with characteristic strong amplitude reflections noticed as previously described.

As previously mentioned two channel types characterize the channels observed in this study based on their sinuosity. The high sinuosity channel with sinuosity index (SI) greater than 1.5 index (SI ranging from 1.7 to 1.9), is called meander channel (Figure 5.5 a and b, Figure 5.8 c and Figure 5.11). This channel type suggest a low bed load component (sand and pebbles) to higher suspension fractions (silt and clay), this is interpreted from the seismic sections as the meandering channel has well developed levees, crevasse splays are interpreted within the overbank area (Figure 7.4).

The second channel type within the units II is identified by lower sinuosity channels with sinuosity index ranging from 1.2 to 1.4. This suggests a channel with higher bed load composition to lower suspension fractions. In this case the channel levee and flood plain deposits are less well developed with no evidence of levee ridges as seen in the higher sinuosity case, which then would lead to classify this channel as unconfined. The higher bed load composition suggests the prevalence of higher sandy channel facies with less flood plain and levee facies observed. The prevalence of sandy bodies suggest a higher rate of aggradation in vertical successions, also the channel width to length ratio is higher which suggest a lateral sand body connectivity of this channel type (Figure 7.4).

It is suggested that the later lower sinuosity channels tend to have good sand body connectivity laterally and vertically, more sandy channel facies with high bed load dominated composition, when compared to the former higher sinuosity meandering channels.

Possible trapping mechanisms and structures present in this interval include pinch-out, faults, sediment wedges and depocentres. These associated features were mainly a result of the salt halokinesis in a process of creating space. The pinch-out features with wedge-shaped channel geometries form as the sediments were confined by the salt and the stratigraphic bodies tapers and pinches out against the salt flanks. These structures are common salt related tectonic stratigraphic features and possible exploration targets. Also observed, are fault displacements, within part of the salt wedge sediments in the pinch out areas and channel sediments within the units. This suggests that the channel sediments were affected by post deformational tectonism by the salt halokinesis, which also could form fluid barriers.

Depocentres form primarily because of the salt movement and sediment deposition. Due to the large volume of sediment being deposited, increased loading leads to increased subsidence creating a depression. This may form areas where could be found high percentage of vertically stacked channels due to increased sediment supply rates.

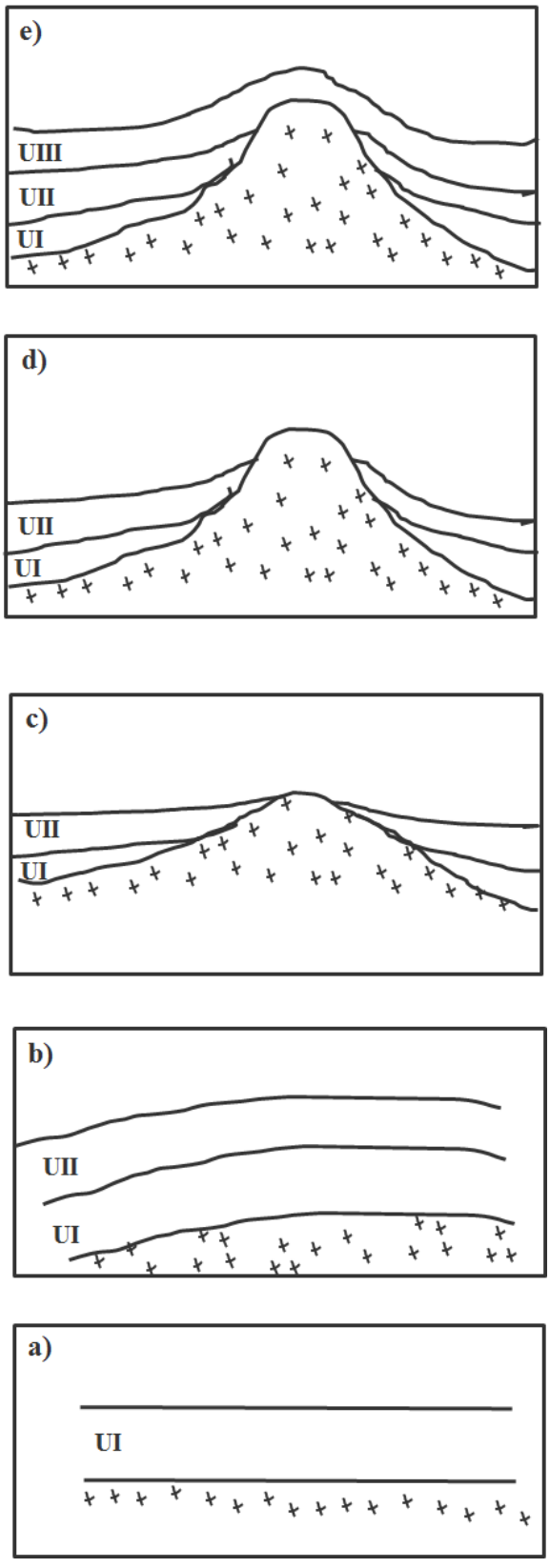

Figure 7.1: Schematic sketch of study case. a) shows initial condition, where the salt was deposited and the sediments were deposited above it. In this case, the sediment layer represents unit I. b) shows the second stage of deposition. More sediment was deposited above the unit I. The salt started moving a bit and the layers above it became a bit bend. c) and d) show high intrusions of salt dome, and start to cut the channels in unit I and II. e) shows the present day, which the new sediments are filling all the spaces and following the salt shape. This sediment layer we call unit III.

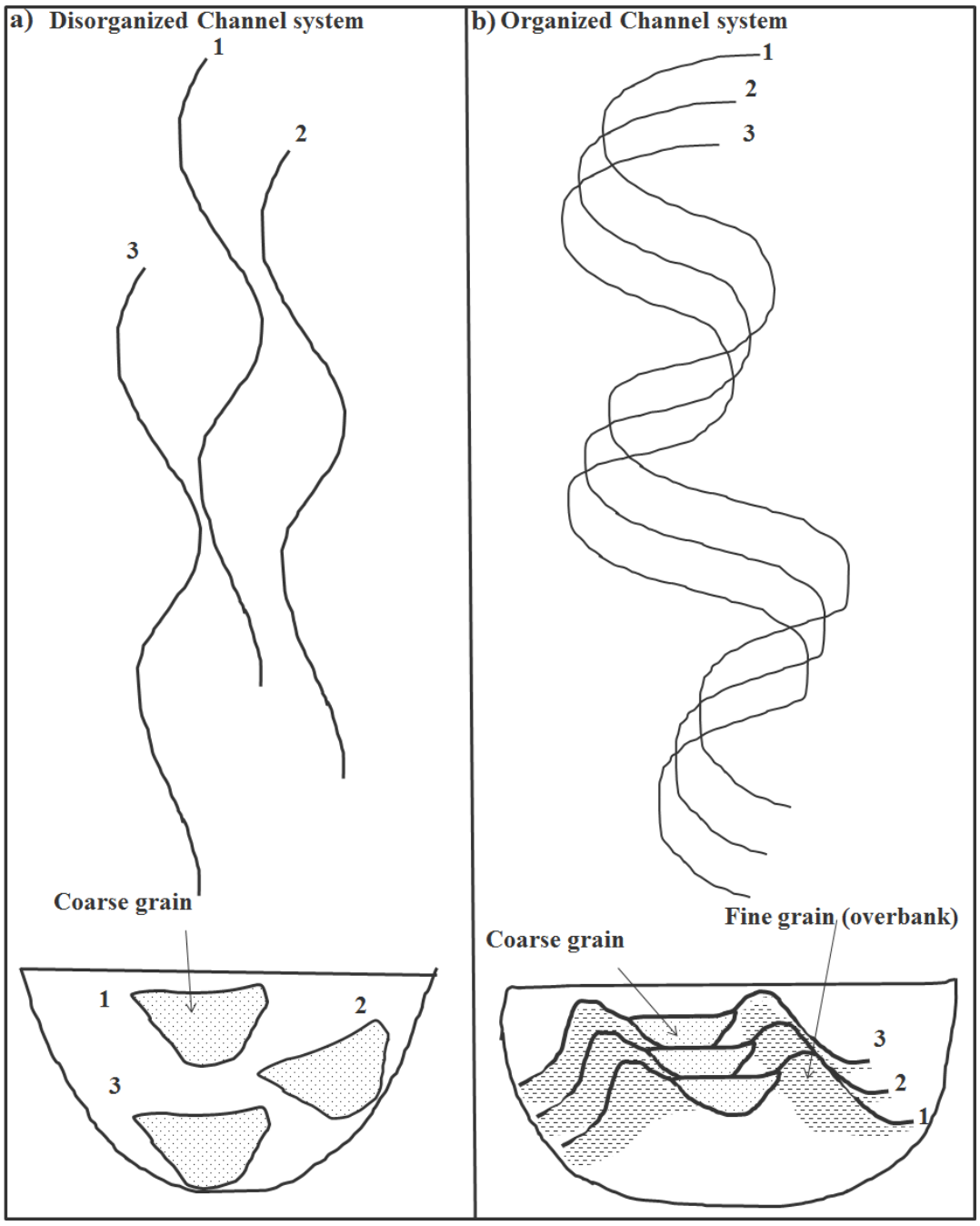

Figure 7.2: Sketch of disorganized and organized channel complex typically in deep water. a) illustrates an example of disorganized channel complex. It shows that this system is mainly identified by bed load composition (coarse grain) with no presence of suspension fractions (Fine grain). Therefore means that, it is high net gross system. This kind of system is similar to study case. b) illustrates an example of organized channel complex. It shows that they are deposited in vertically stack, which tends to have low bed load composition (coarse grain) with high presence of suspension fractions (Fine grain). Therefore means that, it is lower net gross system.

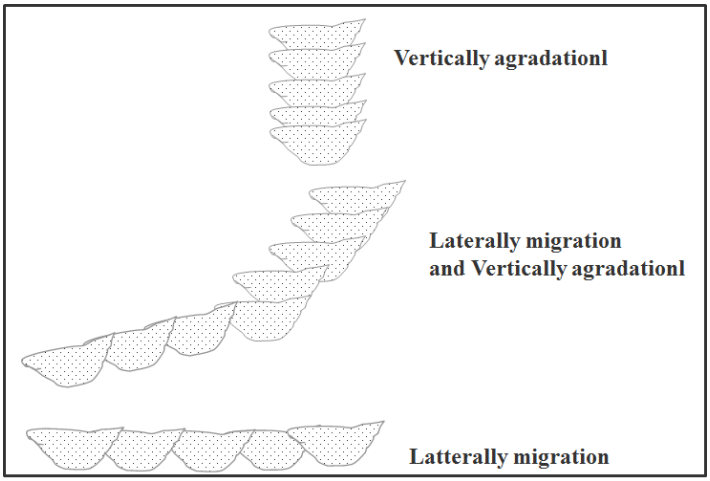

Figure 7.3: Sketch of common channel complex arquitecture in deep water, with lateral migration, vertical aggradation and lateral migration and vertical aggradation.

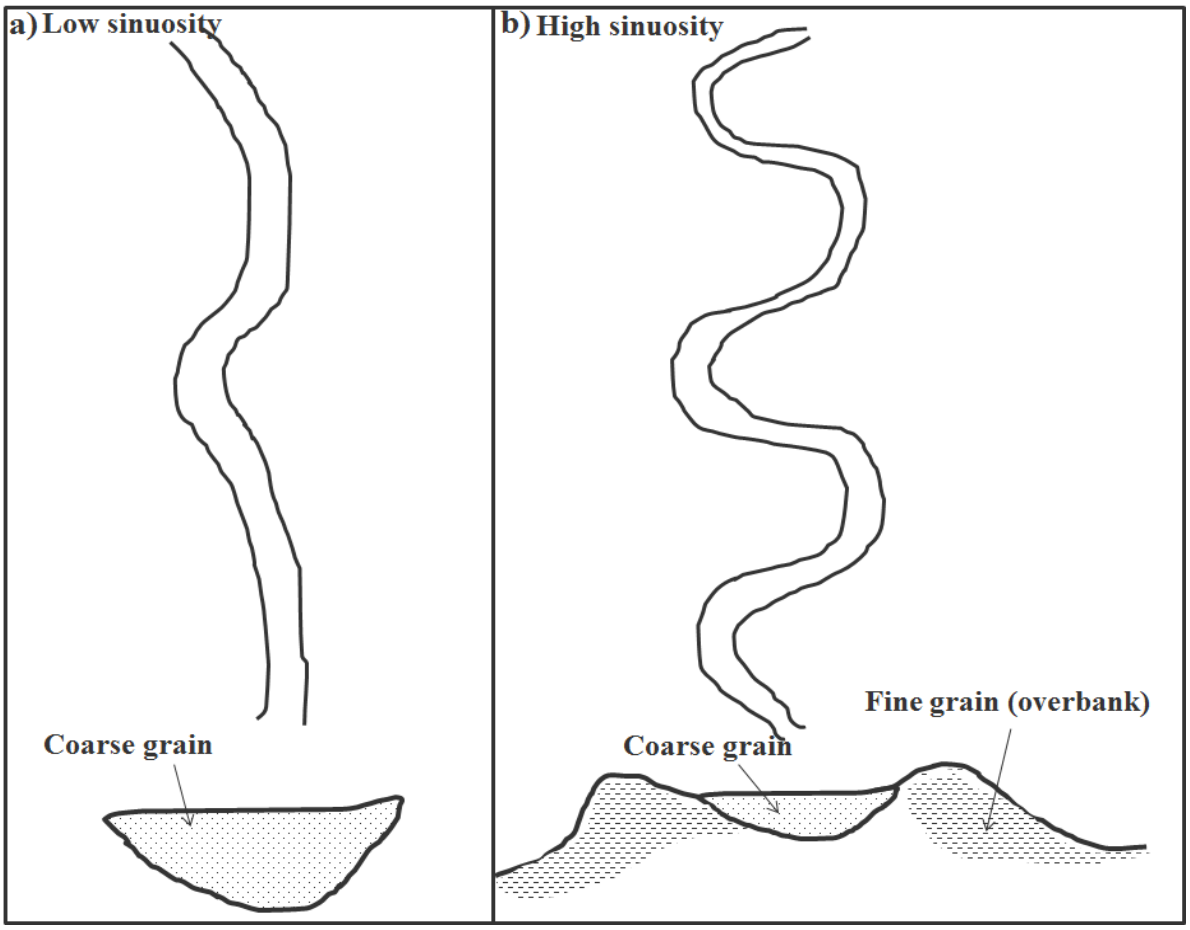

Figure 7.4: Sketch of low and high sinuosity channels typical in deep water. a) illustration of low sinuosity channel. It is a sinuous channel with high bed load composition (coarse grain) and less flood plain and levee facies. Therefore means that, it has high net gross. b) illustration of high sinuosity channel. It is a meander channel with low bed load composition (coarse grain) and high flood plain and levee facies. Therefore means that, it has lower net gross system.

Chapter 8 Conclusion and recommendation for further work

8.1 Conclusion

3D seismic data from Angola, Congo Basin were used to identify the main channels in deep marine environment and analyze how the channels are forming and migrating. Application of 3D seismic attributes was used to support the interpretation. From the analyzed data, it can be concluded that:

- The study area is strongly affected by salt tectonics. The formation and development of the channels were strongly influenced by salt movements.
- Three stratigraphic units were identified in the interpreted interval, comprising four horizons, Horizon A (HA), Horizon B (HB), Horizon C (HC) and Horizon D (HD). Unit I is bounded by HD and HC. Unit II is bounded by HC and HB. Unit III is bounded by HB and HA.
- Unit I is characterized by channels that exhibit components of both lateral migration and vertical aggradation, with a dominant east to west flow direction. Depositional features such as crevasse splay and point bar were also identified. Unit I comprises two main channel systems. It is classified as high sinuosity channel, with a sinuosity index of 1.9 to 1.53. The channels within this unit are interpreted to represent meander channels because the sinuosity index is greater than 1.5.
- Unit II is also characterized by channels that exhibit components of both lateral migration and vertical aggradation, are oriented roughly east-west and interpreted to represent dominant paleoflow towards the west. The unit comprises three main channel systems. The first two channel systems were classified as low sinuosity, with approximately 1.4 and 1.2 of sinuosity index. Therefore, the channels are interpreted as a low sinuosity channel (since the have a SI less than 1.5). The third channel system is classified as high sinuosity channel, with approximately 1.7 of sinuosity index.
- Unit III is characterized by channels with a strong component of vertical aggradation, with northern to western flow direction. The main channel within Unit III is classified as a high sinuosity channel, with approximately 1.7 of sinuosity index.
- Seismic facies of sinuous channels commonly exhibit high amplitude semi-continuous to discontinuous seismic response. However, the associated overbanks have a relatively weak amplitude response. The interpreted sands are associated by with strong amplitudes.

8.2 Recommendation for further work

To better constrain and test the interpretations made in this study we recommend:

- ✓ Wells log analyses, to have an idea of lithology type in the study area.
- ✓ Seismic data with pre-stack depth migration (PSDM), to have good reference depth calculation of the feature.
- ✓ Needs to perform fluid investigations such as AVO (Amplitude Versus offset), to indicate fluid composition within the channel complex and to have an estimation of the net gross within the channels.

References

Abilio, M.S., 1986. The Geology and hydrocarbon potential of Angola. In SADCC Energy sector Techinical and Administractive Unit, TAU, pp. 129-150.

Abreu, V., Sullivan, M.D., Pirmez, C., and Mohrig, D.C., 2003. Lateral Accretion Packages (LAPs): An important reservoir element in deep water sinuous channel, Marine and Petroleum Geology, Elsevier, 20, pp. 631-648.

Amaral, J., Biteau, J.J., Zaroslinska, P., 1998. Angola- the lower Congo Basin Tertiary petroleum systems hydrocarbon distribution in relation with strutural and sedimentary evoluition. AAPG International conference and exhibition, extended abstracts, pp. 924-925.

Anderson, J. E., 1998. Corretating Miocene turbidite sands, Block 4 offshore Angola. Petroleum Exploration Society of Great Britain, West Africa Conference. London (Abstr.).

Anderson, J.E., Cartwright, J., Drysdall, S.J., Vivian, N., 2000. Controls on turbidite sand deposition during gravity-driven extension of a passive margin: examples from Miocene sediments in Block 4, Angola. Marine and Petroleum Geology (17), pp.1165-1203.

Bartolomeu, I., 2012. 2D seismic regional analysis of Kwanza Basin in offshore, Master project, NTNU.

Beaubouef, R. T., Friedmann, S.J., 2000. High-Resolution seismic/sequence stratigraphic Framework for the evolution of Pleistocene Intra Slope Basins, western Gulf of Mexico: Depositional Models and reservoir Analogs, In: P. Weimer, R.M. Slatt, A.H Bouma and D.T. Lawerence, eds., Gulf Coast Section, SEPM, 20th Annual Research Conference: Deep-Water Reservoirs of the world.,. pp. 40-60.

Beaubouef, R.T., Abreu, V., Van Wagoner, J.C., 2003. Basin 4 of the Brazos-Trinity Slope system: The terminal portion of a late Pleistocene lowstand systems tract. In:H. Roberts, et al., eds., Shelf Margin Deltas and Linked Down Slope Petroleum systems: Global Significance and Future Exploration Potential, Proceedings of 23rd Annual Research Conference, Gulf Coast Section SEPM Foundation, pp. 45-66.

Bishop, MS., 1960 surface mapping. John willey, New yourk, pp.198.

Bouma, A.H., 1962. Sedimentology of Some Flysch Deposits; a Graphic Approach to Facies Interpretation: Amsterdam, Elsevier, pp.168 p.

Brice, S.E., Cochran, M.D., Pardo, G., Edwards, A.D., 1982. Tectonics and Sedimentation of the South Atlantic Rift Sequence: Cabinda, Angola. Gulf Exploration and Production Company Houston, Texas.

Cole, G. A., Requejo, A. G., Ormerod, D. Z., Clifford, A., 2000. Petroleum geochemical assessment of the Lower Congo Basin, in Mello, M. R., Katz eds, B. J., Petroleum systems of South Atlantic margins: AAPG Memoir 73, pp. 325–339.

Campion, K. M., A. R. Sprague, and M. D. Sullivan, 2005, Architecture and lithofacies of the Capistrano Formation (Miocene Pliocene), San Clemente, California: Pacific Section SEPM Field Trip Guide Book 100, pp. 42.

Campion, K.M., Sprague, A.R., Mohrig D., Lovell, R.W., Drzewiecki, P.A., Sullivan, M.D., Ardill, J.A., Jensen, G.N., Sickafoose, D.K., 2000, Outcrop expression of confined channel complexes, in P. Weimer et al., editors, Deep-Water Reservoirs of the World: SEPM (Society for Sedimentary Geology), Gulf Coast Section, Houston, TX, pp. 127-150.

Droz, L., Marsset, T., Ondre´as, H., Lopez, M., Savoye, B., and Spy-Anderson, F.-L., 2003. Architecture of an active mud-rich turbidite system:The Zaire Fan (Congo–Angola margin southeast Atlantic): Results from Zai¨Ango 1 and 2 cruises. AAPG Bulletin, v. 87, pp. 1145-1168.

Emery,D., Myers, K., 1996. Sequence Stratigraphy. Blackwell Science Ltd. pp. 297.

Faria, E., 2011. Geological Interpretation of Turbidity Marine Channels using 3D Seismic Data, Master, NTNU.

Fejerskov, M., Dongala, M., Seque, M., and Fort,X., 2009. Salt tectonic modeling. A method for finding more oil in Angola. SPE meeting, Luanda, 16th September 2009.

Fort, X., Brun, J-P., Chauvel, F., 2004. Salt tectonic on the Angolan margin, synsedimentary deformation processes. AAPG Bulletin, v. 88, pp.1523–1544.

Funk, J.E., Slatt, R.M., Pyles, D.R., 2012. Quantification of static connectivity between deep-water channels and stratigraphically adjacent architectural elements using outcrop analogs. AAPG Bulletin, v.96, pp.277-300.

Gee, M.J.R., Gawthorpe, R.L., 2006. Submarine channels controlled by salt tectonics: Examples from 3D seismic data offshore Angola. Marine and Petroleum Geology (23), pp. 443-458.

Gjelberg, J., Valle, J. P., 2003. Tectonostratigraphic evolution of the offshore Angolan margin, Statoil, unpublished report.

Gluyas.J., Swarbrick.R., 2004. Petroleum Geoscience. Blackwell published pp. 359.

Imran, J., Parker, G., and Pirmez, C., 1999. A non-linear model of flow in meandering submarine and subaerial channels: Journal of Fluid Mechanics, v. 400, pp. 295–331.

Kolla,V., Bouurges, Ph.,Urruty, J-M., Safa, P., 2001. Evolution of deep-water Tertiary sinuous channels offshore Angola (West Africa) and implications for reservoir architecture. AAPG Bulletin, v.85, pp. 1373-1405.

Kolla, V., 2007. A review of sinuous channel avulsion patterns in some major deep-sea fans and factors controlling them, Marine and Petroleum geology 24, pp. 450-459.

Leopold, L. B., Wolman, M. G., and Miller, J. P., 1964. Fluvial processes in geomorphology. Freeman, San Francisco, pp. 522.

Mateus, P., 2009. Imaging of Tertiary Turbidite Channel offshore Angola, West Africa, Master, NTNU.

Mitchum, R.M., Jr., Van Wagoner, J.C., 1991. High frequency sequences and their stacking patterns: sequences-stratigraphic evidence of high- frequency eustatic cycles, Sedimentary Geology, v. 70, pp. 131-160.

Mitchum, R.M., Jr., 1977. Seismic stratigraphy and global changes of sea level, Part 1: Glossary of terms used in seismic stratigraphy. In: C.E. Payton, ed., Seismic Stratigraphy- Applications to hydrocarbon Exploration, Am. Assoc. Petrol. Geol., Memoir 26, pp. 205-212.

Rowan.M.G., 2008. Salt Effects on Petroleum Systems. Geo Expro volume 5, 2008. Pp. 56-58.

Savoye, B., Babonneau, N., Dennielou, B., Bez, M., 2009. Geological overview of the Angola–Congo margin, the Congo deep-sea fan and its submarine valleys. Deep Sea Research Part II: Topical Studies in Oceanography Volume 56, Issue 23, pp. 2169-2182

Sikema, W., Wojcik, K.M., 2000. 3D visualization of turbidite systems, lower Congo, offshore Angola. GCSSEPM foundation 20th Annual Research Conference Deep-water Reservoir of the world.

Serqueira, J., Campbell, M., and Smith, P., 1998. Comparison of key play elements of proven and potential petroleum systems of the south Atlantic margin margin-offshore Brazil and West Africa. AAPG International Conference and exhibition, extended abstracts, pp. 104-105.

Sonangol report, 2003. Post N`Demba-1 Tertiary Evaluation Block 34 Angola, pp, 9, 22-26.

Sullivan, M.D., Jensen, G.N., Goulding, F.J., Jenette, D.C., Stern, D., 2000. Architectural analysis of deep water outcrops: Implications for exploration and production of the Diana sub-basin, western Gulf of Mexico. In: P. Weimer, R.M. Slatt, A.H. Bouma, and D.T. Lawerence, eds., Gulf Coast section, SEPM, 20th Annual Research Conference: Deep-Water Reservoirs of the world, pp. 1010-1032.

Sprague, A.R.G., Garfield, T.R., Goulding, F.J., Beaubouef, R.T., Sullivan, M.D., Rossen, C., Campion, K.M., Sickafoose, D.K., Abreu, V., Schellpeper, M.E., Jensen, G.N., Jennette, D.C., Pirmez, C., Dixon, B.T., Ying, D., Ardill, J., Mohrig, D.C., Porter, M.L., Farrell, M.E., Mellere, D., 2005. Integrated Slope Channel DepositionalModels: The Key to Successful Prediction of Reservoir Presence and Quality in Offshore West Africa, CIPM, cuarto EExitep 2005, February 20e23, 2005, Veracruz, Mexico, pp.1-13.

Schlumberger (2013). Glossary oil field.

Stark, D.M., Well evaluation conference Angola 1991. Paris, Schlumberger, pp. 329.

Taner, M.T., 2001. Seismic attribute. Rock Solid Images, Houston, U.S.A. CSEG pp.58.

Valle, J. P., Gjelberg, J.G., Helland-Hansen, W., 2001. Tectonostratigraphic development in the eastern Lower Congo Basin, offshore Angola, West Africa. Marine and Petroleum Geology (18), 909-927.

Van wagoner, J.C., Posamentier, H.W., Mitchum, R.M., Vail, P.R., Sarg, J.F., Loutit. T.S., Hardenbol, J., 1988. An overview of the fundamentals of sequence stratigraphy and key definitions. Exxon production research company, P.O. Box 2189, Huston, Texas 77252-2189.